DETERMINING THE FUNCTION OF *PLASMODIUM* HEMOLYSIN III AND DISCOVERY OF NOVEL ANTIMALARIAL DRUGS

by
Natalie Robinett

A dissertation submitted to Johns Hopkins University in conformity with the requirements for the degree of Doctor of Philosophy

Baltimore, Maryland

September, 2015

ABSTRACT

Elimination of the malaria parasite from endemic areas requires a multi-faceted approach, including development of novel antimalarial drugs and a deeper understanding of parasite-host interactions. Here we describe functional characterization of a *Plasmodium* hemolysin III (PfHlyIII) along with various approaches to determine whether hemolysin is a virulence factor in malaria, contributing to severe malaria anemia. In addition we also describe two antimalarial drug discovery projects including characterization of novel quinine and quinidine derivatives as efficacious, non-toxic antimalarials, as well as the development of a robust high throughput assay to screen for gametocytocidal compounds.

Regarding characterization of *Plasmodium* hemolysin III, we have evidence for heterologous pore formation of recombinant PfHlyIII in *Xenopus* and also show expression of soluble native PfHlyIII in asexual blood stage parasites. Together these data support our hypothesis that PfHlyIII may be available upon schizont egress as a cytolytic protein that could damage and increase clearance of bystander erythrocytes. Unexpectedly, genetic disruption of *P. berghei* HlyIII (PbHlyIII KO) resulted in *greater* virulence in Balb/c mice leading to an early death phenotype and altered parasitophorous vacuole morphology in the asexual blood stages. We hypothesize that early death in mice infected with the PbHlyIII KO parasite may be a result of altered deformability of infected erythrocytes and increased sequestration leading to brainstem hemorrhage. Though we did not prove or disprove our hypothesis that PfHlyIII may damage uninfected erythrocytes and contribute to severe malaria anemia, our knockout phenotype of severe membrane defects suggests PfHlyIII may play a role in membrane homeostasis

or remodeling, either directly or indirectly through functioning as a receptor, similar to yeast homolog Izh2p.

Synthesis and characterization of hydroxyethylapoquinine and derivatives involved revisiting an old quinine derivative with promising historical data supporting greatly reduced toxicity in humans and comparable efficacy against bird malaria compared to quinine. The modifications to quinine included hydroxyethylation at the methoxy side chain and isomerization of a vinyl group. Our studies included a novel synthetic approach to hydroxyethylapoquinine in addition to synthesis of three novel compounds: hydroxyethylapoquinidine and quinine and quinidine derivatives with only the hydroxyethyl substitution. We demonstrate antimalarial efficacy of all four derivatives against three strains of *P. falciparum in vitro*, with nanomolar IC_{50}s against a quinine-sensitive strain 3D7, and elevated IC_{50}s against quinine tolerant strains INDO and Dd2. In a murine malaria model the quinidine intermediate, hydroxyethylquinidine (HEQD) showed the greatest potency, similar to quinine and also performed the best in the *in vitro* assays. Furthermore the hydroxyethyl modifications greatly reduced the hERG channel inhibitory properties of all derivatives compared to the parent drugs, and further derivation of HEQD may yield a safer alternative to quinine or quinidine and be a potential long-half life partner drug in artemisinin-based combination therapies.

SYBR Green I and a green fluorescence background suppressor from CyQUANT were used in conjunction with exflagellation media to develop a novel transmission blocking assay that can be used to screen for gametocytocidal compounds. Following optimization of the assay, we screened the Johns Hopkins Clinical Compound Library version 1.3 as well as the Medicines for Malaria Venture malaria box, a total of over

2,000 compounds, resulting in 43 hits with good efficacy against late stage gametocytes. Quaternary ammonium compounds and acridine-like compounds were novel drug classes revealed in our screen. Transmission blocking activity of top hits was confirmed using membrane feeding assays and correlation with other assays strengthened the validity of our assay. Overall our data supports use of the SYBR Green assay to screen for novel transmission blocking compounds for use in malaria elimination strategies.

Dissertation Readers:

Advisor:

David J. Sullivan, M.D.	Molecular Microbiology and Immunology – BSPH
Gary Ketner, Ph.D.	Molecular Microbiology and Immunology – BSPH
Jürgen Bosch, Ph.D.	Biochemistry and Molecular Biology – BSPH
Caren Meyers, Ph.D.	Pharmacology and Molecular Sciences – SOM
Sean Prigge, Ph.D.	Molecular Microbiology and Immunology – BSPH
Sanjay Jain, M.D.	Pediatric I.D. and Center for Tuberculosis Research – SOM
Michael Matunis, Ph.D.	Biochemistry and Molecular Biology – BSPH

ACKNOWLEDGEMENTS

I would first like to thank Dr. David Sullivan for being such a patient, insightful and supportive mentor. He has helped me grow as a scientist and as a person, and I really appreciate his careful and constructive criticism of my work. He has been so instrumental in shaping how I approach scientific questions and has always pushed me to think outside the box. I will always admire his intellect, integrity, and care for his students. I am thankful for both the attention and independence he has given me over the years, and I value his trust in my work and his investment in my future. I am also grateful for the many opportunities he has made possible for me to mentor and teach students through the undergraduate research programs as well as to be a teaching assistant in the parasitology class.

To my lab mates who have been indispensable over the years and have been a constant source of joy, commiseration, laughter and support - you have all become such good friends, and I cannot imagine my life without you. I first want to acknowledge Tamaki Kobayashi for her kind and quiet spirit and open attitude. She is always available for any questions I might have, and her work ethic, integrity and positive attitude are qualities I have deeply admired and which I hope have rubbed off on me. I also want to thank Patty Ferrer for being such a good friend – I enjoyed all of our many adventures in and out of lab. After spending four years in lab together, I have missed Patty's company and spending time with her, but am grateful for getting to know her. Shannon Moonah was one of the first people I got to know in our lab and his passion for science and for life left a deep impression on me. Thanks to Shannon I was able to become part of a very interesting project that ended up developing into a major part of my doctoral research. I

have missed his wit and sense of humor, but am very thankful for getting to spend two years with him in our lab. Kei Mikita was a visiting PhD student from Japan, and he spent a year working in our lab, with his desk opposite mine. Kei is one of the most cheerful, hard working people I have ever met. He taught me how to have a positive outlook even when research was not going well and how to balance a strong work ethic with a healthy lifestyle. Kei is so dedicated to his work, but he also really loves his family. He and David are both excellent examples to me of keeping a healthy balance of work and family. My favorite memory of Kei is when he used an analogy of baseball (which he loved) to encourage me in my troubleshooting woes. In short, he said that having a batting average of 0.33 meant that you were able to hit the ball one third of the time, and if you could get at least one in three experiments to work, you didn't have a bad batting average. I have remembered that every time I have been tempted to be discouraged. To Leah and Kristin – our new PhDs in the lab – I am so happy to have gotten to know each of you – and I know you are going to be amazing scientists. You are both such fun and wonderful women – I am sad to be leaving you, but it is nice to know the lab will be in good and organized hands ☺.

To my classmates who have also been so instrumental in shaping the person I've become over the past few years: Smita, June, Aleah, Priyanka, Jason and Pike. I have so enjoyed getting to know each of you and what a journey the PhD has been. I am so thankful for each of you, for your friendship, encouragement and support. We had the chance to explore Baltimore together and have seen each other through so many life changes including marriage, new jobs and even children. I am excited to see where each of you end up and am blessed to have known you. I could not have made it through this

program without you. Along the same lines, there are so many people who have taught me techniques and helped with my scientific growth during the last five years, and it is only fair for me to list all of the folks who have made it possible for me to be where I am today: Egbert Hoiczyk, David Zuckerman, Colleen McHugh, Jay Bream, Dilini Gunasekera, Lirong Shi, Abhai Tripathi, Godfree Mlambo, Kyle McLean, Ryan Smith, Joel Vega-Rodriguez, Krista Matthews, Jolyn Gisselberg, Teegan Delli-Bovi Ragheb, Daniel Rhageb, Christine Hopp, Gundula Bosch, Clive Shiff, Julia Romano, Gail O'Connor, Leonid Shats, Connie Liu, Isabelle Coppens and Jonathan Pevsner. Thank you for all of your help, for making time to explain a concept or technique to me, and for answering all of my questions. So many of you went above and beyond and I so much appreciate your time. Thanks also to Thom Hitzelberger, Debbie Bradley, Maryann Smith, and Chad Barnwell for all of your help with managing stipends, fellowships, etc.

I would like to thank all of the faculty members who have served on my different committees over the years, most especially my thesis committee members: Sean Prigge, Jürgen Bosch, and Gary Ketner. Thanks also to the recent additions to my committee: Caren Meyers, Sanjay Jain and Michael Matunis. I am so grateful for your time and input into my thesis research, for working me through all of the scheduling and for taking the time to read my thesis carefully and help me submit a polished final dissertation.

Of course I would like to thank my family for all of their encouragement and support over the years. My parents have been so instrumental in helping me stay motivated in pursuing a good education, all the way through graduate school. Thanks to my mom for her own example of determination – you have inspired me as no one else could. Thanks to my dad for his sense of humor and interest in everything I do – you

have reminded me of the importance of what I have been studying and helped me to be positive and see the humor in even hard situations. Thanks to my brother and sister who, though they have been in different parts of the world, have always been supportive and loved me from afar – I love you both and am so thankful you are my siblings. And to my husband Robby- thank you for putting up with long distance dating for three years, followed by a long-distance engagement, and your willingness to move across the country to do your residency. I could not have finished this program without your love and support. Thank you for being there for me and sacrificing so much for me – glad we get to make our next move together next time, wherever that happens to be.

Finally, I would like to thank God for granting me the endurance and skills needed to complete this program – all that I do is first and foremost for Him.

TABLE OF CONTENTS

LIST OF TABLES

LIST OF FIGURES

CHAPTER ONE:
GENERAL INTRODUCTION

Malaria: Etiology and Epidemiology

Malaria is a protozoan parasitic disease, with historical references from as early as 2700 BC China to 400 BC Greece that described periodic fevers and enlarged spleens (1). While there are over one hundred twenty *Plasmodium* species, only five currently infect humans and result in human malaria: *Plasmodium falciparum, P. vivax, P. malaria, P.ovale,* and *P. knowlesi*. That malaria fevers were the result of parasite reproduction was first suggested by Rasori in 1816, but Laveran was the first to identify the *Plasmodium* parasite in the blood of malaria patients, observing the sexual gametocyte stages of the parasite in 1880 and later convincing the leading malariologists in Italy that the cause of malaria was a protozoan, not a bacterium (2). Ross and Grassi are together attributed with linking the *Anopheline* mosquito vector to malaria transmission. Ross successfully identified *Plasmodium* oocysts in the mosquito in 1897 and further elucidated the *Plasmodium* life cycle in the mosquito (1). Grassi and his colleague Bignami fed mosquitoes on infected travelers and then transmitted the disease to uninfected individuals by mosquito bite, observing that only female *Anopheline* mosquitoes could successfully transmit malaria in 1898 (2).

Since the initial discovery of *Plasmodium* as the causative agent of malaria and requirement for transmission by female *Anopheline* mosquitoes, many other scientists have worked to gain a deeper understanding of the parasite biology and have more finely tuned our understanding of the parasite life cycle in both the mammalian hosts and mosquito vectors. Of particular importance was the observation of a liver stage development by Shortt and Garnham in 1947 that preceded the blood stages responsible for clinical disease (1). The dormant hypnozoite stages of the parasite in the liver that

later develop and result in relapse of the disease were finally identified in 1982 by Krotoski, who was working with Garnham's team (1). Overall, the entirety of the parasite life cycle was gradually revealed over a period of seventy plus years of diligent and rigorous research. Our current understanding of the human malaria life cycle is represented in Figure 1.1.

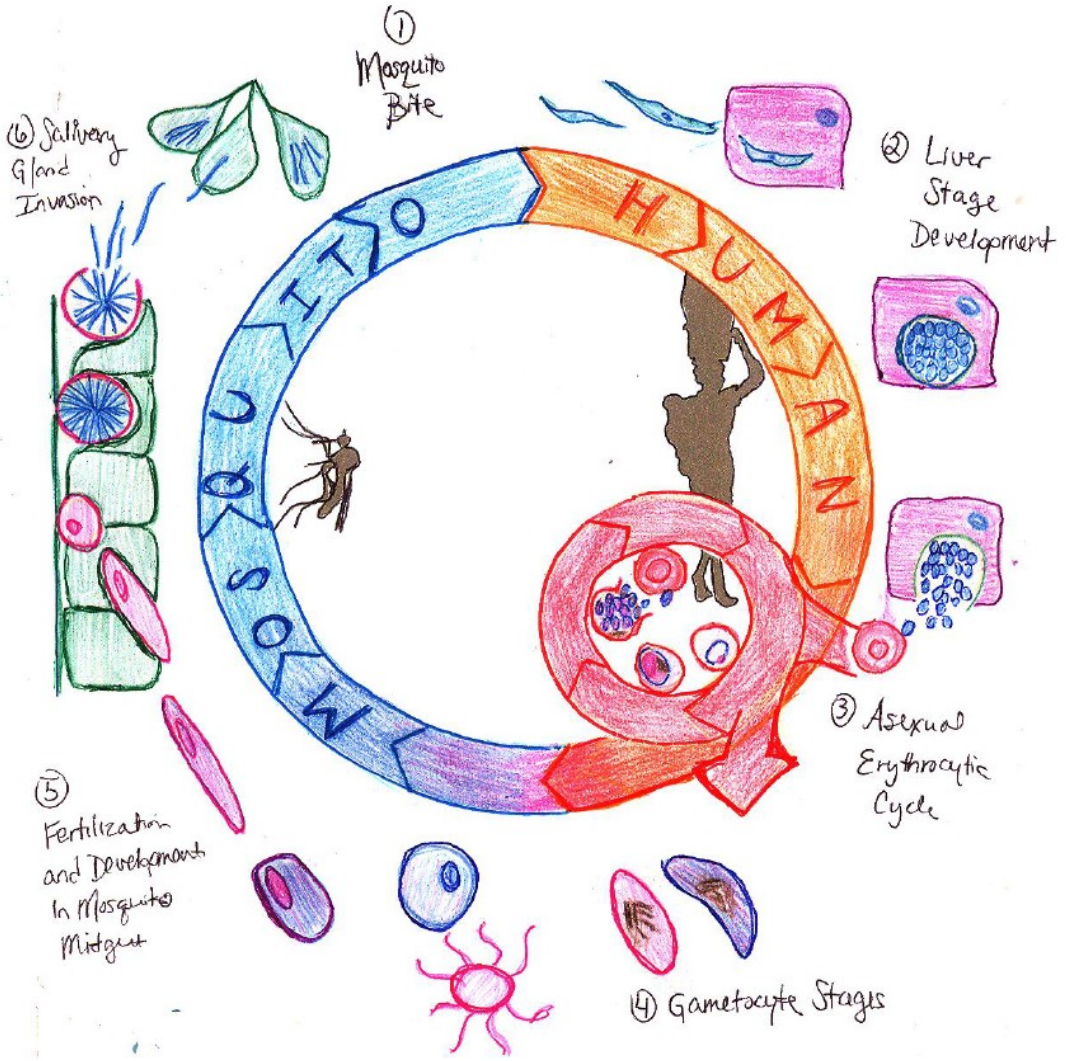

Figure 1.1 *Plasmodium* life cycle in the *Anopheline* mosquito and human host.

In brief, an infected female *Anopheline* mosquito takes a bloodmeal from a human host, and inoculates approximately 100 *Plasmodium* sporozoites into the dermis and bloodstream. The sporozoites travel through the dermis until they reach a blood vessel, after which they migrate to the liver and invade, traverse and develop in hepatocytes. After a seven to ten day development and schizogeny, mature liver schizonts rupture and release merozoites into the bloodstream, beginning the erythrocytic cycle of maturation from a ring trophozoite to a metabolically active, hemoglobin degrading trophozoite, followed by DNA replication and segmentation into a mature schizont, ready for egress and release of new merozoites for reinvasion of erythrocytes. Some early erythrocytic stages undergo a different route of development into the sexual gametocyte stages of the parasite, and in *P. falciparum* in particular, there are five morphologically distinct stages of gametocyte development. Mature gametocytes are taken up in a bloodmeal by *Anopheline* vectors where male and female gametes mature and undergo fertilization in the midgut to form a zygote. These zygotes elongate and become motile, developing into ookinetes that invade the mosquito midgut wall and develop into oocysts. The oocysts then mature and produce sporozoites, which upon oocyte rupture, migrate through the hemocoel and invade the salivary glands of the mosquito, where they are poised for inoculation into a new host.

Humans and the malaria parasite have a unique relationship that has undergone evolutionary changes over the past 10,000 years, due to each organism exerting selective pressure on the other. As a result, *Plasmodium* became distributed geographically over larger areas and multiple continents as humans dispersed across the globe. Interestingly, the map of global malaria distribution as estimated from around the year 1900 has shrunk

geographically over the years as a result of different factors, including human antimalarial interventions and development of infrastructure, but also aided by temperate climates being less amenable to sustaining endemic malaria, making it easier to eliminate malaria in these areas (3,4).

Overall the geographical area at risk for human malaria has been halved, from around 53% of the total earth land area to 27% (4). In addition, malaria deaths have also seen a decline over the past two decades, with a 31.5% decline in malaria-attributed child mortality in sub-Saharan Africa from 2004 (5,6) and a continual decline in global malaria deaths outside of Africa since 1990 (6). Nevertheless, malaria continues to pose a public health threat with 3.3 billion people at risk for malaria infection every year, and an estimated 200 million cases in 2013, resulting in approximately 584,000 deaths (7). Africa, southern Asia, and Central and South America all continue to have malaria transmission, with most of the deadly malaria outbreaks occurring in Sub-Saharan Africa due to *P. falciparum* (7). While great strides have been made to reduce mortality and morbidity over the past decade, ultimately control alone will not be sufficient as malaria control has no definitive end point beyond reducing morbidity and mortality. Elimination is defined as interrupting transmission until no parasites remain in a given geographical area and should be the ultimate goal for each country. Eradication takes the concept of elimination further, applying it on a global scale, describing a time point when no *Plasmodium* parasites are left in the human population or to be transmitted by mosquitoes. All countries with varying levels of malaria transmission have been classified according to stage of elimination from initial stages of control to prevention of re-introduction (Figure 1.2). As each country moves toward elimination they must be

evaluated on several levels of feasibility, including technical, operational, and financial feasibility, as done for Zanzibar in 2009 (8). Most scientists agree that while the available antimalarial interventions are effective and should be used to control malaria (curb disease, prevent death and interrupt transmission), improving upon the current interventions is vital in order to achieve elimination in some settings and ultimately eradication. Funding for control strategies and continued pressure on the vector and parasite are crucial for future success and elimination efforts.

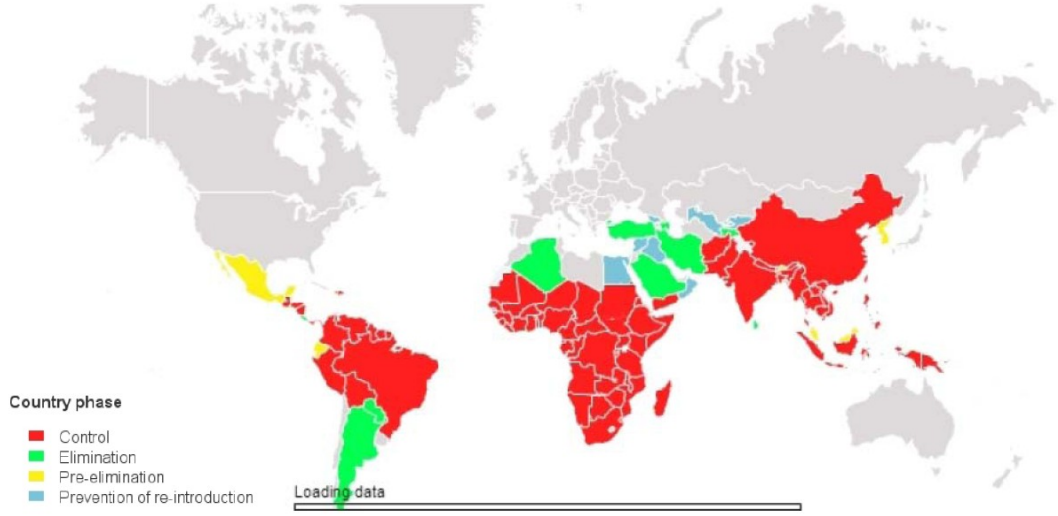

Figure 1.2 Global map of countries with endemic malaria classified according to stage of elimination: Control (red), Elimination (green), Pre-elimination (yellow), and Prevention of re-introduction (blue). Made using the Global Malaria Mapper, June 2015.

Disease and Pathology of *Plasmodium* Infection

Malaria disease can manifest with a variety of symptoms including fever, chills, sweating, headache, nausea and body aches (9). Patients with uncomplicated malaria may present with fever, enlarged liver or spleen, and mild jaundice or anemia, whereas more severe disease occurs when malaria infection is complicated by organ failures or blood or metabolic abnormalities. Manifestations of severe malaria include cerebral malaria, severe malaria anemia, hemoglobinuria, and acute respiratory distress syndrome (9).

Symptoms such as fever and anemia of malaria are the result of asexual stage parasites undergoing their replication cycle and the resulting inflammatory response initiated by the host, in addition to the destruction and clearance of erythrocytes. More severe symptoms are often the result of parasite sequestration, often seen with late asexual stages of *P. falciparum,* which bind to endothelial surfaces in capillaries and small blood vessels via a surface protein PfEMP1, resulting in restricting blood flow and oxygen deprivation in tissues. Dormant liver stage hypnozoite forms of the parasite are found in *P. vivax* and *P. ovale* infections and can reactivate, resulting in relapse after patients have recovered from the illness months or years after the original infection.

Older children and adults in endemic countries who have prolonged exposure to the parasite develop clinical immunity where they no longer exhibit classic symptoms of malaria, such as fever or malaise. However these infected individuals continue to act as reservoirs for the parasite, perpetuating the transmission cycle and resulting in continued infection and disease for the more vulnerable populations including infants, pregnant women, and young children.

Treatment: An Overview of Antimalarial Drug Classes

Currently antimalarial drugs are available to treat liver stages, asexual and sexual erythrocytic stages of the *Plasmodium* parasite in the human host. However the efficacy and safety of some of these compounds is limited, with many no longer useful due to the development of drug resistance. There are five well-described classes of antimalarial compounds with historical success, as well as several new classes of antimalarial compounds in the process of development, and all target various stages of the malaria parasite. The most well-studied and commonly used classes of malaria drugs include the quinolines, antifolates, antibacterials, atovaquone and the endoperoxides (Figure 1.3). Emerging novel drug classes currently listed in the global antimalarial portfolio development stage include aminopyridines (MMV390048) imidazolopiperazine (KAF156) , spiroindolones (KAE609), triazolpyrimidines (DSM265) and ozonides (OZ439) (Figure 1.4).

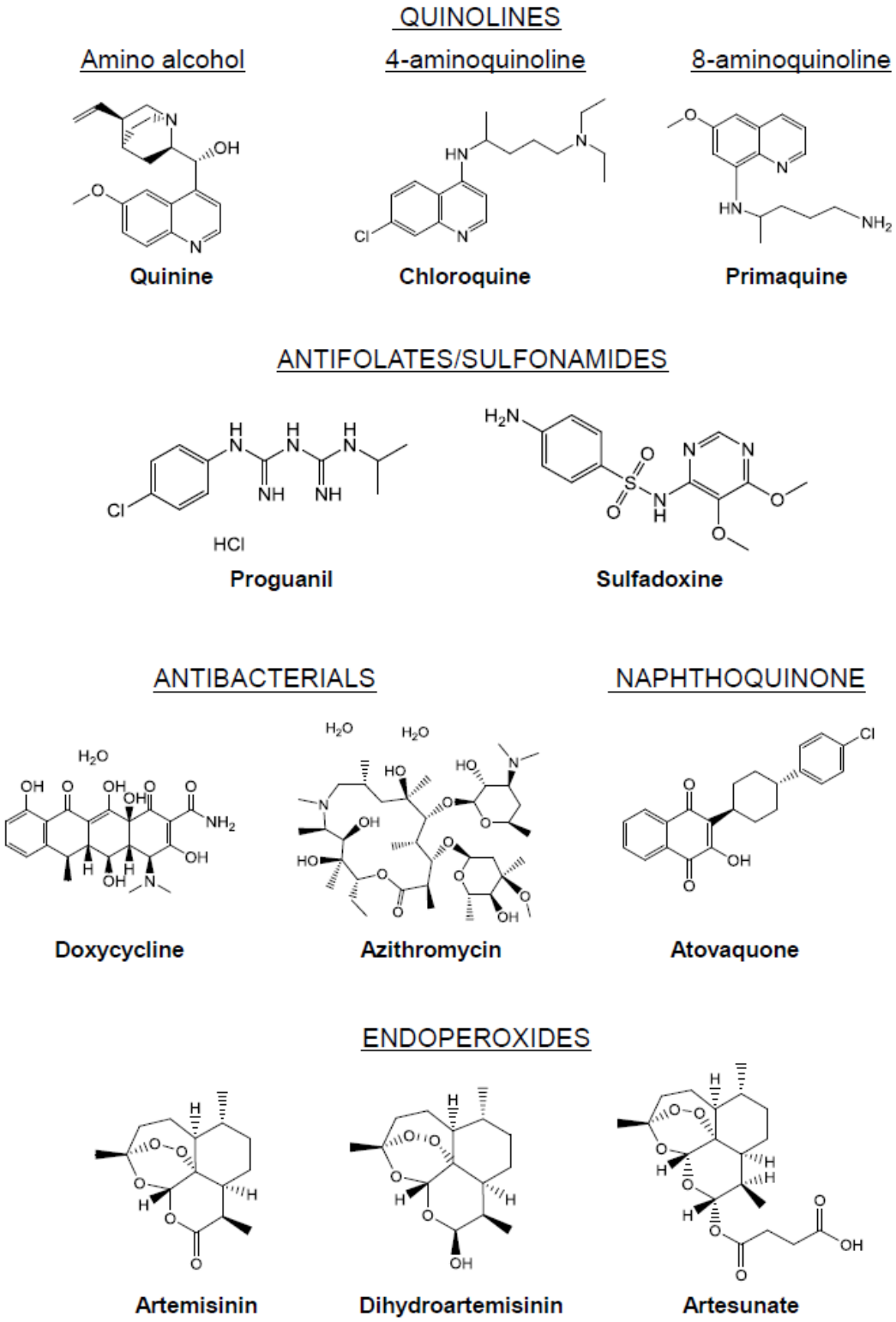

Figure 1.3 Current antimalarial drug classes and examples from each class.

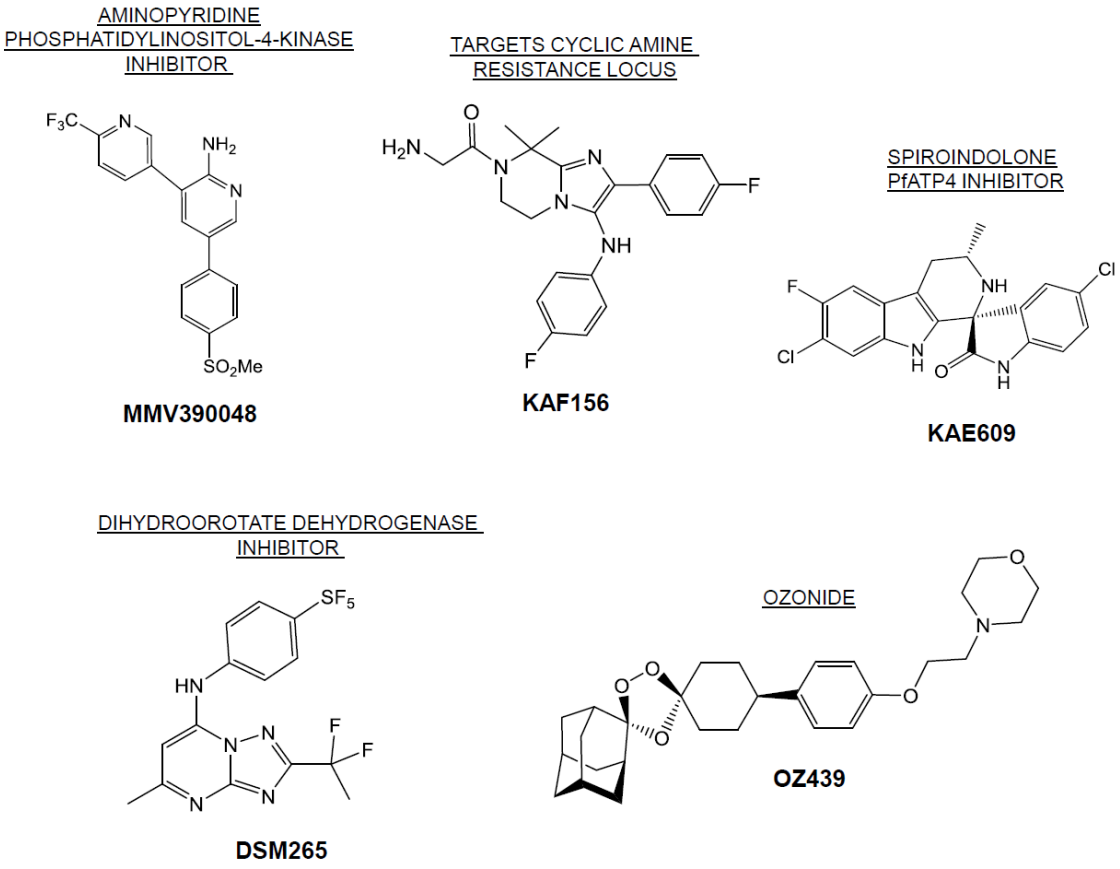

Figure 1.4 Novel antimalarial drugs in development phase in the global portfolio of antimalarial medicines 2015, Medicines for Malaria Venture (10,11).

Quinolines have been derivatized such that we have several different classes of these compounds including the original cinchona-derived alkaloids quinine and quinidine and modified amino-alcohols like mefloquine, as well as the 4-aminoquinolines such as chloroquine and amodiaquine, and the 8-aminoquinolines such as primaquine. Quinolines are commonly thought to inhibit hemozoin formation in the parasite and chloroquine in particular has been shown to bind to the growing face of the heme crystal through atomic force microscopy, and accumulates to high levels in the digestive vacuole of the parasite (12–14).

However, not all quinolines may accumulate to sufficient concentrations in the food vacuole to inhibit hemozoin crystallization, and compounds such as quinine and mefloquine are likely to have other antimalarial targets in addition to their inhibitory action against hemozoin (15–17). Primaquine has a unique and somewhat unclear mechanism of action, but is thought to inhibit *Plasmodium* mitochondrial function and selectively generate oxidative stress through reactive intermediates, but shows little activity against heme crystallization, and thus little inhibition against asexual stages (18,19). Importantly, primaquine is currently the only licensed antimalarial that can kill liver stage parasites, including the dormant hypnozoite stages, and also has cidal activity against *P. falciparum* gametocytes (20,21). Unfortunately primaquine also has safety issues for patients with glucose-6-phosphate dehydrogenase (G6PD) deficiency and requires metabolism by CYP 2D6 in order to be active against parasites, making it challenging to treat infected individuals with deficiencies in either G6PD or CYP 2D6 (22,23).Tafenoqine, a primaquine derivative, is currently under clinical trial investigation, and hopefully will prove equally effective and less toxic than its counterpart (10,11,19).

Resistance against the quinolines has developed at various levels, with chloroquine no longer effective in many parts of the world, and increasing levels of resistance emerging against partner drugs such as mefloquine and amodiaquine. Quinoline resistance is likely due to alterations in the transporters which control drug flux as a result of mutations in *pfcrt*, *pfmdr1*, and *pfnhe* (24). Nevertheless, quinolines continue to be important as partner drugs in artemisinin-based combination therapies as well as malaria prophylaxis, and primaquine in particular is important in malaria elimination strategies to kill both hypnozoites as well as deplete the asymptomatic reservoir of gametocytes.

The artemisinin-based endoperoxides were first isolated from the Chinese medicinal plant sweet wormwood, *Artemisia annua*, which had been historically used to treat fevers, much like the cinchona bark used in South America from which the quinolines were isolated (25). As a response to the failure of chloroquine and the spread of resistance during the 1950's and 1960's, the Vietnamese turned to China for help in finding a replacement antimalarial drug. The result was the launch of the 523 research program in 1967 and the eventual isolation of the active component artemisinin in the 1970's, which was later derivatized into a methyl-ether, artemether, in addition to a water soluble artesunate. It was eventually found that these compounds required metabolism into an active form, dihydroartemisinin, which was responsible for their antimalarial action (25). The mechanism of action of the artemisinins is thought to be damage to biomolecules including bystander proteins and perhaps membrane potential depolarization as a result of reaction oxygen species (ROS) production after iron-dependent bioactivation of the endoperoxide bridge (26). The artemisinins are active

against the late ring to mature schizont asexual blood stages and also show activity against early and late stage gametocytes (27).

The discovery of K13 loci mutations conferring artemisinin 'resistance', better described as a delayed parasite clearance phenotype, support ROS-mediated parasite killing as a mechanism for the endoperoxides as the kelch superfamily of proteins mediate responses to oxidative stress and ubiquitin-regulated protein degradation (28–30). While no significant or sustained increase in IC_{50} has been recorded for the termed 'artemisinin resistant' parasites, multiple accounts of delayed parasite clearance and treatment failure with ACTs have been reported in South East Asia, and this delayed clearance remains an indirect measure of drug efficacy (29,31,32).The *pfkelch* mutation linked with artemisinin 'resistance' results in increased levels of *P. falciparum* phosphatidylinositol-3-kinase (PfPI3K) expression in ring stage parasites which may be important for the altered stress response and survival of these stages, pointing to PfPI3K as a selectively inhibited target of the artemisinins in the early ring stages (33).

It has been proposed that extending the ACT dosing time from three to four days, including at least two parasite life cycles, will prevent treatment failure and allow clearance of the 'resistant' or slow-clearing parasites (28). Currently the artemisinin-based combination therapies are the most effective and safe antimalarial drug regimens available, and until compounds are discovered that are equally rapid in their killing ability, the artemisinins and ACTs will continue to be the gold standard for antimalarial treatment. Altering the dosing strategies and improving the partner drugs in ACTs may protect this vital class of antimalarials from being lost to drug resistance.

The three other main classes of antimalarial compounds are termed 'magic bullet' type compounds (27) as they target a single enzyme or process, and include the antibacterials, antifolates, and atovaquone. Antibacterials with activity against *Plasmodium* typically inhibit the apicoplast ribosomes, resulting in inhibition of protein biosynthesis, or inhibit DNA gyrases (34). The tetracycline derivatives like doxycycline bind to the 30S subunit, whereas the macrolide reagents azithromycin target the 50S subunit, both classes causing a delayed death phenotype (35). The fluoroquinolones such as ciprofloxacin are DNA gyrase inhibitors but may also have additional targets and also result in a delayed death for asexual blood stage parasites (36).

Drugs targeting the folate pathway can be divided into two groups based on their specific targets, one group inhibiting dihydrofolate reductase (DHFR) and the other inhibiting dihydropteroate synthase (DHPS). Drugs targeting DHFR include proguanil, pyrimethamine, and dapsone which bind to DHFR and inhibit folic acid metabolism and downstream nucleic acid biosynthesis. DHPS is an enzyme upstream of DHFR, and sulfonamides such as sulfadoxine that act as para-aminobenzoic acid analogs competitively inhibit DHPS, resulting in formation of dead end metabolites.

Atovaquone is a unique antimalarial that acts as an analog of coenzyme Q, targeting the cytochrome bc_1 complex of the mitochondrial electron transport chain, targets asexual blood stages and has some activity against liver stages (37,38). Because each of these drugs (antibacterials, antifolates, atovaquone) inhibits a specific enzyme or protein, target site mutations in these proteins can confer resistance, making it less difficult for the parasite to quickly evolve resistance (38,39). Nevertheless, many of these compounds are used alone for malaria prophylaxis like doxycycline, or in combination as

in the case of sulfadoxine-pyrimethamine (SP) or Malarone, a formulation of atovaquone and proguanil.

As antimalarial drug resistance continues to pose a challenge for treatment and elimination of malaria, novel classes and derivations of currently effective pharmacophores are being pursued at multiple levels in the drug development phase. Some of the more promising leads that have made it to the later stages of development are pictured in Figure 1.4. The artemisinins are a highly successful group of compounds and derivations of this class have resulted in novel synthetic endoperoxides such as OZ439, also known artefenomel, which is currently being tested in combination with piperaquine (40). Artemisone and a tetraoxane TDD E209 are also in late stage development. DSM265 is a novel compound with a novel target, *Plasmodium* dihydroorotate dehydrogenase and is currently being tested in phase IIa monotherapy trials (40,41).

In a collaborative approach between Novartis Institute for Tropical Diseases in Singapore and the Swiss Tropical and Public Health Institute the spiroindolone class was found to have activity against *P. falciparum*, and subsequent improvements resulted in the compound KAE609, which was found to target the *Plasmodium* Na^+ -ATPase 4 ion channel (PfATP4) (42). KAF156 is another new compound with a novel mechanism of action, targeting the cyclic amine resistance locus, and is also in phase II clinical trials (40,41). In addition this compound has been shown to have activity against multiple stages of the parasite in the mouse model, including protecting mice against sporozoite challenge, killing asexual stages and preventing transmission (43). Finally, MMV390048 is part of a novel class of compounds, the aminopyridines and is an inhibitor of

phosphatidylinositol-4-kinase and is currently in clinical trials (10,40). Considering the paucity of novel targets and classes of antimalarial compounds discovered in the past century, these emerging new compounds discovered within the past decade are an exciting step forward for the malaria community and promise to provide alternatives and support to the current antimalarials challenged by resistance.

Elimination of Malaria: Challenges for Transmission Control and Diagnosis

Ultimately the goal for the global malaria community is elimination and eventually eradication. However antimalarial drugs alone will not be sufficient to accomplish this task, in part due to drug resistance, but also due to the complexity of the vector, the poverty, poor infrastructure and conflict in many endemic areas, as well as the large asymptomatic population. Vector control, diagnostics and vaccines are all tools that will be necessary components in any elimination strategy, in addition to antimalarial drug administration. In order to eliminate malaria, transmission of the parasite must be interrupted, which can be accomplished by preventing mosquito-human interactions, making mosquitoes no longer infectious to humans, or making humans no longer infectious to mosquitoes.

The first strategy involves vector control measures such as long lasting insecticide treated nets (LLINs), indoor residual spraying (IRS), or larviciding to reduce vector populations as well as create a physical barrier between humans and mosquitoes in the case of LLINs (44). LLINs are a popular intervention strategy due to their low cost and ease of distribution, but insecticide resistance and improper use have resulted in LLINs being less effective than expected. Indeed insecticide resistance and behavorial changes in *Anopheles* mosquitoes will continue to challenge control efforts and novel insecticides are vital for future success (45).

There are also efforts to make mosquitoes less competent vectors of *Plasmodium* through genetic modifications or introduction of bacteria to mosquito microbiota which inhibit *Plasmodium* development in the mosquito. Some approaches involve genetically modifying the mosquito itself to express anti-*Plasmodium* genes such

as immune factors that play a role in anti-*Plasmodium* defense in the mosquito (46,47). Other strategies involve paratransgenesis, or modifying symbiotic bacteria to deliver anti-pathogen factors and reduce vector competence (46,47). The challenge for these models is stably introducing them into the population and ensuring that the mosquitoes or bacteria will spread throughout a population.

Finally, a largely untouched strategy involves breaking the transmission cycle by making humans no longer infectious to mosquitoes. The obvious solution is to kill parasites in every infected individual, but doing so may prove very challenging. First infected individuals must be identified, and as mentioned earlier, there is a large asymptomatic population, particularly in endemic areas, that do not present with clinical illness and remain untreated (48). Active case detection of these individuals and treatment is one solution; another would involve mass drug administration of a safe and effective drug that would kill all parasite stages, including gametocytes and active or dormant liver stages. Primaquine in combination with an ACT would accomplish killing of all stages, but MDA of primaquine is ethically questionable as it can cause hemolysis in individuals with G6PD deficiency and is not really appropriate for mass administration to all of a population. Furthermore, MDA efforts would need to be combined with vector control to prevent new infections from occurring.

Ultimately a vaccine that could prevent infection and also block transmission would be ideal, to simultaneously drain the gametocyte reservoir and also prevent transmission of *Plasmodium* to mosquitoes. The only vaccine that is currently in phase III trials is the RTS,S/AS01 which targets *P. falciparum* sporozoites, aimed at preventing infection. Phase III trials of this vaccine resulted in only partial efficacy, with 50%

protection in older children, and only 30% efficacy in the target population, infants (49,50). For elimination purposes, development of a vaccine to prevent transmission would be a means of eliminating access for mosquitoes to the gametocyte reservoir in even asymptomatic individuals and is worth pursuing along with a more effective vaccine to prevent infection (51). Finally, diagnosis of low parasitemia individuals is also crucial to identify and eliminate every last case of malaria and warrants further research in the development of high sensitivity diagnostic tools (52).

All available tools including antimalarial drugs, vaccines, vector control strategies and diagnostics will be required to achieve the goal of elimination and eventually eradication. Each tool requires innovative strategies for improved design and implementation. My dissertation work has involved studying drug design and development for improved antimalarials, designing an assay to identify transmission blocking compounds, and finally understanding basic parasite biology and pathogenesis of the malaria parasite in the human host through the characterization of a *Plasmodium* hemolysin III. While varied in their scope, all three projects have one end goal in mind: the elimination of the malaria parasite.

REFERENCES

1. Cox FE. *History of the discovery of the malaria parasites and their vectors.* Parasit Vectors. 2010 Jan;3(1):5.
2. Schlagenhauf P. *Malaria: from prehistory to present*. Infect Dis Clin North Am. 2004 Jun;18(2):189–205.
3. Feachem RG a, Phillips A a, Hwang J, Cotter C, Wielgosz B, Greenwood BM, et al. *Shrinking the malaria map: progress and prospects.* Lancet. 2010 Nov 6;376(9752):1566–78.
4. Hay SI, Guerra C a, Tatem AJ, Noor AM, Snow RW. *The global distribution and population at risk of malaria: past, present, and future*. Lancet Infect Dis. 2004 Jun;4(6):327–36.
5. Murray CJL, Rosenfeld LC, Lim SS, Andrews KG, Foreman KJ, Haring D, et al. *Global malaria mortality between 1980 and 2010: a systematic analysis.* Lancet. Elsevier Ltd; 2012 Feb 4;379(9814):413–31.
6. Murray CJL, Ortblad KF, Guinovart C, Lim SS, Wolock TM, Roberts DA, et al. *Global, regional, and national incidence and mortality for HIV, tuberculosis, and malaria during 1990–2013: a systematic analysis for the Global Burden of Disease Study* 2013. Lancet. 2014 Jul 21;384(9947):1005–70.
7. WHO | World Malaria Report 2014. World Health Organization; Available from: http://www.who.int/malaria/publications/world_malaria_report_2014/en/
8. UCSF | *Malaria elimination in Zanzibar: A Feasibility Assessment* October 2009. Available from: http://www.malariaeliminationgroup.org/malaria-elimination-zanzibar-feasibility-assessment

9. CDC - Malaria - *About Malaria - Disease*. 2010. Available from: http://www.cdc.gov/malaria/about/disease.html

10. Olliaro P, Wells TNC. *The global portfolio of new antimalarial medicines under development. Clin Pharmacol Ther. Nature Publishing Group*; 2009;85(6):584–95.

11. Medicines for Malaria Venture. *Interactive R&D Portfolio*. 2015. Available from: http://www.mmv.org/research-development/rd-portfolio

12. Olafson KN, Ketchum MA, Rimer JD, Vekilov PG. *Mechanisms of hematin crystallization and inhibition by the antimalarial drug chloroquine*. Proc Natl Acad Sci U S A. 2015 Mar 23; 26

13. Sullivan DJ, Gluzman IY, Russell DG, Goldberg DE. *On the molecular mechanism of chloroquine's antimalarial action*. Proc Natl Acad Sci U S A. 1996 Oct 15;93(21):11865–70.

14. Sullivan DJ, Matile H, Ridley RG, Goldberg DE. *A common mechanism for blockade of heme polymerization by antimalarial quinolines*. J Biol Chem. 1998 Nov 20;273(47):31103–7.

15. Foley M, Tilley L. *Quinoline antimalarials: Mechanisms of action and resistance.* Int J Parasitol. 1997 Feb;27(2):231–40.

16. Dorn a, Vippagunta SR, Matile H, Jaquet C, Vennerstrom JL, Ridley RG. *An assessment of drug-haematin binding as a mechanism for inhibition of haematin polymerisation by quinoline antimalarials*. Biochem Pharmacol. 1998 Mar 15;55(6):727–36.

17. Dassonville-Klimpt A, Jonet A, Pillon M, Mullié C, Sonnet P. *Mefloquine derivatives: synthesis, mechanisms of action, antimicrobial activities*. Sci against Microb Pathog Commun Curr Res Technol Adv - Vol 1. 2011;10275:23–35.

18. Egan TJ, Rossa DC, Adamsb PA. *Quinoline anti-malarial drugs inhibit spontaneous p-haematin (malaria pigment) formation of*. FEBS Lett. 1994;352(1):54–7.

19. Vale N, Moreira R, Gomes P. *Primaquine revisited six decades after its discovery.* Eur J Med Chem. 2009 Mar;44(3):937–53.

20. Ashley EA, Recht J, White NJ. *Primaquine: the risks and the benefits*. Malar J. 2014 Jan;13:418.

21. Butterworth AS, Skinner-Adams TS, Gardiner DL, Trenholme KR. *Plasmodium falciparum gametocytes: with a view to a kill.* Parasitology. 2013 Dec;140(14):1718–34.

22. Luzzatto L, Seneca E. *G6PD deficiency: a classic example of pharmacogenetics with on-going clinical implications*. Br J Haematol. 2014 Mar;164(4):469–80.

23. Pybus BS, Marcsisin SR, Jin X, Deye G, Sousa JC, Li Q, et al. *The metabolism of primaquine to its active metabolite is dependent on CYP 2D6*. Malar J. Malaria Journal; 2013;12(1):1.

24. Roepe PD. *Molecular and physiologic basis of quinoline drug resistance in Plasmodium falciparum malaria*. Future Microbiol. 2009;4(4):441–55.

25. Faurant C. *From bark to weed: the history of artemisinin*. Parasite. 2011;18(3):215–8.

26. Antoine T, Fisher N, Amewu R, O'Neill PM, Ward SA, Biagini GA. *Rapid kill of malaria parasites by artemisinin and semi-synthetic endoperoxides involves ROS-dependent depolarization of the membrane potential*. J Antimicrob Chemother. 2014 Apr 1;69(4):1005–16.

27. Sullivan DJ. *Plasmodium drug targets outside the genetic control of the parasite*. Curr Pharm Des. 2013 Jan;19(2):282–9.

28. Dogovski C, Xie SC, Burgio G, Bridgford J, Mok S, McCaw JM, et al. *Targeting the Cell Stress Response of Plasmodium falciparum to Overcome Artemisinin Resistance*. PLoS Biol. 2015 Apr;13(4):e1002132.

29. Takala-Harrison S, Clark TG, Jacob CG, Cummings MP, Miotto O, Dondorp AM, et al. *Genetic loci associated with delayed clearance of Plasmodium falciparum following artemisinin treatment in Southeast Asia.* Proc Natl Acad Sci U S A. 2013 Jan 2;110(1):240–5.

30. Ariey F, Witkowski B, Amaratunga C, Beghain J, Langlois A-C, Khim N, et al. *A molecular marker of artemisinin-resistant Plasmodium falciparum malaria. Nature*. 2013 Dec 18

31. Kyaw MP, Nyunt MH, Chit K, Aye MM, Aye KH, Lindegardh N, et al. *Reduced susceptibility of Plasmodium falciparum to artesunate in southern Myanmar*. PLoS One. 2013 Jan;8(3):e57689.

32. Rogers WO, Sem R, Tero T, Chim P, Lim P, Muth S, et al. *Failure of artesunate-mefloquine combination therapy for uncomplicated Plasmodium falciparum malaria in southern Cambodia*. Malar J. 2009 Jan;8:10.

33. Mbengue A, Bhattacharjee S, Pandharkar T, Liu H, Estiu G, Stahelin R V., et al. *A molecular mechanism of artemisinin resistance in Plasmodium falciparum malaria.* Nature. Nature Publishing Group, a division of Macmillan Publishers Limited. All Rights Reserved.; 2015 Apr 15;520(7549):683–7.

34. Dahl EL, Rosenthal PJ. *Multiple antibiotics exert delayed effects against the Plasmodium falciparum apicoplast*. Antimicrob Agents Chemother. 2007 Oct;51(10):3485–90.

35. Lee Y, Choi JY, Fu H, Harvey C, Ravindran S, Roush WR, et al. *Chemistry and biology of macrolide antiparasitic agents.* J Med Chem. 2011 Apr 28;54(8):2792–804.

36. Tang Girdwood SC, Nenortas E, Shapiro TA. *Targeting the gyrase of Plasmodium falciparum with topoisomerase poisons*. Biochem Pharmacol. 2015 Jun 15;95(4):227–37.

37. Stickles AM, Ting L-M, Morrisey JM, Li Y, Mather MW, Meermeier E, et al. *Inhibition of Cytochrome bc1 as a Strategy for Single-Dose, Multi-Stage Antimalarial Therapy.* Am J Trop Med Hyg. 2015 Apr 27;92(6):1195–201.

38. Siregar JE, Kurisu G, Kobayashi T, Matsuzaki M, Sakamoto K, Mi-ichi F, et al. *Direct evidence for the atovaquone action on the Plasmodium cytochrome bc1 complex*. Parasitol Int. 2015 Jun;64(3):295–300.

39. Ecker, A, Lehane, AM, Fidock D. *Molecular Markers of Plasmodium Resistance to Antimalarials*. In: Staines, HM, Krishna S, editor. Treatment and prevention of malaria. 2012. p. 249–71.

40. Wells TNC, van Huijsduijnen RH, Van Voorhis WC. *Malaria medicines: a glass half full?* Nat Rev Drug Discov. Nature Publishing Group; 2015 May 22;14(6):424–42.

41. Held J, Jeyaraj S, Kreidenweiss A. *Antimalarial compounds in Phase II clinical development*. Expert Opin Investig Drugs. 2015 Mar;24(3):363–82.

42. Spillman NJ, Allen RJW, McNamara CW, Yeung BKS, Winzeler EA, Diagana TT, et al. *Na(+) regulation in the malaria parasite Plasmodium falciparum involves the cation ATPase PfATP4 and is a target of the spiroindolone antimalarials*. Cell Host Microbe. 2013 Feb 13;13(2):227–37.

43. Kuhen KL, Chatterjee AK, Rottmann M, Gagaring K, Borboa R, Buenviaje J, et al. *KAF156 is an antimalarial clinical candidate with potential for use in prophylaxis, treatment, and prevention of disease transmission*. Antimicrob Agents Chemother. 2014 Sep;58(9):5060–7.

44. Killeen GF, Seyoum A, Sikaala C, Zomboko AS, Gimnig JE, Govella NJ, et al. *Eliminating malaria vectors*. Parasit Vectors. 2013 Jan;6:172.

45. Sokhna C, Ndiath MO, Rogier C. *The changes in mosquito vector behaviour and the emerging resistance to insecticides will challenge the decline of malaria*. Clin Microbiol Infect. 2013 Oct;19(10):902–7.

46. Ramirez JL, Garver LS, Dimopoulos G. *Challenges and approaches for mosquito targeted malaria control.* Curr Mol Med. 2009 Mar;9(2):116–30.

47. Wang S, Jacobs-Lorena M. *Genetic approaches to interfere with malaria transmission by vector mosquitoes*. Trends Biotechnol. 2013 Mar;31(3):185–93.

48. Lindblade K a, Steinhardt L, Samuels A, Kachur SP, Slutsker L. *The silent threat: asymptomatic parasitemia and malaria transmission*. Expert Rev Anti Infect Ther. 2013 Jun;11(6):623–39.

49. Jindal H, Bhatt B, Malik JS, SK S MB. *Malaria vaccine: A step toward elimination*. Hum Vaccin Immunother. 2014;10.

50. Tran TM, Portugal S, Draper SJ, Crompton PD. *Malaria Vaccines: Moving Forward After Encouraging First Steps*. Curr Trop Med Reports. 2015 Jan 27;2(1):1–3.

51. Group ERAC. *A Research Agenda for Malaria Eradication: Vaccines*. PLoS Med. 2011 Jan 25;8(1):e1000398.

52. Lin JT, Saunders DL, Meshnick SR. *The role of submicroscopic parasitemia in malaria transmission: what is the evidence*? Trends Parasitol. 2014 Apr;30(4):183–90.

CHAPTER 2:
PLASMODIUM HEMOLYSIN III: A ROLE IN THE PARASITE AND IN SEVERE MALARIA ANEMIA

***Xenopus* and native PfHlyIII expression data previously published, adapted from following manuscript (remaining data unpublished):**

Moonah S, Sanders NG, Persichetti, JK, Sullivan, DJ. Erythrocyte lysis and *Xenopus laevis* oocyte rupture by recombinant *Plasmodium falciparum* hemolysin III. Eukaryot Cell. 2014 Oct;13(10):1337-45. Epub 2014 Aug 22. PubMed ID PMID: 25148832

ABSTRACT

Severe anemia is a hallmark of malaria pathogenesis and contributes significantly to the morbidity and mortality seen in children, but also in pregnant women infected with malaria. Together, clearance of infected and uninfected erythrocytes in conjunction with inhibition of erythropoiesis is thought to be responsible for the dramatic decline in hemoglobin levels to less than 5 g/dL that defines severe malaria anemia. However the host and parasite factors that mediate the processes of uninfected erythrocyte clearance are still under investigation. We hypothesized that a cytolytic protein produced by the *Plasmodium* parasite, such as a hemolysin, might act as a virulence factor and damage uninfected host erythrocytes, contributing to severe malaria anemia.

Initial characterization of PfHlyIII in our lab had demonstrated that recombinant *Plasmodium* hemolysin III (recPfHlyIII) expressed in *E. coli* was capable of binding to erythrocytes and lysing them in a time and temperature dependent manner. Size dependent inhibition of recPfHlyIII-associated hemolysis by osmotic protectants of increasing hydrodynamic radii supported a pore-forming mechanism with recPfHlyIII pores approximated to be 3-3.5 nm in diameter. Furthermore, transfection and integration of a C-terminally GFP-tagged recPfHlyIII into the Dd2attB *P. falciparum* strain resulted in localization of the recPfHlyIII protein to the digestive vacuole of the parasite. Based on these previous findings, we modified our hypothesis to suggest that soluble PfHlyIII in the digestive vacuole of *Plasmodium* could be released upon parasite egress in infected individuals, resulting in damage to bystander erythrocytes, facilitating uninfected erythrocyte clearance and contributing to severe malaria anemia.

For my thesis, I developed the following aims to test our new hypothesis: (1) Demonstrate PfHlyIII forms a functional pore in a heterologous *Xenopus* oocyte expression system, (2) Determine whether soluble PfHlyIII is expressed and present in late asexual blood stages, and (3) Characterize host effects of a *Plasmodium berghei* hemolysin knock-out on severe malaria anemia.

Demonstration of functional pore formation in a eukaryotic system was accomplished by expressing recPfHlyIII in *Xenopus laevis* oocytes, and observing that recPfHlyIII expressing oocytes were sensitive to hypotonic lysis, similar to oocytes expressing human aquaporin 1, a well-described water channel. Furthermore, oocyte rupture was inhibited by the addition of an osmotic protectant, similar to what was seen in previous studies with inhibition of erythrocyte lysis by recPfHlyIII.

We generated and affinity purified rabbit polyclonal antiserum against the eighty-amino acid N-terminal tail of PfHlyIII in order to study native protein expression in the parasite. Using our PfHlyIII-specific antibody to probe parasite lysates, we found that PfHlyIII was expressed in all asexual blood stages as both a soluble and integral membrane protein, with increased expression of the protein throughout the infected erythrocyte maturation. In addition we also found evidence that PfHlyIII may be expressed in gametocyte stages, but is not detectable by immunoblot in the sporozoite stages. Our evidence for native expression in asexual blood stages supports our hypothesis that soluble PfHlyIII could be released upon parasite egress and come into contact with bystander erythrocytes in patient plasma.

We next used two separate approaches to test whether *Plasmodium* hemolysin III contributes to severe anemia, utilizing the murine malaria model. The first approach

involved construction and characterization of a genetic knockout of PbHlyIII (PbHlyIII KO), in order to determine whether PbHlyIII KO parasites lacking hemolysin would be less virulent and result in less anemia compared to WT *P. berghei* infected mice. To test our hypothesis that knocking out PbHlyIII would result in decreased virulence and anemia, we infected Balb/c mice with either WT or PbHlyIII KO *P. berghei* ANKA and monitored the mice for parasitemia, survival and hemoglobin levels to follow the progression of anemia as the disease progressed. To our surprise, the PbHlyIII KO infected mice died 8-15 days *earlier* than WT infected mice, with no significant difference in parasite growth rate between the groups. To confirm this phenotype we generated a separate PbHlyIII KO parasite in the GFP-Luc *P. berghei* ANKA strain and showed that both knockout parasites resulted in earlier death compared to the wild type. However, because the mice infected with the knockout parasite died so early, we were unable to determine whether these mice would be protected from anemia, thus preventing us from using this model to determine whether PbHlyIII plays a role a severe malaria anemia.

The second approach involved immunizing mice against PbHlyIII using a GST-fusion peptide followed by parasite challenge and observing whether mice with antibodies against PbHlyIII would be protected against severe anemia. With the immunization approach we found that mice with the strongest antisera reactivity after PbHlyIII immunization died very quickly, albeit with low parasitemia, and that those with weak sera reactivity were not protected from parasitemia or severe anemia compared to non-immune or the GST-immunized controls. Based on the pathology of the mice, we suspect that the method of immunization and challenge may have resulted in the

development of severe fibrosis and an adverse immunization reaction that resulted in early death. We were unable to measure anemia in these mice due to their early death and thus were unable to resolve the question regarding the role of PbHlyIII in severe anemia using this approach.

While we were unable to provide sufficient evidence to support or reject a role for the *Plasmodium* protein in severe murine malaria anemia, we were intrigued by the fact that knocking out the *P. berghei* hemolysin resulted in increased virulence of the parasite. We decided to further characterize the knockout parasite in order to determine the functional role of hemolysin III for *Plasmodium.* First pursuing the lethality phenotype, we found that the PbHlyIII KO infected mice had slightly higher parasite loads and also hemorrhages in the spleen, as well as some hemorrhages in the brain, which may have contributed to their early death. Furthermore, transmission electron microscopy images of the PbHlyIII KO asexual stage parasites show striking morphological differences, with undulating membranes and extra vacuolar spaces compared to the WT parasites. Further investigation of these alterations may lead to a clearer understanding of the function of hemolysin in the parasite, perhaps as a receptor or transporter. Finally, by following the PbHlyIII KO parasite through the mosquito life cycle we observed a growth defect in the parasite resulting in decreased oocyte number in the mosquito midgut and a large reduction in sporozoite load in the salivary glands. Further investigation of these mosquito stages to determine where the hemolysin protein is required for normal development may further reveal the functional role of this protein in the *Plasmodium* parasite.

Future directions for this project include further study of the mosquito stages of the PbHlyIII KO parasite to determine which step(s) of development between gamete fusion and sporozoite invasion of the salivary glands require PbHlyIII for normal maturation. In addition the hemolysin gene in *P. falciparum* should also be knocked out and the knockout parasite characterized to confirm what we have found in *P. berghei* to also hold true in the human malaria parasite. While we have confirmed by PCR and Southern Blot that we have successfully disrupted the *pbhlyiii* loci in two separate strains, we have not done whole genome sequencing to rule out other genetic changes that may have occurred as a consequence of knocking out the gene encoding hemolysin III in *P. berghei.* Finally, a different immunization approach should be developed to try and answer our initial question of whether *Plasmodium* hemolysin III contributes to severe malaria anemia.

INTRODUCTION

The Complex Etiology and Pathophysiology of Severe Malaria Anemia

As described earlier, malaria infection can result in either uncomplicated or severe disease. Severe malaria can present with a variety of manifestations, including cerebral malaria (convulsions, impaired consciousness), pulmonary edema, jaundice, abnormal bleeding, and severe anemia (1). The WHO defines severe malaria anemia (SMA) as a hematocrit less than 15% or hemoglobin less than 5 g/dL along with a parasite positive bloodfilm, though patients can present with anemia even with low or undetectable parasitemia (1,2). While *P. falciparum* is often associated with the most severe disease, *P. vivax* can also cause severe anemia and results in the removal of a large quantity of uninfected cells despite often low parasitemia (3).

The etiology of SMA is complicated, with additional factors beyond *Plasmodium* infection that can influence anemia status, including infection with other pathogens (helminths or bacteria), vitamin deficiencies (iron or Vitamin D) and genetic disorders (G6PD deficiency,beta or alpha thalassemias) (4–7). Broadly, anemia as a result of malaria infection is due to the removal of infected and uninfected erythrocytes combined with the decrease or inhibition of erythropoiesis preventing red blood cell replenishment. Influencing each of these mechanisms is a complex dynamic of immune pathways and host defense mechanisms which ultimately may protect the host from high parasitemia, but often result in severe symptoms of anemia.

On the one hand, removal of parasitized erythrocytes is anticipated through the destruction of the red cell upon egress of the parasite during the asexual cycle. In addition infected cells may be targeted for antibody-mediated clearance through recognition of

surface proteins or complement deposition, as well as splenic removal of immature ring stages due to reduced deformability (8–11). Some immature ring infected erythrocytes may undergo a process called 'pitting' whereby the parasite is removed in the spleen and the red cell is returned to circulation, though these erythrocytes experience reduced survival because of parasite antigens retained on the surface (11,12). *P. falciparum* mature blood stage parasites express PfEMP1 concentrated on knobs on the surface of the erythrocyte , resulting in cytoadhesion and sequestration of these later stages, essentially protecting them from removal by the spleen, whereas *P. vivax* mature stages are more deformable and can be seen in circulation (11) . Eventually the infected red blood cells are destroyed upon egress of the parasite.

The contribution of uninfected red blood cell (uRBC) clearance to anemia is surprisingly high, with approximately 10 or 34 uninfected erythrocytes removed for every *P. falciparum* or *P. vivax* infected red cell, respectively(13,14). Similar to the removal of parasitized erythrocytes, uninfected cell removal is largely attributed to erythrophagocytosis through a combination of mechanisms including antibody-mediated clearance, complement activation, oxidation and parasite-related senescence (8,9,15–17). Rhoptry-associated proteins from infected erythrocytes have been shown to recognize the surface of uRBCs in a parasitemia-dependent manner which can result in opsonisization followed by phagocytosis or complement activation (9). Other data suggests that the loss of CR1 and CD55 from the surface of uRBCs due to parasite product derived immune complex formation and removal may result in increased complement component C3b deposition and increased removal of uRBCs (18–22). One murine malaria study suggests a factor extrinsic to either erythrocytes or antibodies is responsible for uRBC clearance.

SCID mice, devoid of T or B cells, developed less anemia than wild type Balb/c or nude mice (lacking T cells only), but transferring serum from infected Balb/c mice to infected SCID mice did not result in increased clearance rates, signifying an antibody-independent clearance mechanism (23). In a separate study, red blood cells transferred from mice experiencing severe malaria anemia into healthy animals did not undergo similar clearance, suggesting that these cells were not permanently or sufficiently changed to warrant their removal. In the same study, depletion of macrophages and CD4+ T cells reduced anemia in semi-immune mice, supporting the idea that a hyperphagocytic response might be responsible for enhanced clearance of uRBCs, though the trigger for this response is still not well-defined (24). A very recent study confirms the role of activated CD8+ T cells in the splenic clearance of parasitized erythrocytes related to an increase in the removal of uRBCs (25). Finally, deformability may also play a role in uRBC clearance, as uRBCs have been shown to have reduced deformability in patients with SMA (26). Overall, there is evidence for increased erythrophagocytosis in hosts experiencing SMA, but the triggers for this response remain undefined and appear to be antibody-independent.

In the face of such aggressive removal of both infected and uninfected erythrocytes, one would expect the replacement mechanisms to be equally vigorous. However erythropoiesis has been shown to be disrupted in SMA patients, preventing the production and development of new erythrocytes to replace those which have been removed through the afore-mentioned processes. In a murine malaria model, impaired responses to erythropoietin during reticulocytosis (27) and decreased expression of the transferrin receptor CD71on red blood cells (28) were demonstrated to prevent

maturation of erythroid precursors, suggesting potential downstream effects of *Plasmodium* infection on erythropoiesis. Interestingly, the parasite product hemozoin has been shown to affect erythropoiesis on multiple levels including: inhibiting macrophage activation which could disrupt erythroblastic islands, preventing production of reticulocytes (29,30),stimulating the production of endoperoxides by macrophages which may affect growth of erythrocytes (30–34), and finally suppressing erythropoietin induced proliferation of erythroblasts (35). Parasites may also contribute directly to dyserythropoeisis by infecting and destroying erythroblasts, as has been shown in the case of *P. vivax* (36).

Strongly correlated with the inhibition of erythropoiesis in SMA is immune dysfunction and imbalance, often skewed toward inflammation and Th-1 type mechanisms. For example, multiple studies have shown relationships between high tumor necrosis factor alpha (TNF-α) to interleukin ten (IL-10) ratios and SMA (37–40). Other research suggests cerebral malaria and SMA are influenced by separate TNF-α promoter alleles (41), while one study points toward uniquely programmed monocytes and T cells as the source of the skewed TNFα:IL-10 ratio (39). The origins of imbalanced inflammatory responses may return full circle to parasite-produced hemozoin which can be phagocytosed and influence macrophage activation and production of downstream inflammatory mediators (42,43). Other immune mediators such as migration inhibitory factor (MIF) and stem cell growth factor (SCGF) have also been suggested as contributors to severe anemia and malaria pathogenesis through suppression of erythropoiesis, though the MIF studies have been done in mice and not proven in humans (44–47). While inhibition of erythropoiesis is obviously detrimental for the host, one

modeling study suggests that decreasing production of new red blood cells may prevent even more severe anemia in the host by reducing the number of cells the parasite can invade and destroy (48).

Unfortunately current treatment options for SMA are limited to antimalarial drugs and transfusion for very severe cases. However transfusions may not be beneficial and also carry the risk of HIV transmission. Furthermore, drug treatment of uncomplicated malaria in endemic areas does not have a significant impact on hemoglobin levels, and prevention of infection or prophylaxis is really the only way to prevent severe malaria anemia and other acute pathologies of the disease (49).

It is evident from the complexity of SMA and the paucity of treatment options available that further study of SMA is urgently needed in order to better understand the mechanisms and identify and test potential interventions. Animal models of severe malaria and specifically severe malaria anemia have their own limitations. The severe malaria mouse model of *P. berghei* ANKA infected C57Bl/6J mice is often used to mimic cerebral malaria (CM), but is not a good model for SMA as the mice progress quickly to CM and develop acute rather than chronic anemia, due more to parasite destruction of infected cells than loss of uRBCs (30,50). Balb/c mice infected with the same strain of parasite can develop anemia over a longer period of time, but development of high parasitemia may make it difficult to differentiate between anemia due to parasite egress and anemia due to uRBC clearance. However, it has been shown that anemia is not always correlated with the peak parasitemia in both mouse and *Aotus* monkey malaria models (30,51), which is in agreement with a human study with evidence for a higher correlation with anemia and 90-day parasitemia history, rather than current parasite

burden (2). Specifically a study of *P. chabaudi* infection in Balb/c mice demonstrates that the percentage of infected erythrocytes rather than total parasite number correlated more strongly with a decrease in total circulating erythrocytes, suggesting that available uninfected erythrocytes are the limiting factor in these infections (52). Semi-immune animal models may the best way to study the contribution of uRBC removal in human SMA, where animals have similarly low levels of parasitemia but continued clearance of uninfected red blood cells and development of severe anemia (30,51,53).

Overall it appears that severe malaria anemia is a complex pathology of *Plasmodium* infection, and that the immune response to parasite infection and products may result in downstream effects on erythropoiesis as well as enhanced erythrophagocytosis of infected and uninfected erythrocytes. The exact parasite-related mediators of clearance and dyserythropoeisis have yet to be clearly identified.

Pore-forming Toxins and Hemolysins

Cytolytic proteins have been described for many pathogenic microorganisms and are often responsible for invasion and egress of the pathogen into and out of the host cell, or are classified as toxins or virulence factors with pathogenic effects for the host. Bacterial cytolysins in particular make up a diverse class of proteins, differing by size, secondary structure, target cell, pore diameter, and mechanism of pore-formation/lysis. In general bacterial cytolysins can be divided into either alpha-helical or beta-barrel pore-forming toxins resulting in the formation of homogenous (consistently the same composition) or heterogenous (range in number of monomer components) pores, or in some cases disruption of the membrane without formation of a discrete lesion. The size of pores formed by many of the cytolysins ranges from small (0.5-5 nm) such as the pore formed by *E. coli* hemolysin A, to the much larger pores (20-100 nm) like those formed by the cholesterol dependent cytolysins like perfringolysin O (54). Beta-barrel toxins make up the majority of bacterial cytolysins and tend to form larger pores, while the alpha-helical toxins tend to form smaller pores.

Mechanism of pore-formation and/or membrane disruption has been postulated and in some cases confirmed for different classes of bacterial cytolysins, and can depend on the target cell and availability of certain ligands, such as cholesterol, glycans, lipids, membrane proteins, or GPI-anchored proteins. For many cytolysins the general mechanism of action includes binding to a target ligand or receptor followed by oligimerization and insertion into the membrane to form an aqueous pore (55). Thiol-activated cytolysins such as streptolysin O depend on cholesterol for the initial binding to target membranes, and some studies suggest that binding to cholesterol triggers a

conformational change followed by self-association between monomers, resulting in a oligomeric transmembrane pore (56). *Staphylococcus aureus* alpha-toxin is known to form homogenous hexameric small pores 2-3 nm in diameter and does not require a specific ligand to bind cells, though the toxin does show preferential binding to rabbit erythrocytes compared to human erythrocytes (54). *Clostridium perfringens* produces a cholesterol-dependent cytolysin, perfringolysin O which upon binding to the membrane, triggers formation of heterogenous oligomers containing 35-50 monomers which shift to reveal beta-hairpins, ultimately resulting in insertion of a 25-30 nm beta-barrel pore into the target membrane (57). Some cytolysins disrupt membranes without forming a discrete pore, as has been described for *E. coli* hemolysin A, an alpha-toxin which transiently disrupts membrane bilayers by inserting into the outer membrane monolayer and disrupting the bilateral tension of the lipid bilayer (58).

Consequences of pore-formation in target cells aside from direct cytolysis, include efflux of potassium and influx of calcium which can trigger downstream events including inflammatory responses as well as apoptosis, leading to the destruction of tissue and loss of endothelial or epithelial barriers (55). Pore-forming toxin induced barrier disruption can be the result of direct damage to endothelial or epithelial layer integrity or a downstream consequence of increased inflammation as a result of a toxin-induced pores (55). Ultimately barrier disruption can have lethal outcomes for an infected individual, as toxins like *S. pneumoniae* pneumolysin can destroy lung tissue with a convergence of apoptosis and inflammation, resulting in pulmonary pneumonia (55).

Plasmodium falciparum Hemolysin III: A Pore-forming, Hemolytic Protein Localizing to the Digestive Vacuole

While considering potential mediators of severe malaria anemia, our lab discovered that *Plasmodium* encodes a putative hemolysin III protein, with structural homology to hemolysin III proteins previously described in *Bacillus cereus* (59–61) and *Vibrio vulnificus* (62). *Plasmodium* hemolysin III is part of the hemolysin III superfamily of integral membrane proteins ranging from bacterial proteins with previously described hemolytic activity (59,60,62) to eukaryotic proteins with seven predicted transmembrane domains acting as functional receptors for ligands including progestin and adipo-Q (PAQR) (63). Phylogenetic analysis based on protein sequence data of representative proteins in the hemolysin III superfamily (Figure 2.1) suggests the *Plasmodium* hemolysin III proteins are more closely related to the bacterial hemolysins than the eukaryotic PAQR proteins.

The *Bacillus* and *Vibrio* hemolysin III proteins with similar predicted secondary structure and topology to *Plasmodium* hemolyin III have been previously characterized. Expression of *B. cereus* hemolysin III in *E. coli* resulted in preparation of crude extracts with hemolytic activity but difficulty in attempts to further purify the protein. However hemolysis and osmotic protectant experiments using the crude extract supported a pore-forming mechanism for *B. cereus* HlyIII with a temperature dependent binding and 3-3.5 nm pore-formation step with temperature-independent lysis (59,60). The hemolysin III of *V. vulfnificus* shares 48% identity to *B. cereus* HlyIII, and expression of recombinant *V. vulnificus* HlyIII in *E. coli* also results in hemolytic activity, with insertional inactivation of the gene decreasing the pathogenicity of the bacteria in mice (62).

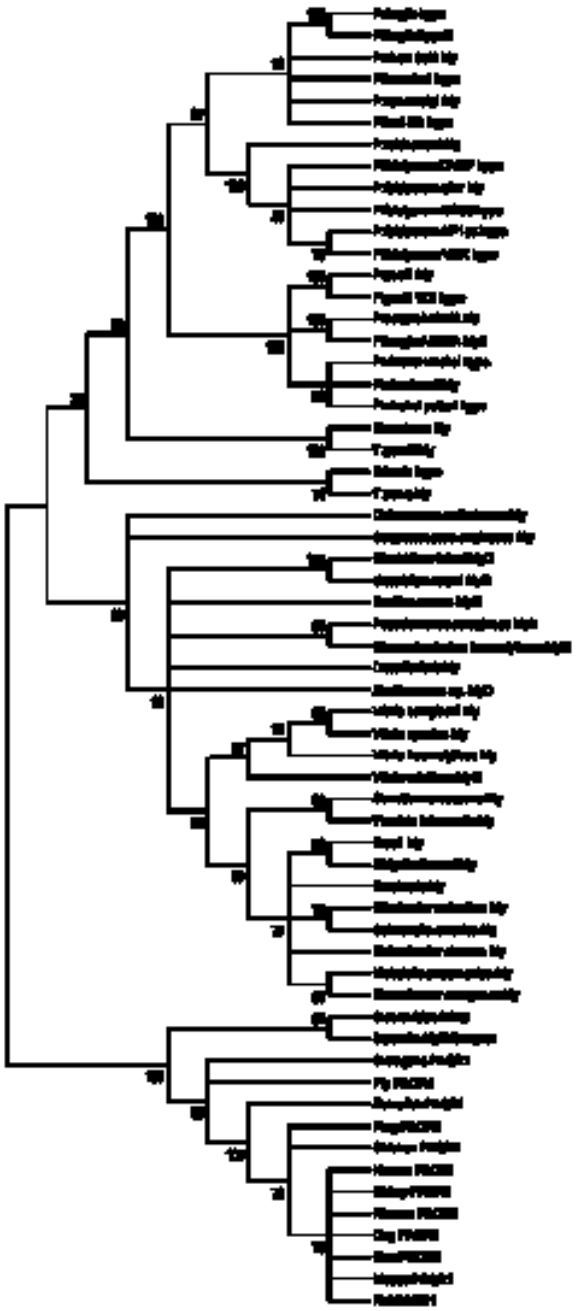

Figure 2.1 Hemolysin III Superfamily Phylogenetic Tree of Representative Proteins including *Plasmodium* hemolysins*,* apicomplexan homologs, bacterial hemolysins, and eukaryotic PAQR proteins. Alignments were made using Muscle and neighbor joining was used to construct the phylogenetic tree with bootstrapping; cutoff 70%.

Multiple sequence alignment of all of the above sequences used in the phylogenetic tree reveals conserved residues including a serine and histidine, as well as a conserved motif, DxxxIxxxIxG (Figure 2.2). These residues were conserved across all species with the exception of one bacteria protein and one yeast protein, suggesting that they are important for protein structure/function. In addition all of the HlyIII superfamily of proteins have seven predicted transmembrane domains with similarly predicted topology as represented in Figure 2.3.

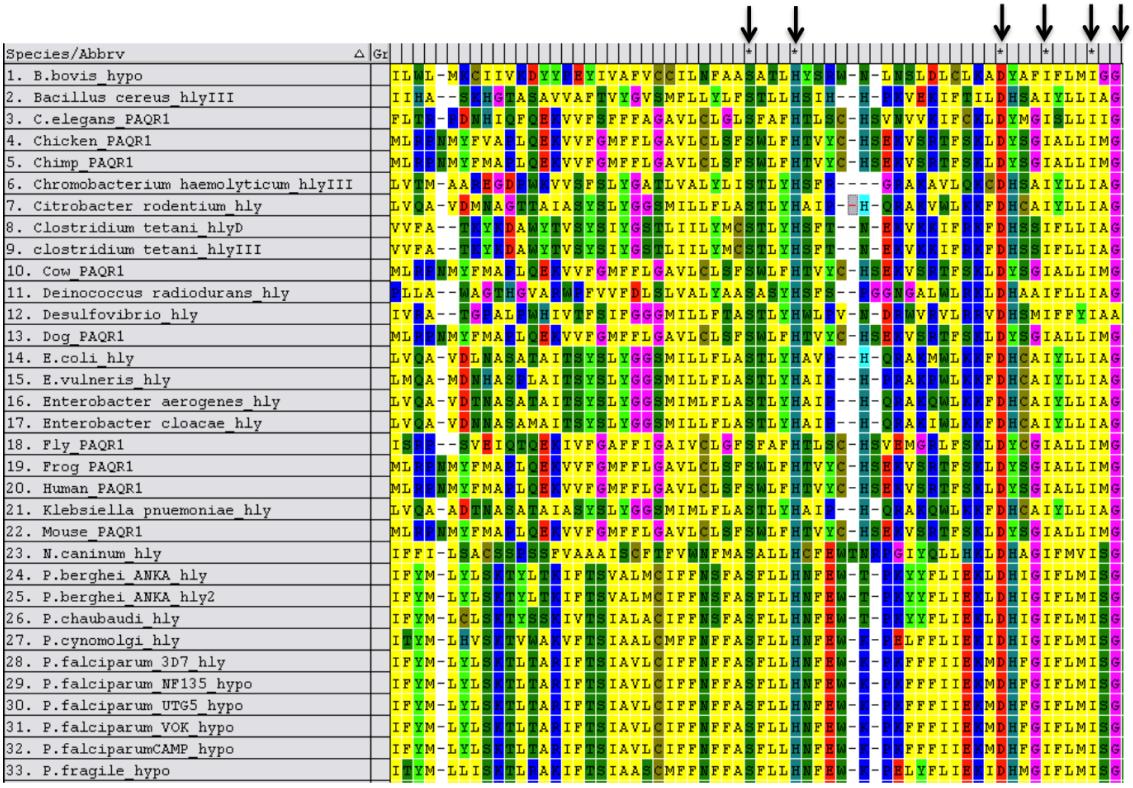

Figure 2.2 Protein sequence alignment of HlyIII superfamily proteins reveals conserved residues and motif across eukaryotes and prokaryote sequences. Arrows point to conserved residues including a serine and histidine, as well as a conserved motif aspartic acid, isoleucine, isoleucine, glycine (DxxxIxxxIxG).

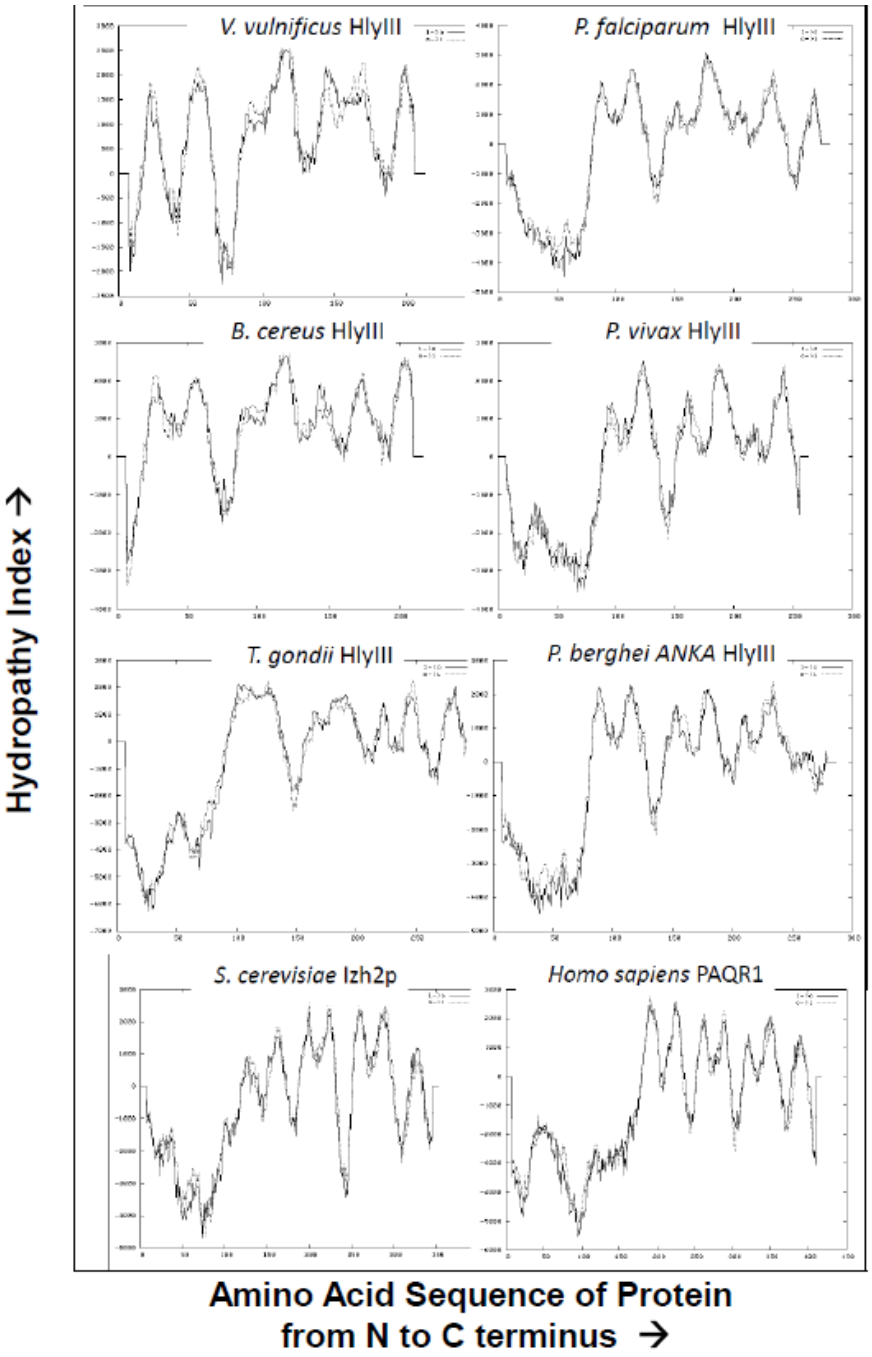

Figure 2.3 Transmembrane domain predictions generated by TMpred for various HlyIII superfamily proteins including *Plasmodium, Toxoplasma, Vibrio*, and *Bacillus* hemolysins and eukaryotic homologs including a yeast protein and human PAQR. Predicted hydrophobic regions have positive hydropathy scores (>0).

Of note, all the representative eukaryotic proteins in the HlyIII superfamily, regardless of function, have an additional N-terminal domain not found in the bacterial hemolysins. Thus, even though the overall sequences of *Plasmodium* hemolysins are more similar to the bacterial hemolysins, structurally, *Plasmodium* hemolysins share conserved N-terminal domains with the other eukaryotic members of the family that may be important for function.

The eukaryotic proteins such as *S. cerevisiae* Izh2p and various PAQR proteins all share homology and unique motifs and are classified as part of the PAQR protein family. Several studies have suggested three subclasses within this family based on differing motifs and physical characterisitics: Class I, Class II, and Class III (64,65).

Class I proteins are restricted to eukaryotes and include yeast proteins such as Izh2p as well as the human adiponectin receptors (PAQR1 and 2). Yeast Izh2p, a homolog to human adiponectin receptors, is an important mediator in cellular metabolism, and has been recently shown to play a role in iron, phosphate and zinc homeostasis, with downstream implications for lipid metabolism (66). In humans, adiponectin is a polypeptide hormone that regulates metabolism, and deficiencies in adiponectin can result in insulin resistance and type 2 diabetes (67). Izh2p has been shown to respond to progesterone in a G-coupled protein receptor (GCPR) independent manner, confirming a functional role as a membrane progesterone receptor that does not rely on GCPRs for function (64), and other studies suggest a role for sphingolipids as downstream effectors of Izh2p (65).

Class II proteins are also progesterone receptors but have a unique eighth transmembrane domain that is C-terminal to the last PAQR domain. Recent studies

confirm the PAQR proteins as functional hormone or steroid membrane receptors, including demonstration of progestin receptors in zebrafish and adiponectin receptors in yeast (68,69), suggesting these proteins are important for downstream signaling after interaction with a hormone or steroid.

Class III proteins include the eukaryotic and prokaryotic proteins with homology to hemolysins which may or may not predict hemolytic functions for these proteins (65). *Plasmodium hemolysin* III falls into the class III protein category and phylogenetically appears more similar to the bacterial hemolysins, despite having the additional N-terminal tail reminiscent of the class I and class II proteins.

Initial work in our lab was done to characterize a putative *Plasmodium falciparum* hemolysin III by expressing a recombinant, his-tagged PfHlyIII in *E. coli* followed by characterization of pore-forming activity of the purified lysate in hemolytic assays as well as immunofluorescent microscopy demonstrating binding of the protein to the surface of erythrocytes in the presence of an osmotic protectant, polyethylene glycol. From this studies we concluded recombinant PfHlyIII was a pore-forming protein that could bind to and lyse erythrocytes in a time and temperature dependent manner, forming pores of approximately 3.5 nm in diameter. Temperature studies suggested a multi-step mechanism of binding followed by insertion into the membrane, similar to what has been described for other hemolytic proteins. Furthermore, glibenclamide, a channel inhibitor, was also able to partially inhibit hemolysis of erythrocytes when incubated in addition to recPfHlyIII lysate. In a separate approach, C-terminal GFP-tagged PfHlyIII was overexpressed in the Dd2attB strain of *P. falciparum* and the PfHlyIII-GFP was localized to the digestive vacuole of the parasite. Interestingly parasites overexpressing PfHlyIII-

GFP were observed to exhibit a swollen food vacuole phenotype. Work from these studies was previously published (70).

While we had demonstrated that recombinant *Plasmodium* hemolysins were functional cytolytic proteins, we were ultimately interested in whether or not they could be virulence factors in malaria, contributing to severe malaria anemia. Specifically we hypothesized that *Plasmodium falciparum* hemolysin III might contribute to damage and destruction of bystander erythrocytes if the protein was released in soluble form upon egress of the parasite from the erythrocyte and subsequent rupture of the digestive vacuole (Figure 2.4).

Thus the aims of my thesis project were the following: (1) heterologous expression of recombinant PfHlyIII in *Xenopus* oocytes followed by confirmation of pore-formation in eukaryotes, (2) determining whether soluble PfHlyIII is expressed and present in late asexual blood stages, and (3) determining the virulence of *Plasmodium* hemolysin III in a mouse model of malaria.

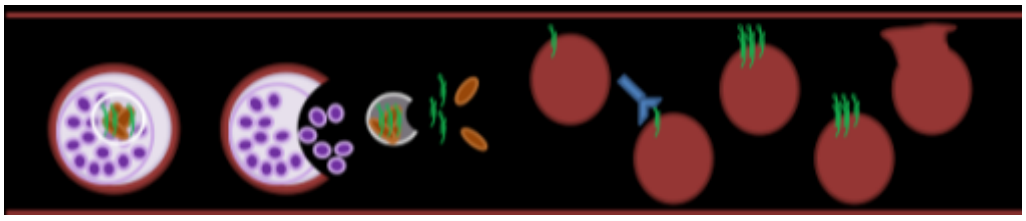

Figure 2.4 Hypothesis: soluble PfHlyIII may damage bystander red blood cells upon parasite egress and rupture of the food vacuole, where recombinant PfHlyIII-GFP has been localized

MATERIALS AND METHODS

Phylogenetic Tree Construction

The evolutionary history was inferred using the Neighbor-Joining method (71). The optimal tree with the sum of branch length = 10.66815406 is shown. The percentage of replicate trees in which the associated taxa clustered together in the bootstrap test (500 replicates) are shown next to the branches (72). The evolutionary distances were computed using the Poisson correction method (73) and are in the units of the number of amino acid substitutions per site. The analysis involved 60 amino acid sequences. All positions containing gaps and missing data were eliminated. There were a total of 142 positions in the final dataset. Evolutionary analyses were conducted in MEGA6 (74).

Xenopus Expression

Plasmid construction: pGS21a_PfHly3-flag with an Nhe site was constructed using the QuikChange Lightning site-directed mutagenesis kit (Agilent Stratagene #210518-5), digested with EcoRI and NheI and ligated into pXβG-ev1-myc to produce pXβG-ev1-myc-PfHly3-flag. We received pXβG-ev1-myc and pXβG-ev1-hAQP1 cDNA as a generous gift from Dr. P. Agre.

Expression in Oocytes: Capped cRNA was produced using *in vitro* transcription from either the pXβG-ev1-myc-PfHly3-flag or pXβG-ev1-hAQP1 plasmid templates, linearized with XbaI, using T3 RNA polymerase and the RNeasy minikit (Qiagen #74104). *Xenopus laevis* oocytes generously donated by Dr. C. Montell were defolliculated and injected with 25-44 ng of cRNA or 50 nl of DEPC-treated water (diethyl pyrocarbonate), followed by incubation at 16 °C for 3-5 days in OR3 medium.

Oocytes were collected 72, 96 and 120h post-injection for Western Blot analysis and swelling assays, described below.

Western Blot analysis: 10 oocytes per treatment were pooled into 200 µl of ice cold lysis buffer (20 mM Tris-HCl, pH 7.5, 140 mM NaCl, 2% Triton X-100, 1x Protease Inhibitors- Sigma Fast Protease Inhibitor Cocktail Tablet EDTA free) and incubated on ice for 30 minutes. Oocytes were homogenized by pipetting samples repeatedly and centrifuged at 4500 x g for 15 minutes at 4°C to removed yolk and cellular debris. The supernatant was transferred to a new tube and incubated on ice for 30 minutes, with occasional vortex. The sample was spun at 15,000 x g to remove insoluble materials and the supernatant was stored in SDS loading buffer at -80°C. Samples were heated for 10 minutes at 95°C and cooled on ice, then run on an SDS-PAGE gel (BioRad Mini-PROTEAN 4-20% TGX Gel, # 456-1093) at 100V for 2 hours. Proteins were then transferred to a nitrocellulose membrane and probed with 10 µg/ml anti-Flag M2 produced in mouse (Sigma F3165) in 5% milk in TBS-T, 1:5,000 anti-*myc*-HRP produced in mouse (Invitrogen R951-25), anti-AQP1 B-11 produced in mouse (Santa Cruz sc-25287), or anti-beta actin produced in mouse (AbCam 8224). HRP-conjugated anti-mouse antibodies produced in goat (IgG+IgM (H+L) Jackson Lab 115-035-068) were used for myc, hAQP1, and beta actin blots, followed by ECL.

Swelling Assays: Method modified from Preston, G. M., Carroll, T. P., Guggino, W. B. & Agre, P. (1992) Science 256 **,** 385-387. Briefly, 5-6 oocytes per group were transferred to a small petri dish of water (hypotonic) and monitored with videomicroscopy at room temperature for swelling and rupture over a time course of 0-60 minutes. Still pictures were taken at 0, 1, 5, 10, 15, 30, 45, and 60 minutes and the

number of intact oocytes was determined based on the number of oocytes which did not rupture in water after each time point.

Recombinant GST and MBP Fusion Protein Expression and Purification, anti-PfHly III antibody production and affinity purification, and Western Blot assays with GSTF80AA competition.

Plasmid construction and GST fusion protein expression and purification: The first 80 amino acids of PfHly III were expressed as a glutathione *S*-transferase (GST) fusion protein (GSTF80AA) by cloning a 240-bp insert encoding the codon-optimized N-terminal 80 amino acids into the pGEXT vector (parent pGEX-4T-3 with inserted Tev protease sequence, gift of Prigge lab, Supplementary Figure 1). Primers for expression from optimized genomic template were as follows:
forward, 5'- GAATTCAATGGAATTTTACAAAAACTTC-3'
reverse, 5'- GAATTCCTAAGCTTGCCGCGAAACAGGGTTTTG-3'. Expression of the GST fusion protein was conducted in BL21*RIL cells in LB broth plus ampicillin and chloramphenicol induced with 1 mM isopropyl-D-thiogalactopyranoside (IPTG) at an optical density at 600 nm (OD600) of 0.6 and incubated for 10 h at 20°C. The GSTF80AA fusion protein was purified after high-pressure cell homogenization (EmulsiFlex C5 cell disruptor; Avestin; 100 MPa) in lysis buffer (50mM Tris, pH 8.0, 1% Triton X 100, 150mM NaCl, 10mM DTT, DNAseI 10 µg/µL, $MgCl_2$ 5 mM, Sigma Protease Inhibitor 1X), followed by centrifugation, and incubation of supernatant with glutathione-Sepharose 4B resin (GE Healthcare), followed by elution with 10 mM glutathione. Similar conditions were used the express and purify recombinant GST fused to the *P. berghei* and *P. chabaudi* hemolysin N-termini.

Primers for these constructing the respective expression constructs were as follows:

Pb80AA forward: 5' – GAATTCAATGGGGAGGTATTATGAATGC – 3'

Pb80AA reverse: 5'-GAATTCCTAAGCTTTCCTCTCAGCAGCGTTTTTTCATG - 3'

Pc80AA forward: 5'- GAATTCAATGATAGGATATTATGAAACC– 3'

Pc80AA reverse: 5'- GAATTCCTAAGCTTTCCTCTCAATAATGTCGCTTC – 3'

Plasmid construction and MBP fusion protein expression and purification: Separately, a maltose binding protein (MBP) construct was also made using a new PCR insert: forward 5'- CGCCATGGAAATGGAATTTTAC – 3' and reverse 5' AGCGGAT CCTCAGCCGCGAAACAG -3' cloned into the *Nco*I and *Bam*HI sites of the MBP-tev-pRSF plasmid (gift from Bosch lab, Supplementary Figure 2), producing a plasmid encoding MBP-F80AA. The MBP-F80AA fusion protein was expressed in LB plus kanamycin and 0.2% glucose, induced as described above for the GST fusion protein, and purified using amylose resin (NEB catalog no. E8021L), eluted with 10 mM maltose.

Anti-PfHlyIII antibody production, purification and verification: Purified GSTF80AA was used to immunize a rabbit at Cocalico Biologicals, and preimmune serum, test bleeds, and the final bleed were received and tested by Western Blotting. The MBPF80AA protein was used for testing of anti-PfHly III antibodies as well as for affinity purification involving coupling the MBPF80AA fusion protein to an *N*-hydroxy-succinimide (NHS)-activated HiTrap column (GE Healthcare), running the antiserum over the column for 1 h, washing with binding buffer (0.05 M NaH2PO4, 0.15 NaCl, 0.01MEDTA), and eluting with 0.1Mglycine, 0.15 M NaCl, pH 2.6. Antibody responses were determined by Western Blot analysis as described above with antiserum concentrations at 1:10,000 and affinity-purified test bleed 2 (APTB2) at 1:1,000. The

GSTF80AA fusion protein was used in competition for native or recombinant PfHly III antigen by preincubating APTB2 anti-PfHly III antiserum (20 _l, 0.34 mg/ml with majority of protein present as bovine serum albumin [BSA] from purification) with 100_l of GSTF80AA fusion protein (0.35 mg/ml), at an approximately 1:50 ratio in 1 ml of blocking buffer (5% milk in PBS-Tween 0.1%) for 1 h, followed by dilution to 20 ml for Western Blot analysis.

PfHlyIII knockout (KO) and single crossover disruption (SXO) constructs

The *pfhly3* (PF3D7_1455400) targeting plasmid designed for double homologous recombination was constructed by cloning regions -1615bp to -811bp (5' arm) and +1104bp to +1952bp (3' arm) with respect to the *pfhly3* initiation codon into *SpeI/AflII* and *EcoRI/AvrII* sites respectively in the pCC1D plasmid (gift from Jacobs-Lorena lab, Supplementary Figure 3), modified from the pHHT-FCU plasmid (75).

PCR primers were:

5' arm forward: 5'- actagtCATGTCCTCTTTTTGATTCACAT – 3'

5' arm reverse: 5'- cttaagTTGGTAAA ATATAAATTGTCCTCATTT – 3'

3'arm forward: 5'- gaattcCGTGGGAATCCCT GAATAAA – 3'

3' arm reverse: 5'- cctaggATGCAATGTTTG AGTAAAAGAAAA – 3'.

Sequencing primers were:

5'arm forward: 5'- CTATGGAATACTAAATATATAT CCAATGGCCCC – 3'

5'arm reverse: 5'- CAAAATGcttaagTTGGTA AAATATAAA TTGTCCTC – 3'

3'arm forward: 5' – CAGAATACCCAGGTGTTCTCTCTGATG – 3'

3'arm reverse: 5'- CGGTGTGAAATACCGCACAGATGCG – 3'

The *pfhly3* (PF3D7_1455400) targeting plasmid for single crossover (SXO) disruption was constructed by cloning region +71bp to +740bp with respect to the *pfhly3* initiation codon into the *AflII* site in the pCC1S plasmid (gift from Prigge lab, Supplementary Figure 4).

Primers for homology region were:

SXO forward:

5'-GCCGGGcttaagGGGTAGTACAAAAATTGATGATAATGAAATTGCG -3'

SXO reverse: 5'- GAGCTCcttaagGGCTTTTTCACAGAATATATA ACTGCTCC – 3'

Sequencing primers were:

pCC1S forward: 5'- CGAACATTAAGCT GCCATATCCttaattaaGTCG – 3'

SXO insert reverse: 5'- GGCTTTTTCACAGAAT ATATAACTGCTCC – 3'

PbHlyIII genetic knockout construct

The *pbhly3* (PBANKA_131910) targeting plasmid designed for double homologous recombination was constructed by cloning regions -834bp to -283bp and +973bp to +1487bp with respect to the *pbhly3* initiation codon into the *ClaI/SbfI* and *EcoRI/XbaI* sites respectively in the pL0001 plasmid (gift from Jacobs-Lorena lab, originally obtained through the MR4 as part of the BEI Resources Repository, NIAID, NIH: *Plasmodium berghei* pL0001, MRA-770, deposited by AP Waters, Supplementary Figure 5).

Parasite strains and transfection

The *P. falciparum* 3D7, *P. berghei* ANKA, and *P. berghei* GFP-Luc strains were used for gene targeting and were obtained through the MR4 as part of the BEI Resources Repository, NIAID, NIH: *Plasmodium falciparum* 3D7, MRA-102, deposited by DJ

Carucci; *Plasmodium berghei* ANKA, MRA-311, deposited by TF McCutchan; *Plasmodium berghei* (ANKA) 676m1cl1, depositied by CJ Janse and AP Waters: Genetically modified parasite of clone cl15cy1 of the ANKA strain; expresses GFP-luciferase fusion. This line has been selected by flow (FACS) sorting, based on GFP fluorescence. Stable transfectant with pL1063 (MRA-852); this line does not contain a drug-selectable marker. The transgene is integrated into the genome by double cross-over integration and therefore parasites should not lose the transgene and will remain fluorescent throughout life cycle. Gametocyte, ookinete, oocysts, sporozoite and liver development is comparable to wildtype P. berghei (ANKA) (76).

For *P. falciparum* transfection, 400 microL of 50% hematocrit uninfected erythrocytes were suspended in 5 ml of cold Cytomix (120 mM KCl, 0.15 mM CaCl2, 2 mM EGTA, 5 mM MgCl2, 10 mM K2HPO4/KH2PO4, 25 mM HEPES) and centrifuged at 500 x g for 5 min. The 200 microL RBC pellet was resuspended in 400 microL of targeting construct (65 µg DNA) suspended in cold Cytomix, and transferred to a 0.2 cm BioRad Gene Pulser cuvette for electroporation at 0.31 kV, 950 µF, infinity resistance, with time constants of 14.2 (KO) and 14.5 (SXO) and voltage of 307 mV. Electroporated RBCs were placed immediately on ice and washed with cold RPMI and then added to 2 ml of 10% synchronized trophozoites at 1% hematocrit and 10 ml of complete media (RPMI 1640, 10% human serum, .005% hypoxanthine, 25 mM HEPES, 0.26% $NaHCO_3$). Cultures were maintained at 5% CO_2, 5% O_2, 90% N_2 at 37 °C. Drug selection with WR92100 began 1 day post transfection and was maintained with media changes every day for 7 days and every other day for 51 days with no positive parasite selection detected.

For *P. berghei* transfection, one donor mouse was injected with frozen stock of desired parasite culture and parasites were harvested by cardiac puncture at 5-10% and used to infect 5 donor mice per transfection with 10^6 iRBCs. When donor mouse parasitemia reached 0.5-3%, parasites were harvested by cardiac puncture, washed and cultured overnight in 150 ml RPMI supplemented with 20% fetal calf serum and 0.36 mg/ml gentamcyin at 36.5°C with gently shaking (50 rpm). Mature schizonts were purified using a Nycodenz gradient (Histodenz, Sigma D2158) with 10ml of 55% nycodenz PBS dispensed beneath culture suspension followed by centrifugation at 450 x g, no brake for 25 min. Schizonts were collected from the interface, pelleted and washed with media from the column supernatant, pelleted again and counted, using between $5x10^7$ and $1x10^8$ schizonts per transfection. Schizonts were resuspended in 100 μL nucleofector solution (Mouse T Cell Nucleofector Solution and Supplement, Lonza VPA-1006) with 20 μg of linear dna targeting construct and electroporated in an Amaxa Nucleofector using program U-033, followed by immediate addition of 100 μL of culture media and injection into the tail vein of a per-warmed Swiss Webster mouse. Drug selection with .07 mg/ml pyrimethamine was started one day post transfection and was maintained 4-7 days until positively selected parasites reached 5% parasitemia. Drug-selected parasites were genotyped by PCR and knockouts were confirmed by Southern Blot.

PCR Analysis

Primers for confirming integration and genetic knockout were:

5’ Integration forward: 5’ – CCCTTATGGTATTCCCCTATCC – 3’

5’ Integration reverse: 5’ – GCTTTCCTCTTAATTCACTTGG – 3’

3’ Integration forward: 5’ – AGATGGCTGTCTAGCGGAAA – 3’

3’ Integration reverse: 5’ – ATAGCACCACGGAAAGTGCT – 3’

Phusion High Fidelity DNA polymerase (NEB M0530S) was used for genotyping using 1-2 µL whole blood from the tail vein of infected mice as the DNA template. The 50 µL reaction contained 1X buffer, 0.2 mM dNTPs, 0.5 µM primers, 3% DMSO and 1U of Phusion Taq Polymerase. Cycling parameters were 98°C (0:30), 35 cycles of 98°C (0:10), 55°C (0:30), 68°C (1:30), followed by 68°C (6:00).

Southern Blot Analysis

A digoxigenin (DIG) labeled probe specific to the 3’ homology region used for targeting the genome, +973bp to +1487bp with respect to the *pbhly3* initiation codon, was synthesized by PCR, using DIG-11-dUTP (Roche Applied Science 11209256910) and 3’ homology arm primers (see above). Next, genomic DNA from WT and HlyIIIKO *P. berghei* ANKA was isolated and subjected to restriction enzyme digest with *HindIII* overnight (10 µg DNA with 5U of enzyme/µg DNA). The genomic DNA digest was then run on a 0.8% TAE agarose gel at 65 mV for 6 hours. The DNA was transferred to a nitrocellulose membrane using downward transfer overnight followed by crosslinking the DNA to the membrane. Following incubation of the membrane in hybridization buffer for 1 hr at 42°C, the DIG-labeled probe was denatured (95°C 5min) and added (300 ng in 25 µL PBS) to the membrane and hybridized for overnight at 42°C. The membrane was washed 2x for 5min with low astringency buffer at room temperature followed by two 20 minute high astringency washes at 65°C. The DIG nucleic acid kit was used for detection (Roche Applied Science 11175041910). Briefly, the membrane was washed in maleic acid buffer and blocked at room temperature for 1 hour with blocking reagent and probed

with anti-digoxigenin 1:10,000 for 30 min, room temperature followed by 3 washes for 15 min and addition of CSPD for detection.

Immunization studies

Recombinant glutathione-S-transferase (GST) or GST fused to the *P. berghei* hemolysin III N-terminus (GSTB80AA) was expressed and purified from *E. coli* as described above. Mice (6 week old, female, Balb/c) mice were prebled (100 µL) and serum was collected (37°C 1hr, 4°C O/N, centrifuge 13,000 rpm 15min 4°C to collect supernatant) and stored at -20°C for baseline serum reactivity analysis. The following day mice were divided into four groups: a non-immunized control group (n=10), GST alone, 25 µg (n=10), GSTB80AA, native, 50 µg (n=10) and GSTB80AA, denatured, 50 µg (n=5) and immunized according to their group with antigen emulsified in 200 µL complete Freund's adjuvant (CFA). Each group received three boost immunizations of the same antigen in incomplete Freund's adjuvant (IFA) on days 18, 32, and 54 post priming.* The non-immunized control group did not receive adjuvant or antigen at any point. Animals underwent a test bleed (100 µL) on day 45 and day 74 and serum reactivity was assessed by Western Blot of whole cell *P. berghei* ANKA parasite lysate run on an SDS-PAGE gel and transferred to a nitrocellulose membrane, probed with 1:1000 antiserum in blocking buffer. Based on serum reactivity, mice were divided into 7 test groups to be challenged with either WT *P. berghei* ANKA or HlyIII KO *P. berghei* ANKA:

Cage	# mice	Immunization Status	Challenge
A	5	Non-immune	WT
B	5	GST alone control	WT
C	5	GSTB80AA – strong responder	WT
D	4	GSTB80AA – weak responder	WT
E	5	Non-immune	HlyIII KO
F	5	GST alone control	HlyIII KO
G	3	GSTB80AA – weak responder	HlyIII KO

Following challenge, mice were monitored for survival, parasitemia and hemoglobin levels using either complete blood count analysis of 50 µL tail blood or 2 µL blood into 0.5 mL Drabkin's reagent dispensed in triplicate and absorbance read at 405 nm.

*Note: All emulsions except the final boost were made by vortexing the antigen and adjuvant, while the final emulsion was made using the syringe emulsifying technique which gave a more stable emulsion.

Histology

Mice were sacrificed and perfused with 25 mL PBS and organs were subsequently removed, rinsed in PBS and fixed in Z-fix (Anatech LTD, #174) and submitted for paraffin processing and staining of sections with Giemsa or H&E to Johns Hopkins Medical Laboratories Reference Histology.

RNA isolation, cDNA preparation and qPCR analysis

Tissues were snap-frozen and stored at -80°C until time for processing. 1mL of Trizol was added to each sample and then samples were placed on ice to thaw briefly. Samples were then transferred to homogenizing tubes and homogenized for 20-30 seconds until frothy and homogenous. The samples were then incubated at room temperature for 5 min followed by addition of 200 µL chloroform and shaking to mix

thoroughly. Samples were centrifuged at 12,000 x g for 15 min at 4°C, the upper phase was transferred to a fresh Eppendorf tube and an equivalent volume of 70% ethanol was added to each tube. Samples were further purified using a PureLink RNA minikit (Life Technologies 12183018A).

Reverse transcription was performed using 1 µg RNA as template with DNAse treatment for 15min followed by addition of 50 µM random hexamers and 0.8 mM dNTPs, 5 min incubation at 65°C. After being chilled on ice, a reverse transcription mix (1X RT buffer with $MgCl_2$, 10 mM DTT, 40U RNAsin (Promega N2611)) was added along with 1 µL MuLV reverse transcriptase (Life Technologies N8080018) and samples were incubated at room temperature for 10 min, 42°C for 50 min, 70°C for 15 min, chilled on ice for 1 min and stored at -80°C.

Multiplex qPCR with primers specific for *P. berghei* ANKA 18s rRNA were used to quantify parasite load in the following mouse tissues: brain, lung, liver, heart, kidney and spleen. Mouse hypoxanthine guanine phosphoribosyl transferase (hprt) functioned as the housekeeping gene. Primers were as follows:

18s forward: 5'- GGAGATTGGTTTTGACGTTTATGCG-3'

18s reverse: 5'- AAGCATTAAATAAAGCGAATACATCCTTA-3'

HPRT forward: 5'- TCCCAGCGTCGTGATTAGC-3'

HPRT reverse: 5'- CGGCATAATGATTAGGTATACAAAACA-3'

Taqman probes (Integrated DNA Technologies, Coralville, IO):

18s: 5' 6-FAM/ZEN-CAATTGGTTTACCTTTTGCTCTTT-3'IBFC

HPRT: 5' Cy5-TGATGAACCAGGTTATGACC-3'BHQ-2

Reaction conditions for qPCR (384 well plate, 10 μL reaction): 1X IQ Multiplex Power Mix (BioRad, Hercules, CA), 0.2 μM 18s primers, 0.5 μM HPRT primers, 0.2 μM Taqman probes, and 3 μL cDNA.

Mosquito Infections and Analysis

Anopheles stephensi mosquitoes were maintained on a 10% sucrose solution at 27°C and kept on a 12 hour light/dark schedule. Day 3-5 old mosquitoes were fed on two subsequent days for 7-10 minutes per day on *P. berghei* ANKA WT or *P. berghei* ANKA HlyIIIKO infected mice with 5-10% parasitemia and 1-2% gametocytemia. Ten days post feeding mosquito midguts were dissected and stained with 0.1% mercurochrome and oocysts were counted. Eighteen days post feeding mosquito salivary glands were removed and sporozoites isolated and counted. In two experiments, naïve mice were exposed to infected mosquito bite prior to salivary gland dissection. Inoculated mice were monitored for parasite patency in the blood by Giemsa stained bloodfilm.

RESULTS

Recombinant PfHlyIII Expression and Hypotonic Lysis in *Xenopus* Oocytes

While recombinant PfHlyIII had been previously expressed and partially purified as a bacterial lysate and shown to have hemolytic properties (70), we were interested in expressing a recombinant *Plasmodium* hemolysin protein in *Xenopus laevis* oocytes in order to confirm heterologous protein expression and pore-formation in a eukaryotic system.

We produced an RNA transcript encoding a myc and flag-tagged recombinant PfHlyIII (myc-PfHlyIII-flag, Figure 2.5A and B) and then injected the RNA into *Xenopus* oocytes along with water injection control and human aquaporin 1(hAQP1) RNA as a positive control for pore formation. Protein expression was monitored by Western Blot from 72 to 120 hours post-injection and myc-PfHlyIII-flag and hAQP1were expressed at all time points (Figure 2.5C).

Next we conducted swelling assays based on those previously described (77) by placing oocytes in a hypotonic solution and monitoring oocyte swelling and lysis using videomicroscopy. Oocytes expressing myc-PfHlyIII-flag swelled and ruptured in a similar manner to hAQP1-expressing oocytes compared to little or no rupture by water-injected controls (Figure 2.6 A and B), suggesting the recombinant hemolysin was able to form pores and disrupt the membrane of the oocyte, making them susceptible to hypotonic lysis. Polyethylene glycol (PEG) can function as an osmotic protectant and has been used to determine pore-size of other hemolysins and pore-forming proteins in other studies (60). Addition of PEG of increasing molecular weight or hydrodynamic radii

resulted in decreased hypotonic lysis of myc-PfHlyIII-flag expressing oocytes (Figure 2.7), further validating pore-formation and an approximate size between 3-6 nm.

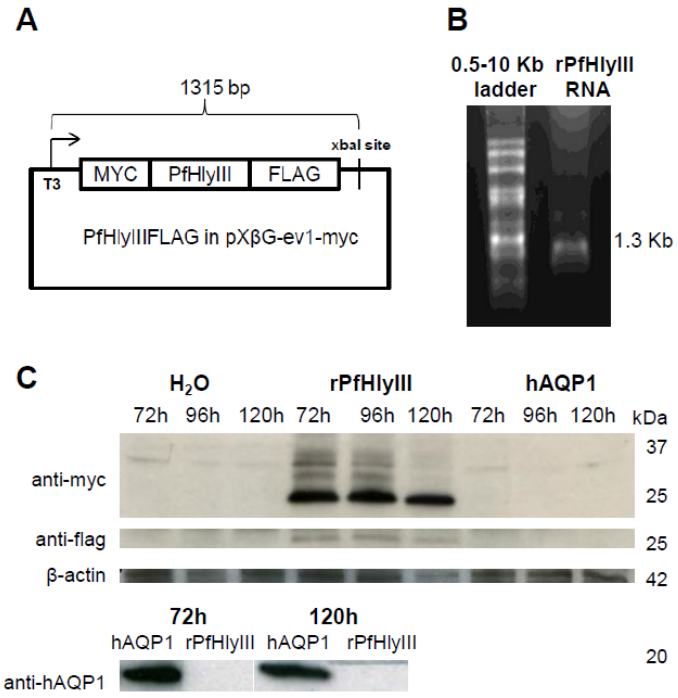

Figure 2.5 *In vitro* transcription of recombinant *P. falciparum* hemolysin III (rPfHlyIII) RNA and expression of recombinant PfHlyIII protein in *Xenopus* oocytes. (A) DNA template for *in vitro* transcription of myc-PfHlyIII-flag RNA. (B) myc-PfHlyIII-flag transcription product on 1% agarose, 6.6% formaldehyde denaturing gel. (C) Protein expression of 10 pooled *Xenopus laevis* oocytes per injection treatment (DEPC H_2O, rPfHlyIII, or human aquaporin 1 (hAQP1)).

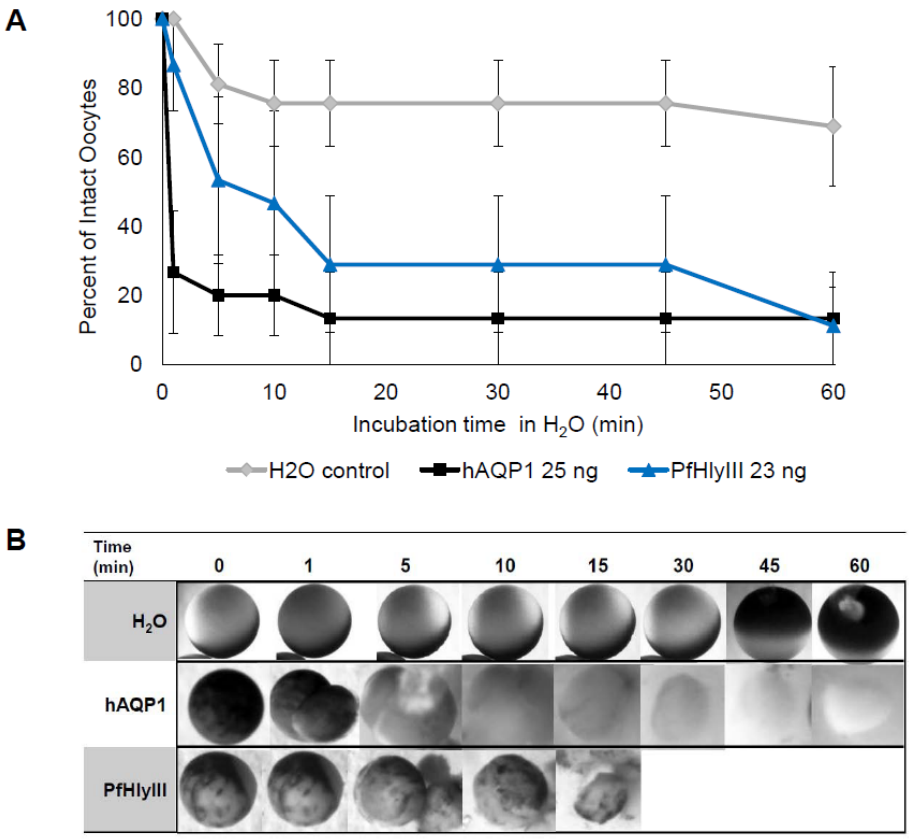

Figure 2.6 Hypotonic lysis of rPfHlyIII expressing oocytes compared to hAQP1 and water injected controls upon incubation in water. (A) Quantification of intact oocytes over time, expressed as mean percent intact oocytes with SEM, average of three independent experiments using 5-10 oocytes per group in each experiment. (B) Time lapse photography of representative oocytes from each treatment.

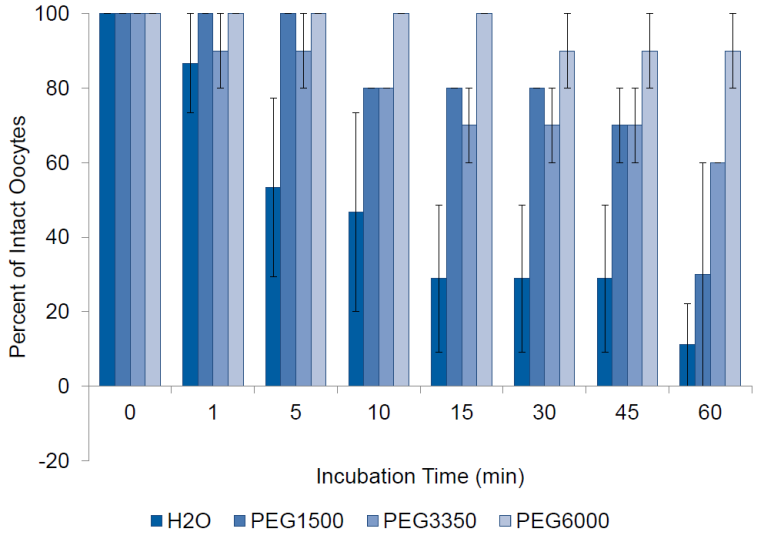

Figure 2.7 Addition of osmotic protectants prevents hypotonic lysis. Polyethylene glycol of increasing hydrodynamic radii protected rPfHlyIII expressing oocytes from hypotonic lysis in a buffer dependent manner: (water, 30 mM PEG1500, PEG3350, or PEG6000). Results are expressed as mean percentage of intact oocytes with SEM, from three independent experiments.

Native HlyIII Expression Studies in *P.falciparum*

According to data from various studies in the PlasmoDB genome database, the transcriptome of *P. falciparum* strains including 3D7 show a cyclical expression of *PfHlyIII* mRNA, with peak mRNA levels at late trophozoite stages (78). We wanted to characterize the PfHlyIII protein expression pattern in asexual blood stages to determine whether soluble PfHlyIII could be present in the clinically relevant stages of *Plasmodium* infection and potentially be released upon parasite egress. Furthermore we hoped understanding protein expression of PfHlyIII would help us further elucidate the function of the protein in the parasite.

In order to look at protein expression, we chose the first eighty amino acids of the PfHlyIII N-terminus as an epitope (Figure 2.8) as this region lacks any predicted transmembrane domains and is sufficient in length to be antigenic, whereas the remaining peptide is predicted to have seven transmembrane domains and is not targetable.

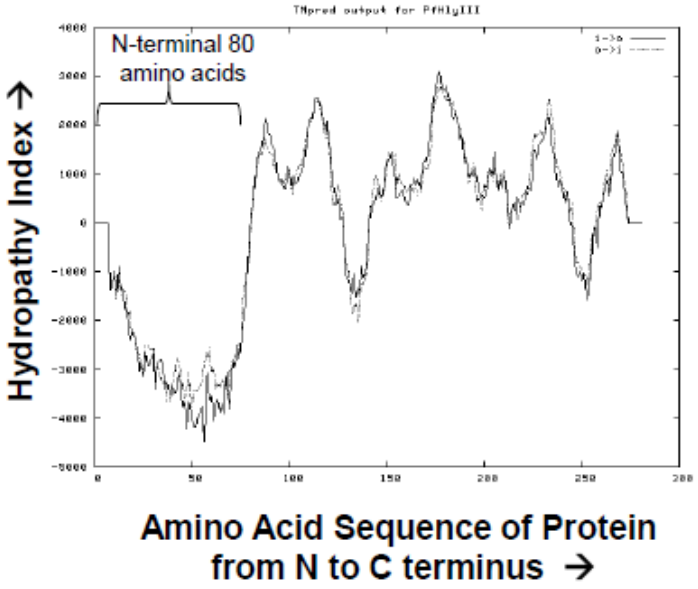

Figure 2.8 TMpred-generated prediction of transmembrane regions I to VII in PfHly III**,** N-terminal 80 amino acids indicated with no transmembrane domains.

Next we designed constructs with glutathione-S-transferase (GST) or maltose binding protein (MBP) fused to the codon-optimized 80 amino acid N-terminus of PfHlyIII (Figure 2.9A, 2.10A), and also produced GST constructs using the *P. berghei* and *P. chabaudi* HlyIII homologous N-terminal regions (Figure 2.9 B,C). Using these constructs we expressed and GST and MBP fusion peptides in *E. coli* and purified them from whole cell lysates (Figure 2.9 C, D and 2.10 C).

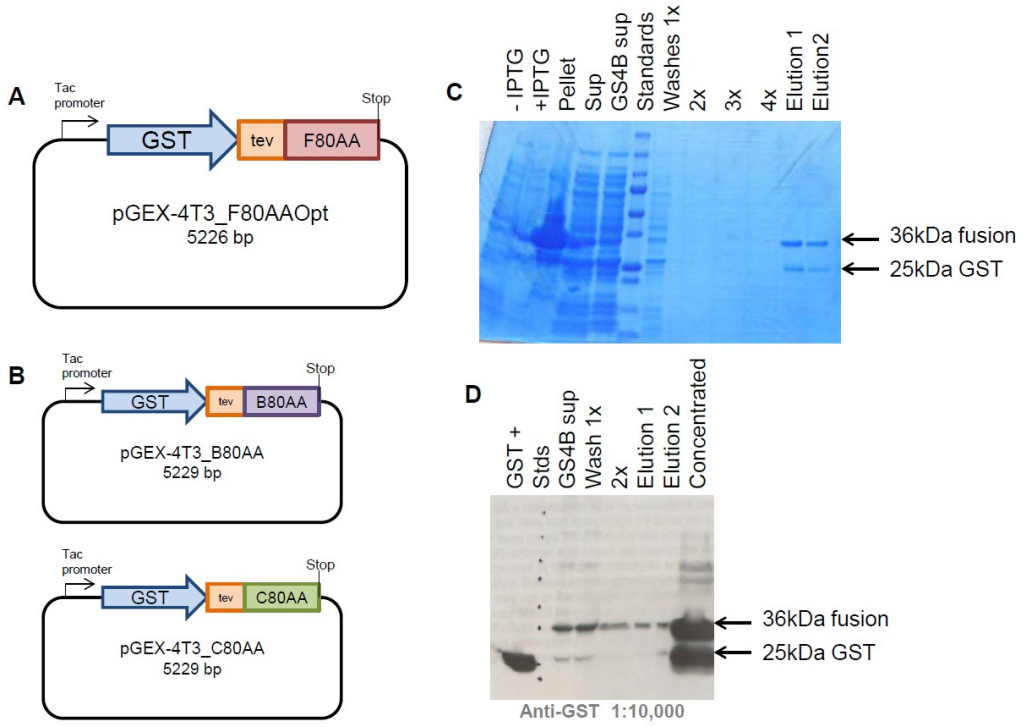

Figure 2.9 Plasmid construction and expression of GST- hemolysin III 80 amino acid N-terminus fusion proteins for *P. falciparum, P. berghei,* and *P. chabaudi*. (A) GST-expression construct for *P. falciparum* codon-optimized 80 amino acid N-terminus. (B) Expression constructs for *P. berghei* (B80AA) and *P. chabaudi* (C80AA). (C) SDS-PAGE analysis of GSTF80AA expression and purification using Glutathione Sepharose 4B beads, resulting in the purified 36 kDa fusion protein and free GST (25 kDa). Gel stained with Coomassie Brilliant Blue. (D) Western Blot of purification fractions using anti-GST specific antibodies at 1:10,000, confirming GST-tagged product.

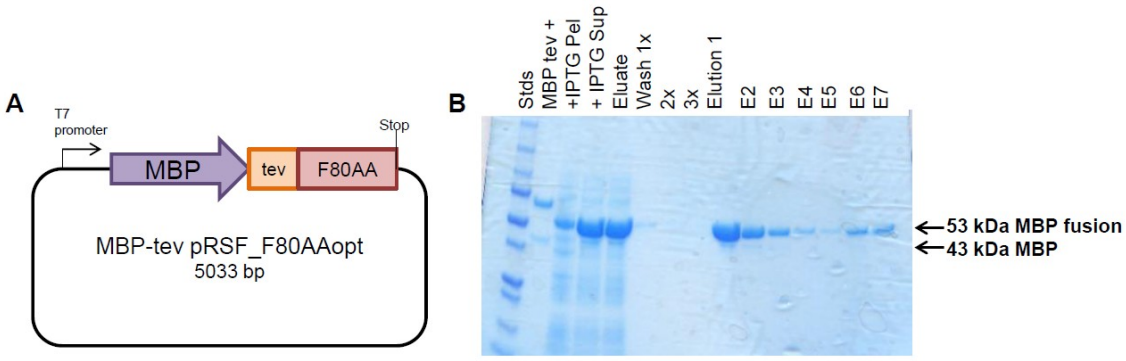

Figure 2.10 Plasmid construction and expression of MBP-tagged hemolysin III 80 amino acid N-terminus fusion protein for *P. falciparum.* (A) MBP-expression construct for *P. falciparum* codon-optimized 80 amino acid N-terminus. (B) SDS-PAGE analysis of MBPF80AA expression and purification using Amylose Resin, Eluting with 10 mM Maltose, resulting in the purified 53 kDa fusion protein and free MBP (43 kDa). Gel stained with Coomassie Brilliant Blue.

Having generated a *P. falciparum* HlyIII antigen, we immunized a rabbit (through Cocalico Biologicals), generating rabbit polyclonal antiserum, followed by verification and affinity purification using the MBPF80AA fusion peptide. Affinity purification of test bleed two (APTB2) using the MBPF80AA increased the specificity of the antiserum, resulting in clear detection of the recombinant MBPF80AA peptide (Figure 2.11A) and also detection of a unique band in *P. falciparum* asexual blood stages (25 kDa, Figure 2.11B). The 25 kDa band was no longer recognized after competition with the GSTF80AA antigen, confirming specificity for PfHlyIII (Figure 2.11B, last panel).

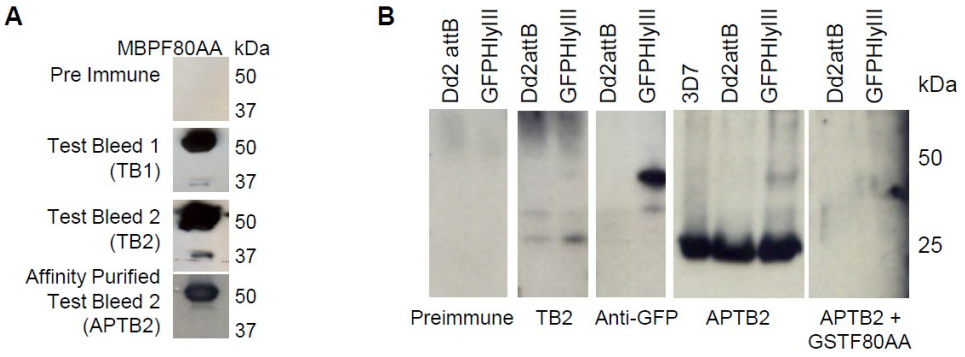

Figure 2.11 Generation of rabbit polyclonal antiserum against the 80 amino acid N-terminus of PfHlyIII, affinity purification and detection of PfHlyIII in asexual blood stages. (A) Test bleed antiserum recognizes recombinant MBP-tagged PfHly III N-terminal 80-amino-acid peptide (MBPF80AA, 53 kDa) compared to the preimmune serum. (B) Affinity-purified test bleed 2 (APTB2) recognizes a unique band of less than 30 kDa in three strains of P. falciparum: 3D7, Dd2attB, and Dd2attB transfected with PfHly III-GFP; anti-GFP and APTB2 both recognize a unique higher-molecular-weight product in the PfHly III-GFP transfected strain. Competition with antigen ablates the unique band.

With the appropriate tool in hand, we used the affinity purified antiserum to determine stage specific expression of native PfHlyIII in asexual blood stages. Using synchronized parasite lysates at different time points (Figure 2.12A), we found that PfHlyIII was expressed in increasing amounts throughout the life cycle, with peak levels of expression at late trophozoite and schizont stages (Figure 2.12B). Furthermore, PfHlyIII was detected in both pellet and supernatant fractions (Figure 2.12C, Figure 2.13A), suggesting the protein is present in both membrane bound and soluble forms in all asexual blood stages.

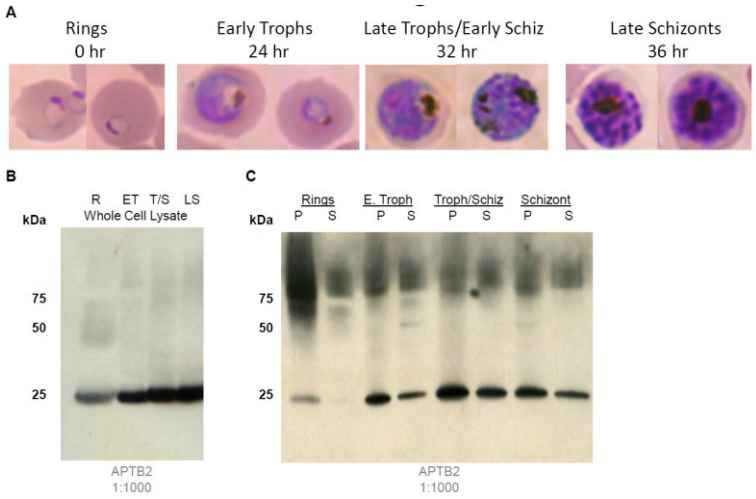

Figure 2.12 Asexual Stage Specific Expression of Native PfHlyIII. (A) Light microscopy images of synchronized asexual blood stages of *P. falciparum,* 3D7 strain, Giemsa stain: Ring (R), early trophozoite (ET), late trophozoite/early schizont (T/S) and late schizont (LS). Whole cell parasite lysates from these cultures were used for the detection of native parasite PfHlyIII by Western Blot using rabbit polyclonal antiserum (APTB2), with 2.5 µg of total protein loaded per well. (B) Native PfHlyIII (25 kDa) was detected in all asexual blood stages.(C) Native PfHlyIII was present in pellet (P) and supernatant (S) fractions in all stages.

Treatment of the *P. falciparum* pellet fraction with a variety of solvents (Figure 2.13B) resulted in complete breakdown of the peptide in strong base (100 mM NaOH), very little release of the membrane bound form in a weak base (100 mM Na_2HCO_3), a moderate amount of solubilized protein with non-ionic detergent (1% Triton-X) and complete solubilization of the membrane bound protein with an ionic detergent (1% sodium dodecyl sulfate). These results confirm native PfHlyIII is present as both a soluble and integral membrane protein in all asexual blood stages, including mature schizonts.

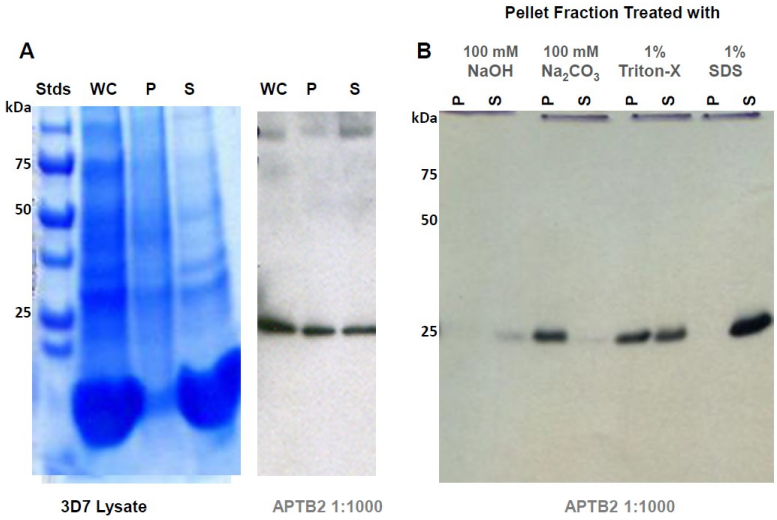

Figure 2.13 Native PfHlyIII is expressed in asexual stages in soluble form and also integrally associated with the membrane**.** (A) Whole cell lysate (WC), pellet or membrane fraction (P) and supernatant or cytosolic fraction (S) were run on an SDS-PAGE denaturing gel and either stained with Coomassie Brilliant Blue (left panel) or probed for native PfHlyIII expression by Western Blot (right panel). (B) Pellet fractions were treated with different solvents to test association of protein with the membrane, including 100 mM NaOH, 100 mM Na2CO3, 1% Triton-X, and 1% SDS.

In addition to looking PfHlyIII expression in asexual blood stages, we were also interested in determining expression levels of PfHlyIII in gametocytes and mosquito stages, specifically sporozoites to determine whether this protein was important for transmission stages of the parasite. In gametocyte cultures collected days 11, 14, and 17 post initiation of gametocytogenesis (days 4, 9, and 12 post treatment with N-acetylglucosamine), PfHlyIII was found to be expressed in early stages as a 25 kDa and 36 kDa protein (Figure 2.14, first panel). However the asexual stage specific merozoite surface protein was also present in the earlier gametocyte preparations, despite purification attempts (Figure 2.14, second panel), suggesting that there was some asexual stage protein carried over in the gametocyte lysate, which may indicate that the 25 kDa band in the APTB2 probed blot may be from asexual stages. Nevertheless, there is a unique 36 kDa band present in the gametocyte prep that was not observed in blots from asexual stages, suggesting PfHlyIII may be expressed in gametocytes in a longer form (closer to the predicted molecular weight of 33 kDa).

In a separate experiment, *P. falciparum* sporozoites were purified from salivary glands and probed for PfHlyIII expression. Even at the highest concentration of sporozoite whole cell lysate (100,000 sporozoites), PfHlyIII was not detected, compared to a high abundance circumsporozoite protein (CSP) that was detected at even very low sporozoite numbers (Figure 2.15).

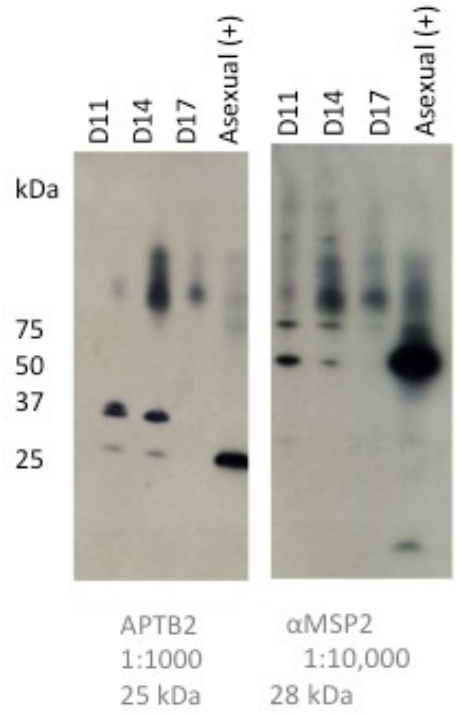

Figure 2.14 Expression of PfHlyIII in early, middle and late stage *P. falciparum* gametocytes. Gametocytes were harvested at day 11, day 14, and day 18 post-gametocytogenesis.

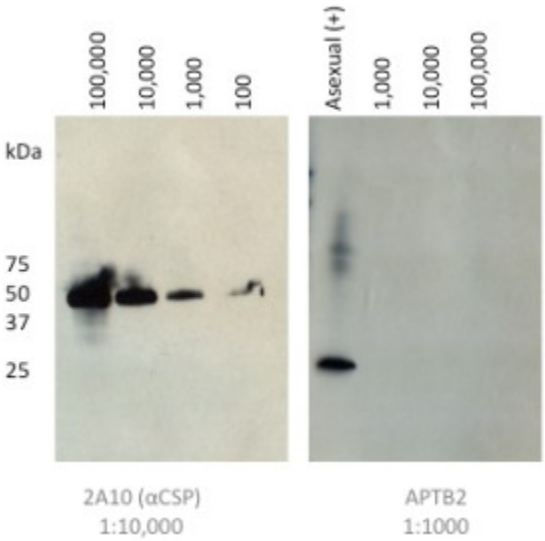

Figure 2.15 Circumsporozoite (CSP) and PfHlyIII expression in *P. falciparum* sporozoites whole cell lysates diluted serially from 100,000 to 100 sporozoites.

In order to address the question of whether *Plasmodium* hemolysin III is a virulence factor in the parasite that can contribute to pathogenesis in the host, we turned to a murine malaria model, Balb/c mice infected with *P. berghei* ANKA. We chose this model due to the chronic nature of the disease and the ability to measure the progression of anemia in these mice. We wanted to determine whether the *P. berghei* homolog of PfHlyIII, PbHlyIII, was influential in the development of anemia in this mouse model.

We took two approaches to address the question of hemolysin associated virulence. The first involved knocking out the PbHlyIII gene and comparing the virulence and development of anemia in mice infected with either wild type or PbHlyIII KO *P. berghei*. We predicted that parasites lacking hemolysin III would be less virulent and cause less anemia in mice. Our second approach involved immunizing mice against PbHlyIII and then challenging them with parasites to determine whether antibodies against PbHlyIII could protect mice from anemia.

Genetic knockout studies in *P. berghei* and attempts in *P. falciparum*

For genetic knockout of *pbhlyiii,* we modified the pL0001 plasmid containing the TgDHFR selection cassette by adding two homology arms, one including part of the 5' UTR of *pbhlyiii* and the other the end of the gene and part of the 3' UTR. These homology regions were chosen in order to completely disrupt the gene, essentially knocking it out upon successful homologous recombination (Figure 2.16A and B). We were successful in obtaining *pbhlyiii* knockouts in two different parasite strains. We originally knocked out PbHlyIII in the WT *P. berghei* ANKA parasite (PbHlyIII KO1), and later repeated the knockout using the *P. berghei* ANKA GFP-Luc parasite (PbHlyIII KO2) in order to strengthen the case for our knockout phenotype. Upon clonal dilution we obtained at least one clone from each knockout transfection. The modified loci were verified for positive integration by PCR (Figure 2.17) and Southern blotting (Figure 2.18).

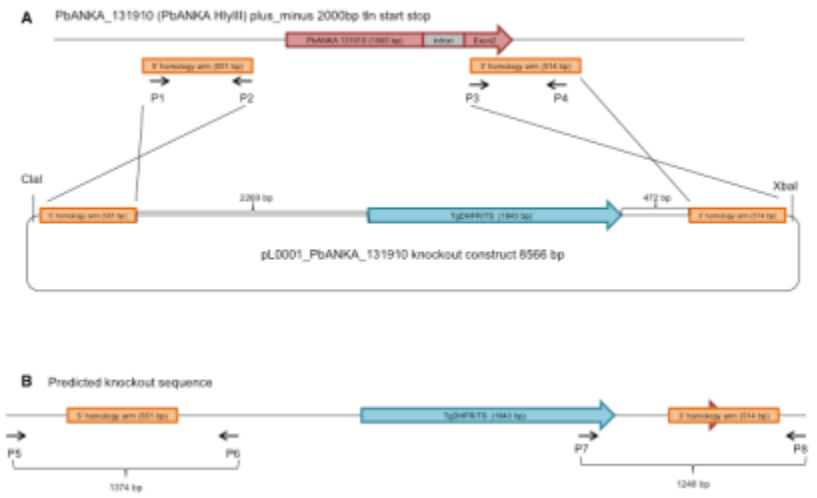

Figure 2.16 Genetic knockout plasmid (A) and predicted locus modification (B) for *P. berghei* HlyIII.

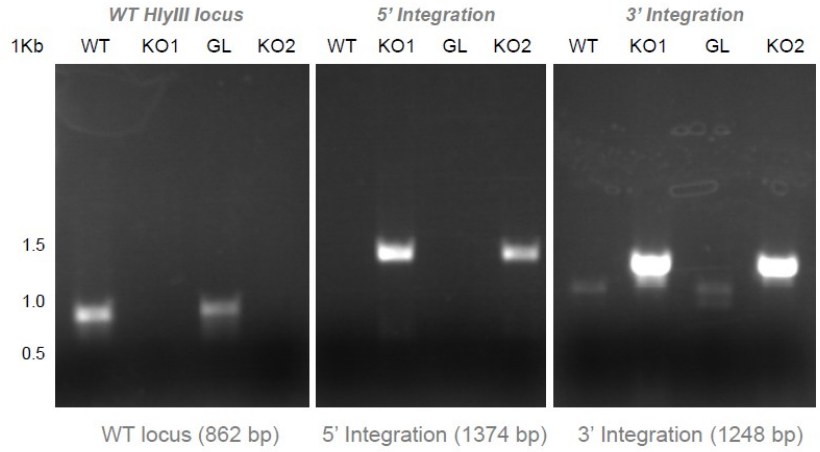

Figure 2.17 PCR verification of drug cassette insertion and disruption of *PbHlyIII* locus from genomic DNA isolated from wild type (WT), PbHlyIII KO1 (KO1), GFP-luciferase (GL), or PbHlyIII KO2 (KO2) *P. berghei* parasites.

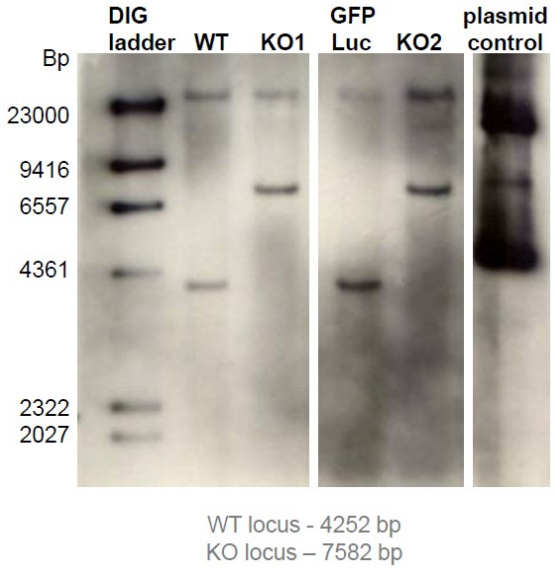

Figure 2.18 Southern Blot verification of drug cassette insertion and disruption of *PbHlyIII* locus using hindIII digest of genomic DNA from wild type (WT), PbHlyIII KO1 (KO1), GFP-luciferase (GL), or PbHlyIII KO2 (KO2)*P. berghei* parasites and a digoxigenin labeled probe (3' homology arm used in the targeting construct).

In order to gain a deeper understanding of the functional role of the *Plasmodium falciparum* HlyIII protein and compare it to the *P. berghei* HlyIII knockouts, we also designed plasmids for genetic knockout or disruption of the hemolysin III gene in *P. falciparum* (Figure 2.19). Unfortunately our attempts to disrupt or knockout the hemolysin-coding gene in *P. falciparum* were unsuccessful, with no parasites detected up to 60 days post drug-selection. Due to the low efficiency and long schedule of *P. falciparum* knockout strategies at the time, we decided to focus on characterization of the PbHlyIII KO parasites.

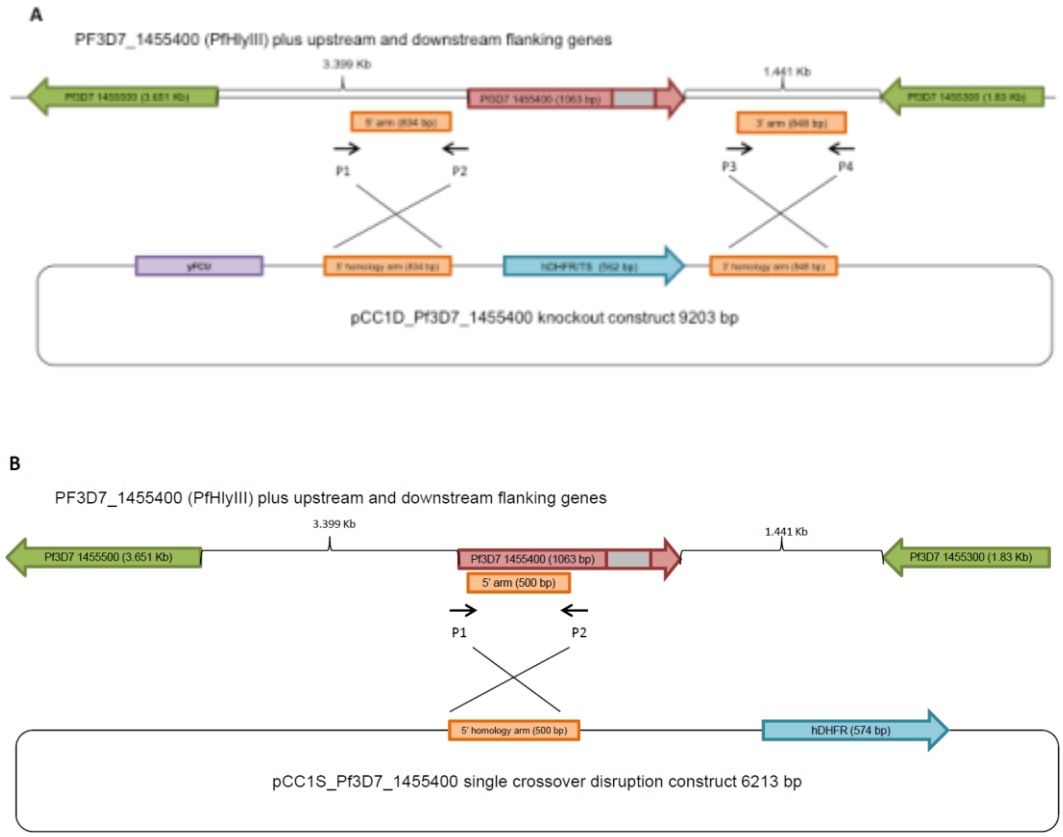

Figure 2.19 Genetic knockout (A) and single crossover disruption plasmid designs for *P. falciparum* hemolysin III.

Virulence and Anemia in PbHlyIII KO vs WT P. berghei infected mice

In our first experiment comparing PbHlyIII KO1 versus WT *P. berghei* infected Balb/c mice we were surprised to find that the knockout parasite was more virulent than the wild type, killing mice between 7-15 days post infection compared to 22-25 days for the wild type infected mice (Figure 2.20A). We did not find a difference in parasite growth rate as both parasitemia and parasite densities were comparable between both WT and PbHlyIII KO1 infected groups (Figure 2.20B and C). Finally, because all but one KO1 infected mouse died before the mice developed anemia (day 14), we were unable to measure a significant difference in anemia between the two groups. For the single KO1 infected mouse that survived until day 30, we noticed a slightly higher hemoglobin level, but were unable to find a statistically significant difference (Figure 2.20D).

We were interested in determining whether this virulence phenotype would be repeated in other mouse backgrounds, so we also compared the WT and PbHlyIII KO1 parasite infections in C57/Bl6 mice. In two separate experiments we found no difference in survival in these mice (Figure 2.21A and C), but did notice a significant difference in parasite growth rate, with PbHlyIII KO1 parasites multiplying more quickly than WT *P. berghei* (Figure 2.21B and D).

While the virulence phenotype was intriguing and suggestive of further study, due to the early death of PbHlyIII KO1 infected mice, we were unable to compare significant differences in anemia in Balb/c mice, and thus turned to an alternative approach, immunization against PbHlyIII.

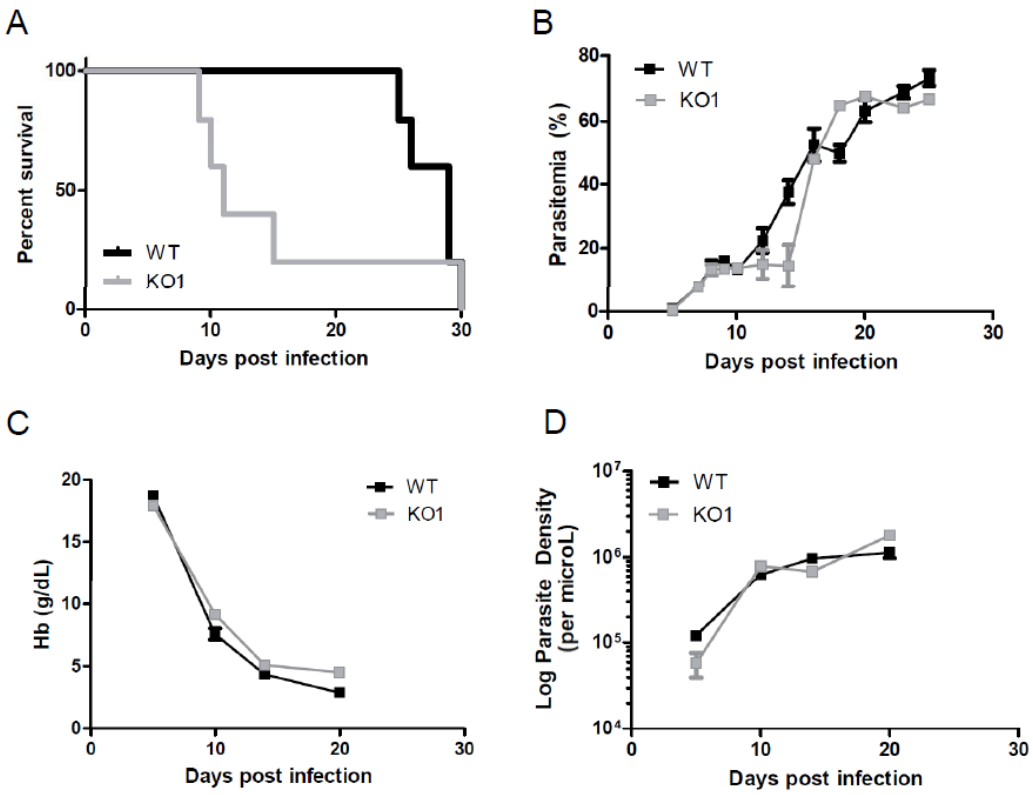

Figure 2.20 Survival, parasitemia and hemoglobin levels in 16 week female Balb/c mice infected i.p. with $1x10^5$ WT or PbHlyIII KO1 *P. berghei* infected erythrocytes. (A) Survival of mice up to day 30 post infection. (B) Parasitemia counted by Giemsa stained bloodfilm beginning day 3 post infection and continuing every other day until day 27. (C) Hemoglobin levels obtained from complete blood count analysis on days 5, 10, 15, and 20 post infection. (D) Parasite densities, calculated as a function of total parasites per microliter, estimated from parasitemia multiplied by the total red blood cell count for each infected mouse.

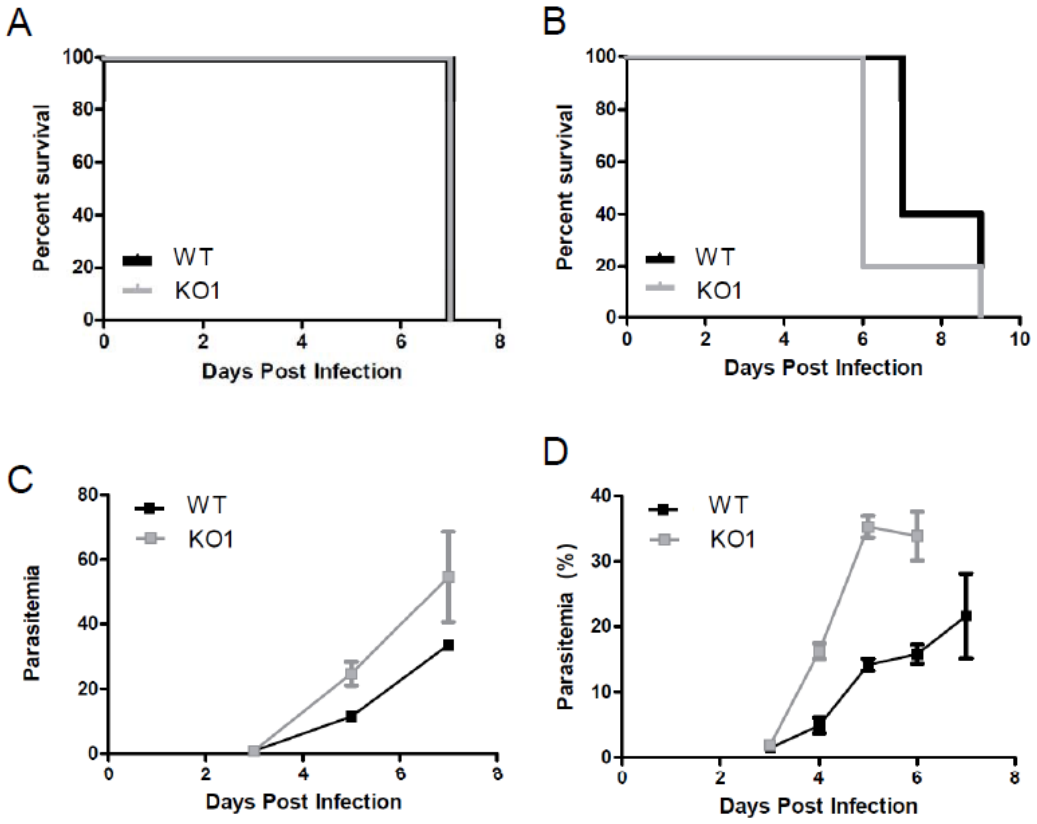

Figure 2.21 Survival and parasitemia of C57/Bl6 mice infected i.p. with $1x10^5$ WT or PbHlyIII KO1 *P. berghei* infected erythrocytes: two independent experiments. (Experiment 1: A and C) (A) 12-week old C57/Bl6 mice die on day 7 in both WT and KO1 infected groups (C) KO1 parasites multiply faster than WT. (Experiment 2: B and D) (B) 9-week old C57/Bl6 mice die between day 6-9 post infection in both WT and KO1 infected groups. (D) KO1 parasites multiply significantly faster than WT.

Immunization against PbHlyIII followed by parasite challenge

Our second approach to determine the contribution of *Plasmodium* hemolysin to anemia in the mammalian host involved immunization of mice against the *P. berghei* hemolysin III homology to determine whether antibodies against HlyIII could protect mice from developing severe anemia. We chose to express and purify a GST-tagged 80 amino acid N-terminus of PbHlyIII (Figure 2.9B) as our hemolysin-specific antigen as we had successfully used the *P. falciparum* construct for our earlier antibody studies. We adapted a prime-boost strategy from the Thermoscientific Pierce Antibodies online protocol for mouse immunization (79) using 50 µg of our GSTB80AA fusion peptide or GST alone as a control emulsified with Complete Freund's adjuvant (CFA) for the priming and Incomplete Freund's adjuvant for the subsequent boosts (Figure 2.22A).

We tested the sera reactivity of the immunization groups by Western Blotting whole cell *P. berghei* parasite lysate and found that there was very little reactivity after the first two boosts (test bleed 1, data not shown). Thus we boosted a third time, using a syringe method rather than vortexing for forming the emulsion, and found that test bleed 2 showed reactivity in all immunized groups (Figure 2.22B). Specifically the non-immunized groups showed no distinct bands, whereas the GST-immunized group had a 25 kDa band and the GSTB80AA-immunized group had two bands, one 25 kDa band likely associated with GST, and another slightly smaller band that was likely specific to the hemolysin peptide. We observed that there was some variability in sera reactivity, especially within the hemolysin III-immunized group, with some mice showing much stronger sera reactivity than others.

Based on the sera reactivity in the different groups, we divided the non-immunized and GST-control groups into 2 groups of 5 mice each for WT or PbHlyIII KO1 *P. berghei* ANKA challenge (Figure 2.22C first and second panels), and we divided the GSTB80AA immunized group into three separate groups for challenge: one 'strong' responder group for WT challenge and two 'weak' responder groups for WT or HlyIII KO1 *P. berghei* challenge (Figure 2.22C third panel). We used the PbHlyIII KO1 parasite challenge as a control, hypothesizing that PbHlyIII immunization would have no effect on survival or disease in the PbHlyIII KO1 challenged mice. Following challenge on day 97 we monitored the mice daily for survival and parasitemia by bloodfilm. Hemoglobin levels were monitored daily in Drabkin's reagent and complete blood count analysis was done on the mice every fifth day up to day 25 post challenge.

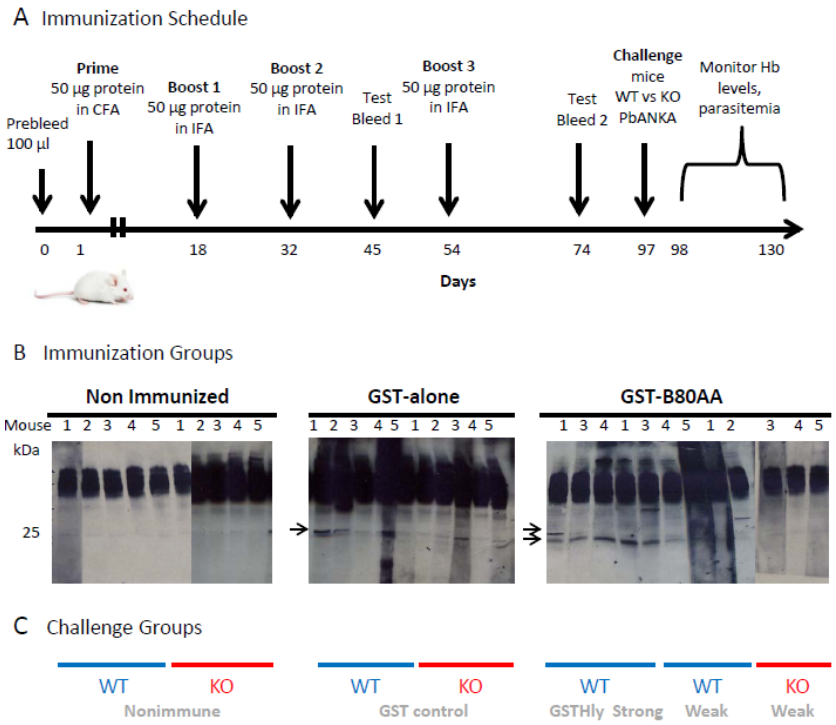

Figure 2.22 Immunization schedule, sera reactivity and experimental groups for HlyIII immunization and parasite challenge. (A) Immunization schedule with priming in Complete Freund's Adjuvant (CFA) followed by three boosts in Incomplete Freund's Adjuvant (IFA), test bleed and challenge. (B) Serum from each mouse was tested for reactivity against WT *P. berghei* whole cell parasite lysate after test bleed: non-immunized (10 mice, no distinct bands), GST control group (10 mice, 25 kDa band), GSTB80AA group (12 mice*, 25 kDa band and one distinctly lower than the GST associated band). (C) Based on sera reactivity, mice were split into 2 groups per immunization group for WT or HlyIII KO *P. berghei* challenge, with the exception of the GSTB80AA immunized mice which were divided into three groups, a strong responder group for WT challenge and two weak responder groups for WT or HlyIII KO challenge. *Three mice died in GSTB80AA group after the third boost, cause of death unknown.

Figure 2.23 summarizes the parasitemia, hemoglobin levels and survival of both WT and KO1 challenged groups. Overall we found that the immunization had no significant effect on parasite growth, hemoglobin levels, or survival, with the exception of the GSTHlyIII immunized, strong responder group, which overall suppressed parasitemia (Figure 2.23A) but also resulted in shorter time to death post-challenge (Figure 2.23E). Because the GSTHly strong responder mice died so quickly, we were unable to calculate a significant difference in parasitemia or anemia, though the single mouse that survived past day 15 did have much lower parasitemia and less anemia than the control groups and 'weak' responders (Figure 2.23A and C).

Severe weight loss was noted for these mice as early as three days post challenge and post-mortem necropsy of the strong responder mice revealed the development of severe fibrosis in the abdominal cavity, suggesting an adverse reaction to the immunizations and subsequent challenge that may have contributed to their early death. We hypothesized that using the same intraperitoneal route of immunization and challenge may have contributed to inflammation and the aforementioned fibrosis.

Due to the complicated results of immunization we were unable to conclude whether antibody strong response to PbHlyIII was protective for these mice and able to suppress parasitemia and protect against the development of anemia. Neither GST alone nor GSTHly weak responders were able to suppress parasitemia and both developed similar levels of anemia and died at similar rates to non-immunized mice after challenge with WT *P. berghei.* We did note that a majority of the KO1 *P. berghei* challenged mice died between day 8 and 15 regardless of immunization status (Figure 2.23F), again confirming our early death KO phenotype.

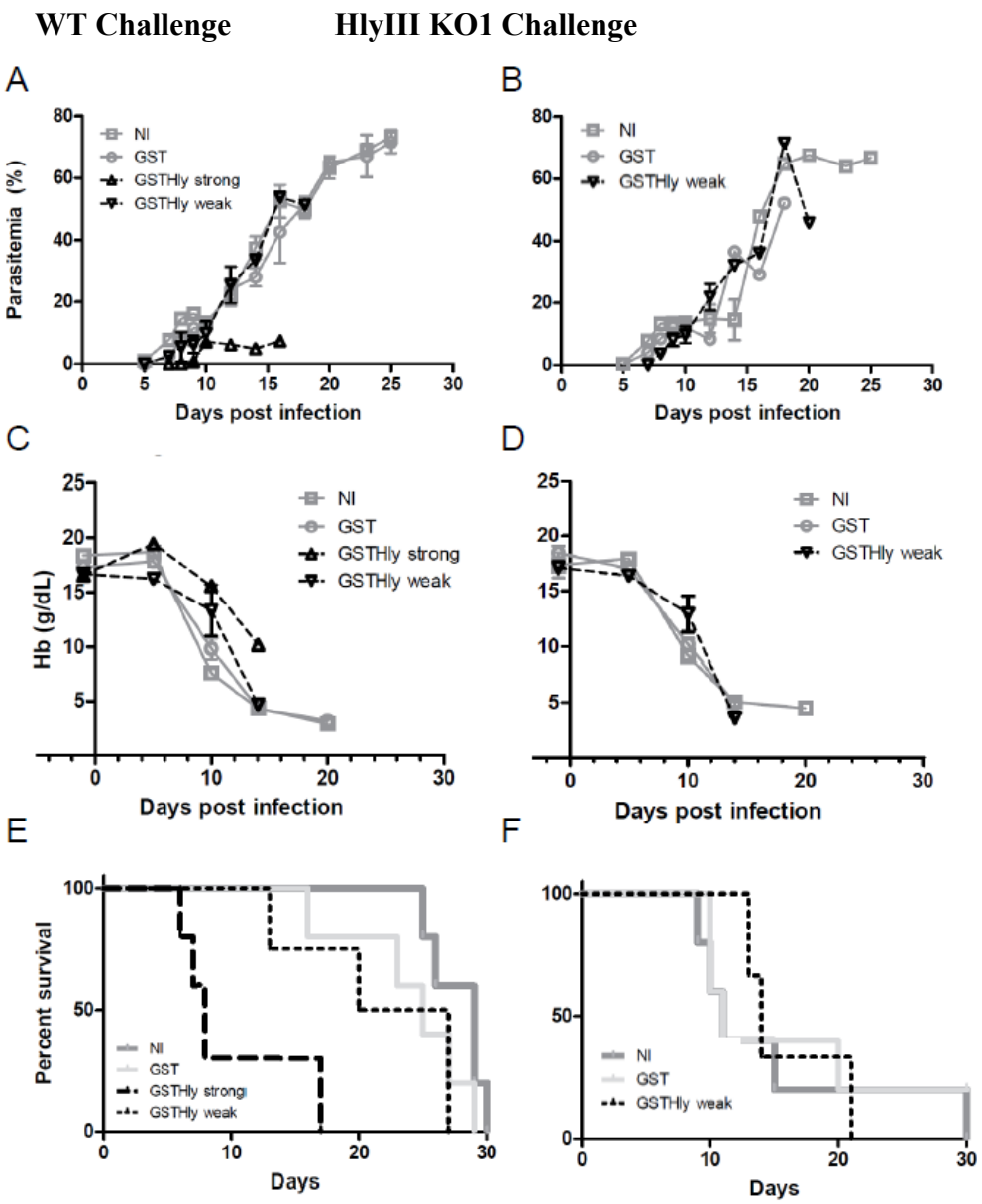

Figure 2.23 Parasitemia, hemoglobin levels, and survival of WT or PbHlyIII KO1 challenged mice after no immunization (NI), immunization with GST alone (GST), or GSTB80AA fusion peptide , strong or weak responders (GSTHly strong or GSTHly weak). (Left panel: A, C, E) Parasitemia, hemoglobin levels and survival of WT *P. berghei* challenged mice. (Right panel: B, D, F) Parasitemia, hemoglobin levels and survival of PbHlyIII KO1 *P. berghei* challenged mice.

As neither the WT vs KO approach, nor the immunization approach were successful in answering our virulence question, we decided to focus on the early death phenotype of the knockout parasite in hopes of uncovering the functional role of hemolysin III in the parasite itself and understanding why lacking hemolysin resulted in a more virulent parasite.

Essentiality of PbHlyIII in the malaria life cycle

First, we wanted to determine whether the gene was essential for all stages of the murine parasite, thinking that if the HlyIII KO parasite was unable to complete any particular stage of its life cycle, we might have a further clue to the functional role of this protein in the parasite. To that end, we had confirmation that the hemolysin gene was inessential for asexual blood stages due to the positive transfection results and observations of asexual blood stage parasites by Giemsa stained blood film (Figure 2.24). We also observed that the HlyIII KO1 and HlyIIIKO2 parasites could both form male and female gametocytes (Figure 2.24, right panel). Of note, we did observe that the HlyIIII KO parasites tended to have larger vacuoles in the asexual blood stages (Figure 2.24, left panel) and pursued this phenotype further with electron microscopy studies covered later.

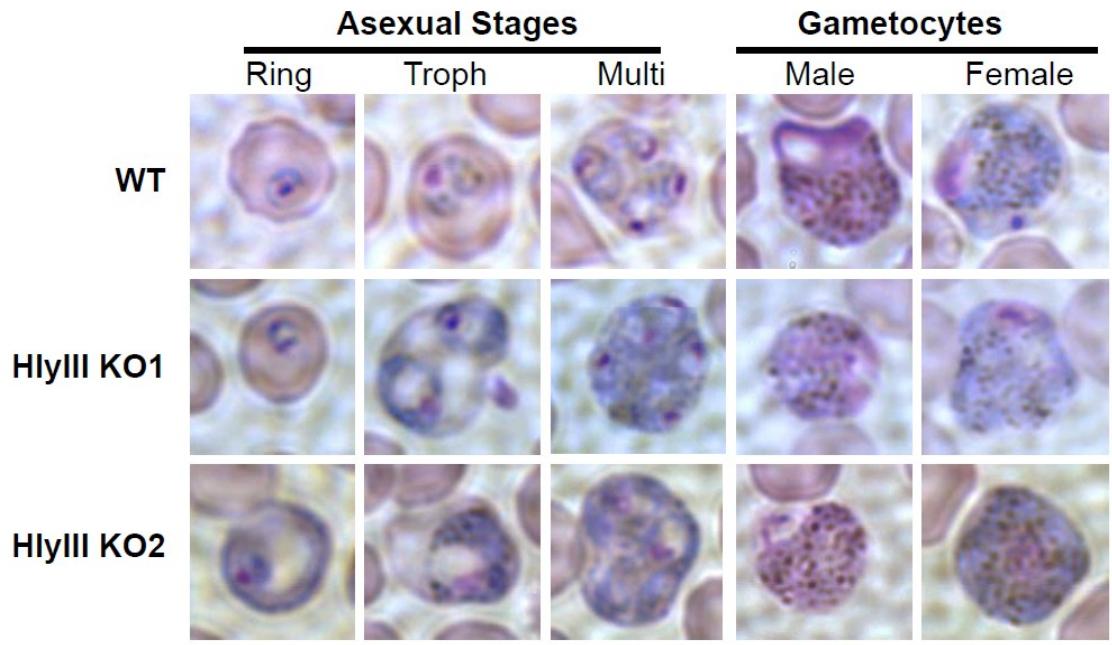

Figure 2.24 Wild type or HlyIII KO *P. berghei* ANKA blood stage parasites appear morphologically comparable by Giemsa stained bloodfilms, with an observation of more vacuoles present in the knockout asexual parasites compared to WT. Asexual blood stages with ring, trophozoite, and erythrocyte multiply-infected with trophozoites (left panel) and sexual blood stages, male and female (right panel).

Once we confirmed that the knockout parasites could form gametocytes, we then needed to ascertain whether these HlyIII KO gametocytes were infectious to mosquitoes and could continue the parasite progression through the mosquito stages, resulting in infectious sporozoites. We therefore fed Day 5 *Anopheles stephensi* mosquitoes on either WT or HlyIII KO1 *P. berghei* ANKA infected Balb/cJ mice with at least one gametocyte per field (~150-200 red blood cells) confirmed by bloodfilm and monitored the mosquitoes for oocyst development and sporozoite production (Figure 2.25A).

In three independent experiments, we observed that the HlyIII KO1 parasite made consistently fewer and smaller oocysts per mosquito midgut (Figure 2.25 B-D) and that the sporozoite yield from salivary glands was at least ten-fold less compared to the WT *P. berghei* ANKA strain (Figure 2.25B). Furthermore, the WT and KO1 infected mosquitoes were allowed to feed on naïve mice in at least two independent experiments, with only the WT inoculated mice developing patency between day 4 and day 7 post feed (Figure 2.25B).

In the third experiment, we significantly increased the number of salivary glands dissected in order to obtain sufficient WT and HlyIII KO1 sporozoites to infect mice directly intravenously and check for patency, but were still unable to obtain sufficient sporozoites in the knockout group for injection (<2000 total estimated, only a single sporozoite counted out of multiple dilutions and more than fifty fields).

Thus we found that the HlyIII KO1 parasite was not essential for mosquito stage development but did have a significant growth defect, resulting in fewer oocysts and less sporozoites in the salivary glands. We were unable to determine essentiality in the liver stage due to insufficient sporozoite recovery from the salivary glands. We did observe that the male to female gametocyte ratio was higher in the KO1 parasite group compared to the WT.

A

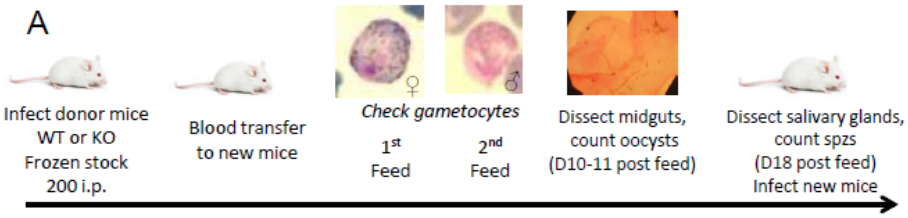

B

		Midgut			Salivary Gland		
		# pos midguts/ total	% positive midguts	# oocysts/ midgut	# Mosquitos dissected	Spz/ mosquito	Patency (M1/M2)
Expt 1	WT	5/10	50%	+	20	-	D7/-
	KO	5/10	50%	+	20	-	-/-
Expt 2	WT	13/22	60%	0-100+	10	737	D4/D4
	KO	9/16	56%	0-100	10	75	-/-
Expt 3	WT	10/23	43%	0-100+	84	3500	na*
	KO	16/21	76%	0-100	128	12.5	na*

*Did not feed mosquitoes on naïve mice to check for patency

C

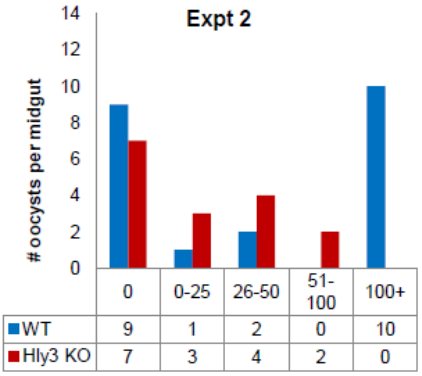

	0	0-25	26-50	51-100	100+
WT	9	1	2	0	10
Hly3 KO	7	3	4	2	0

D

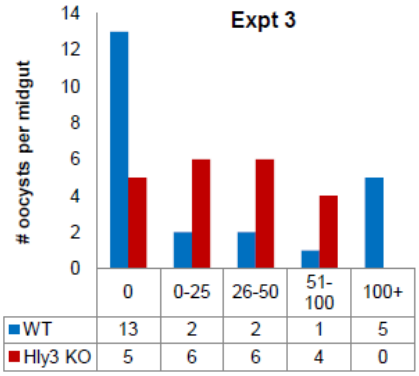

	0	0-25	26-50	51-100	100+
WT	13	2	2	1	5
Hly3 KO	5	6	6	4	0

Figure 2.25 PbHlyIII KO1 *P. berghei* oocyst and sporozoite counts from mosquitoes compared to WT *P. berghei* following bloodfeeding on infected mice in three independent experiments**.** (A) Experimental strategy for infecting mosquitoes with *P. berghei* WT or HlyIII KO1 parasites and assessment of oocyst and sporozoite development. (B) Quantitative results for oocysts and sporozoites determined from midgut and salivary gland dissections. (C and D) Number of oocysts per midgut enumerated for experiments 2 and 3 respectively.

Dissecting the Lethality Phenotype

We were still curious to understand why the PbHlyIII KO parasites were more lethal and to confirm that our virulence phenotype was real and related to disruption of *P. berghei* HlyIII. In order to confirm our phenotype we chose to knockout the same gene in a separate *P. berghei* strain expressing GFP-luciferase, confirming the separate knockout by both PCR and Southern blot as mentioned above (Figure 2.17, 2.18). When we repeated the previous experiment with infection of Balb/c mice with $1x10^5$ *P. berghei* infected erythrocytes, we found that the second knockout parasite PbHlyIII KO2 was equally lethal to the first, killing Balb/c mice between day 8-12 compared to day 18-22 for GFP-luc WT *P. berghei* (Figure 2.26B).

Increased passaging of the original PbHlyIII KO1 parasite through mice seemed to slightly decrease the virulence, with some mice surviving closer to the WT (Figure 2.26A), but as we were unable to successfully passage the PbHlyIII KO parasite through the mosquito, we were unable to confirm this observation. We did note a slight decrease in parasitemia for the PbHlyIII KO1 infected mice that survived past day 10 (Figure 2.26C) that might have played a role in their survival, but the parasitemia quickly rose to match the WT parasitemia by day 15 and the two mice went on to die several days earlier than the WT infected mice. Regardless, infection with either PbHlyIII knockout parasite resulted in significantly earlier death than infection with either the WT or GFP-luc *P. berghei* ANKA strains (Figure 2.26A, B). We did not find a significant difference in parasite growth rate or weight loss between the wild type and knockout groups (Figure 2.26C, D). However, HlyIII KO infected mice had slightly but not significantly higher weights compared to the wild type over time (Figure 2.26 E, F).

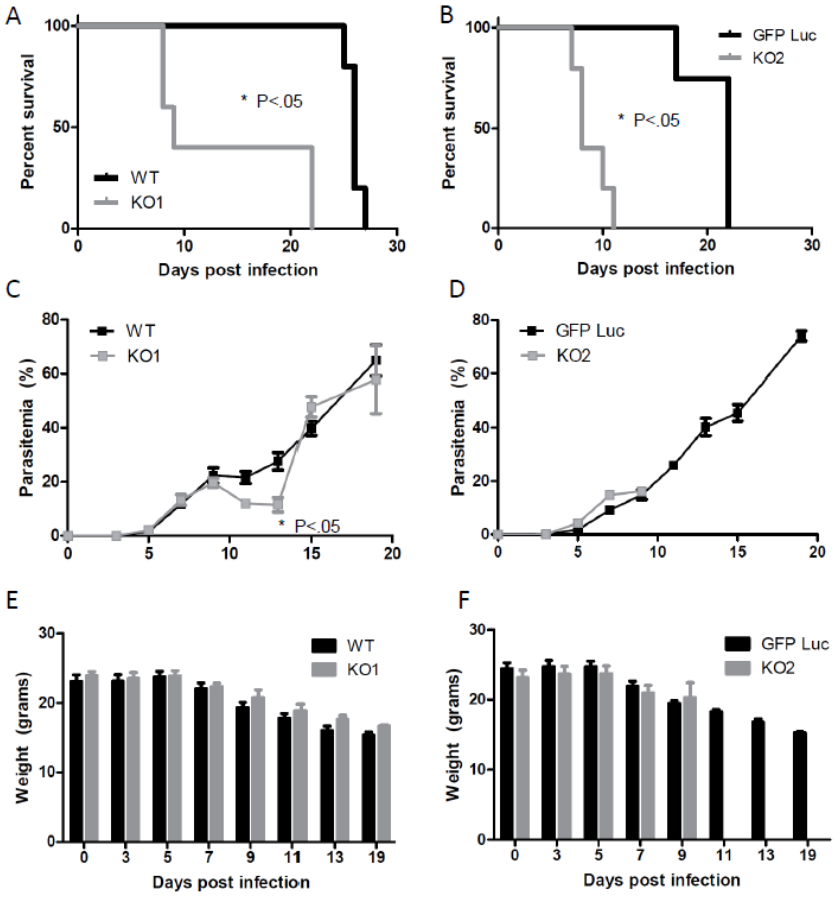

Figure 2.26 Survival, parasitemia and weights of 19 week old Balb/c mice infected with $1x10^5$ *P. berghei* infected erythrocytes (WT, PbHlyIII KO1, GFP-luc, or PbHlyIII KO2). Left panel: Balb/c mice infected with WT compared to PbHlyIII KO1 *P. berghei* ANKA (A, C, E) Survival, parasitemia and weights monitored between day 3 and day 30 post infection. Right panel: Balb/c mice infected with GFP-luciferase compared to PbHlyIII KO2 *P. berghei* ANKA (B, D, F) Survival, parasitemia, and weights monitored between day 3 and day 30 post infection. The Log-Rank test showed significant differences in survival between the WT and KO1 groups and the GFP-luc and KO2 groups with p-values <.05. An unpaired t-test showed a significant difference between WT and KO1 parasitemia on day 13 post infection, p-value <.05.

Once the increased lethality phenotype of our PbHlyIII KO was confirmed, we then turned to histology and qPCR methods in order to determine cause of death. We had observed that our PbHlyIII KO infected Balb/c mice looked similar to the experimental cerebral malaria (ECM) model of *P. berghei* ANKA infected C57/Bl6 mice in that the mice experienced seizures. As ECM is thought to be the result of parasite sequestration and vessel occlusion, we hypothesized knocking out a pore-forming protein like hemolysin III might result in altered deformability and increased sequestration of the parasitized erythrocytes, which might cause increased vascular occlusion and hemorrhage. We decided to infect mice with WT or PbHlyIII KO parasites and harvest organs for histology to look for parasite sequestration and hemorrhage, and concurrently measure parasite load with qPCR to quantitatively determine whether HlyIII KO parasites were sequestering in particular organs.

We infected Balb/c mice with either WT or PbHlyIII KO1 *P. berghei* parasites and sacrificed the mice on D7 post infection, the day that PbHlyIII KO infected mice had begun to die in our earlier experiments. The day of sacrifice we immediately harvested blood as well organs including heart, lung, kidney, liver, spleen, and brain for formalin fixation or RNA isolation. Three independent experiments were completed, one with perfusion to determine sequestered parasite load. qPCR of 18s copy number in the perfused organs showed significantly increased parasite load in both the spleen and the heart in the KO infected mice compared to WT (Figure 2.27) suggestive that there was increased parasite clearance or sequestration in these organs. While no other organs had significant differences in parasite load between the WT and PbHlyIII KO groups, all showed a trend toward more parasites in the KO1 compared to the WT group.

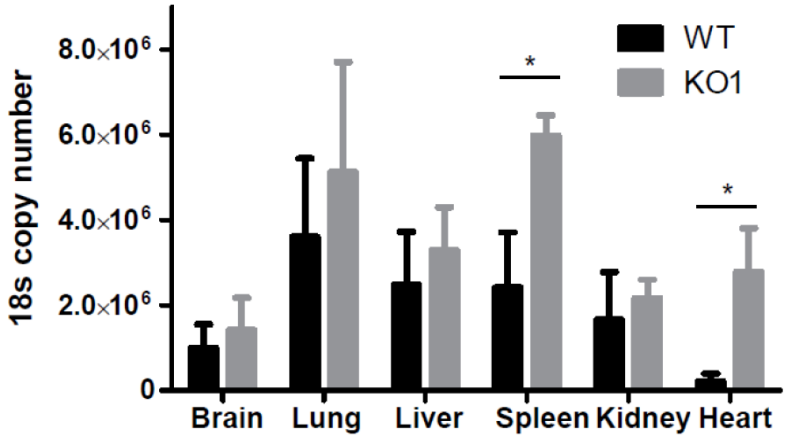

Figure 2.27 Parasite load in Balb/c mouse brain, lung, liver, spleen, kidney and heart on Day 7 post infection with WT or PbHlyIII KO1 *P. berghei,* based on 18s copy number measured by qPCR.. Mouse tissues were perfused with PBS followed by RNA isolation and cDNA synthesis. Equivalent RNA concentrations from both WT and KO1 tissues were used to ensure equivalent comparisons. An unpaired t-test was used to analyze each organ group and only spleen and heart were found to have significant differences between WT and KO1 groups, p-values <.05, n=3 mice per group.

Histology of the different organs revealed evidence of brain hemorrhage (Figure 2.28), edema, fibrosis and immune cell infiltration in the lung, and increased parasitized and uninfected erythrocytes as well as hemorrhage and fibrosis in the spleen (Figure 2.29) in the PbHlyIII KO compared to the WT *P. berghei* ANKA infected mice. Histology of other tissues including heart, liver and kidney were comparable between both WT and KO groups (Figure 2.30). These general trends were seen for both perfused and non-perfused tissues in all three experiments. However, blinded scoring of brain sections in the third experiment without perfusion suggested some mixed results, with varying levels of brain hemorrhage also seen in WT and GFP-Luc groups (Table 2.1).

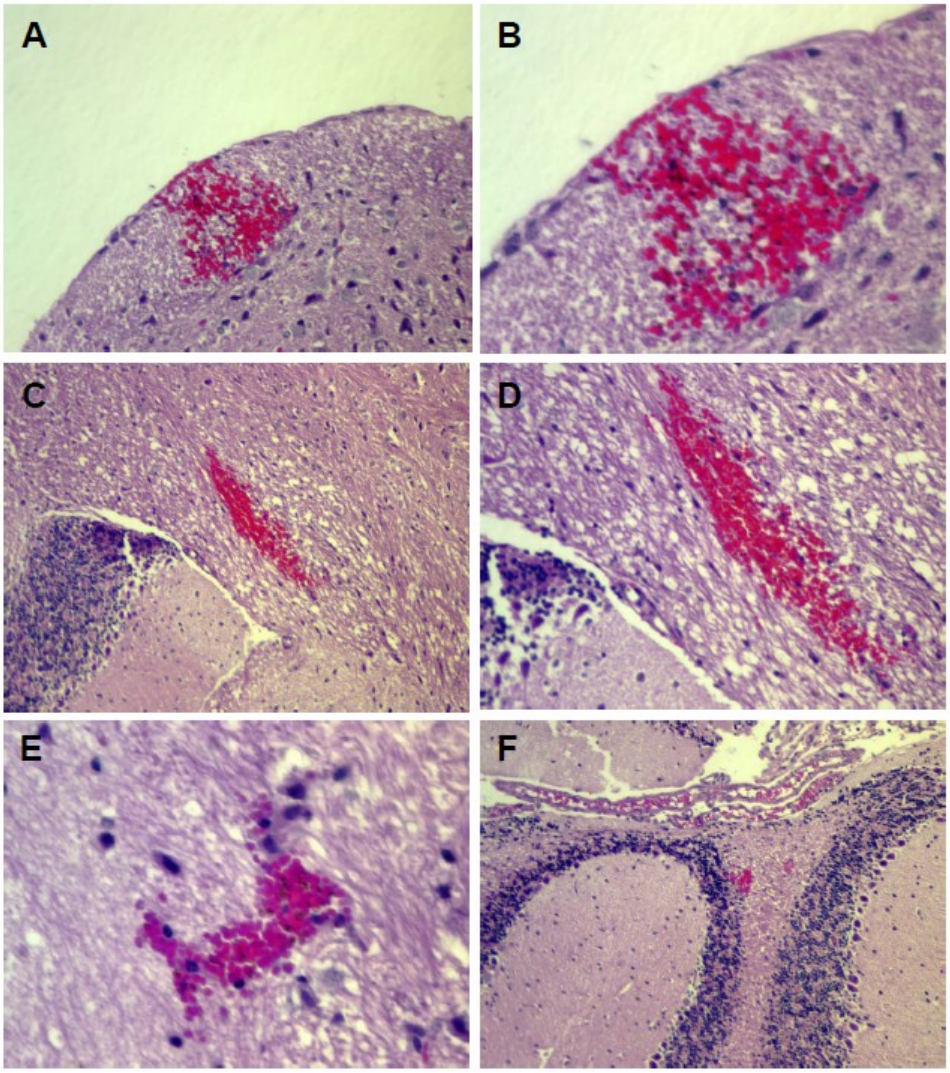

Figure 2.28 H&E stained brain sagittal sections from PbHlyIII KO *P. berghei* ANKA infected Balb/c mice. Brain sections from PbHlyIII KO infected mice had varying levels of peri-mortem hemorrhage in the cerebral cortex, brainstem and cerebellum. (A and B) 10x and 20x views of a peripheral brainstem hemorrhage. (C and D) 10x and 20x views of a central hindbrain hemorrhage. (E) 20x view of a small cerebral cortex hemorrhage. (F) 10x view of a small cerebellum hemorrhage. Representative images from two independent experiments without perfusion (n=3 mice per group per experiment).

Table 2.1 Scoring of WT or PbHlyIII KO Mouse Brain Hemorrhage				
# hemorrhages in four brain sagittal sections				
WT	4	8	13	3
PbHlyIII KO1	10	10	4	-
GFP Luc	20	10	15	-
PbHlyIII KO2	3	10	7	-
mouse	**1**	**2**	**3**	**4**

Specifically brain hemorrhage was noted in the brainstem and cerebellum (Figure 2.28), with a few hemorrhages also seen in the cerebral cortex. Though the final histology experiment suggested the GFP-Luc and to some extent the WT *P. berghei* infected mice had several brain hemorrhages, overall our observations over the course of three experiments were that the PbHlyIII KO infected mice had increased levels of brain hemorrhage compared to the WT strains. In particular, we suspected that brainstem hemorrhage might be a cause of death but this hypothesis requires further investigation.

Other striking findings included increased edema and fibrosis in the lungs seen in one of the two non-perfused biologic replicates (Figure 2.29D) as well as fibrosis and hemorrhage in the spleen (Figure 2.29B) in the PbHlyIII KO groups compared to the WT. Other tissues including kidney, liver and heart showed no evidence of increased parasite sequestration or inflammation in the PbHlyIII KO infected mice (Figure 2.30).

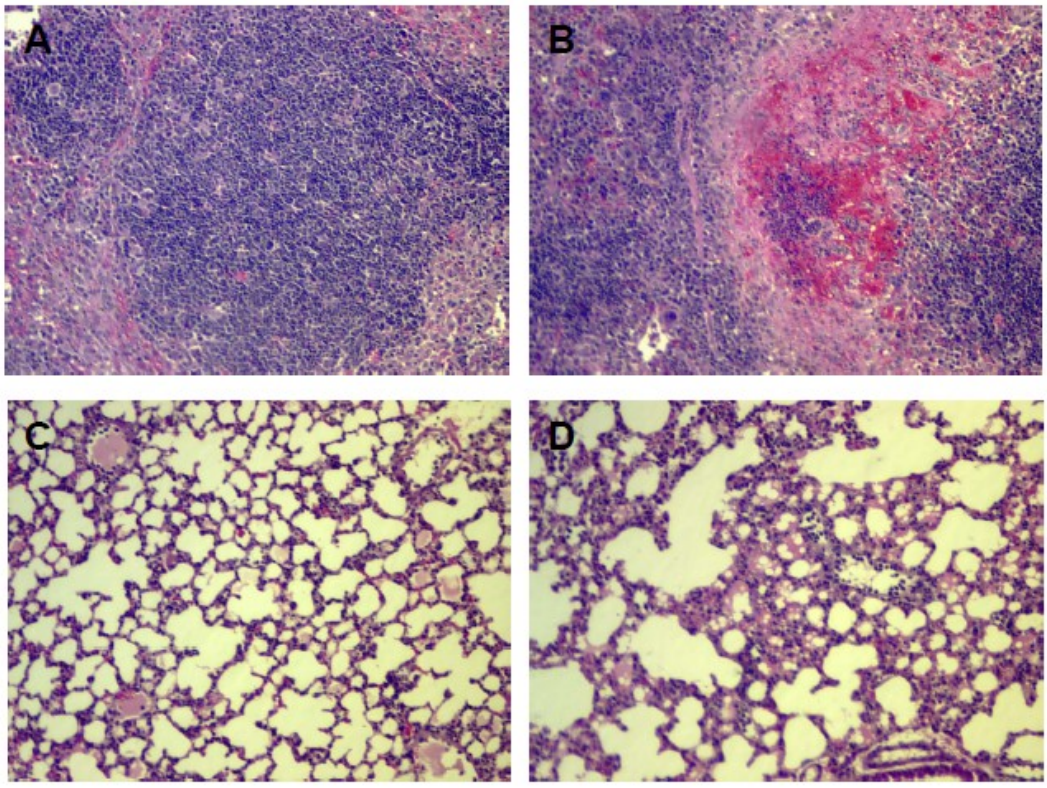

Figure 2.29 H&E stained spleen and lung sections from WT or PbHlyIII KO *P. berghei* ANKA infected Balb/c mice. (Top panel) PbHlyIII KO infected mouse spleens (B) have increased amounts of fibrosis, hemorrhage and both infected and uninfected erythrocytes compared to WT infected mice (A). (Bottom panel) Lung sections from PbHlyIII KO (D) infected mice showed increased levels of fibrosis, edema and immune cell infiltration compared to WT infected mice (C) Representative images from two independent experiments without perfusion (n=3 mice per group per experiment).

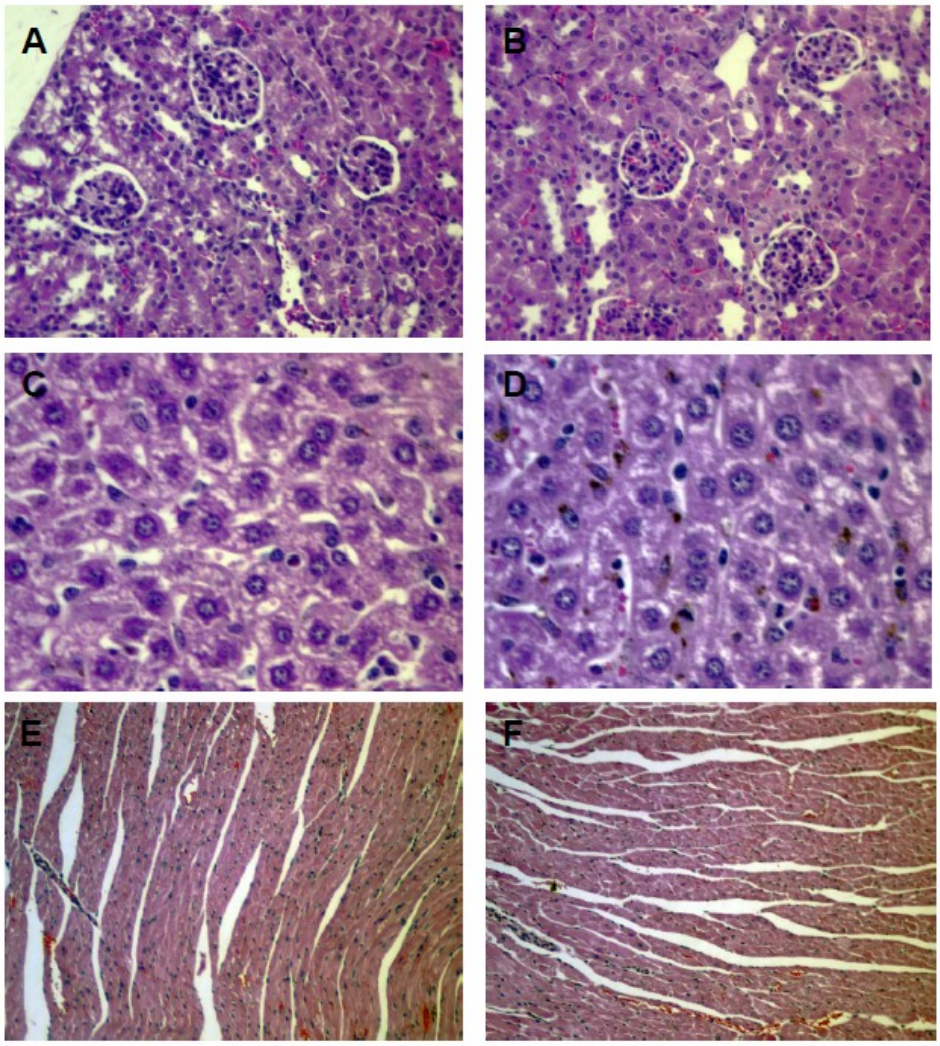

Figure 2.30 H&E stained heart, liver and kidney sections from WT or PbHlyIII KO *P. berghei* ANKA infected Balb/c mice. Heart sections (top panel), liver sections (middle panel) and kidney sections (bottom panel) showed no striking differences in pathology between WT and PbHlyIII KO *P. berghei* infected mice. All tissues contained hemozoin pigment indicative of infection.

Following up on our earlier observation of an increasing number of vacuoles seen in the PbHlyIII KO parasites compared to the WT on Giemsa stained bloodfilms (Figure 2.24), we next pursued higher resolution visualization of these parasites using transmission electron microscopy (TEM). Both WT and PbHlyIII KO1 parasitized red blood cells were harvested by cardiac puncture, washed and immediately fixed for TEM. Using this technique we observed some striking phenotypic differences between the WT and KO parasites. WT *P. berghei* asexual stage parasites are depicted in Figure 2.31.

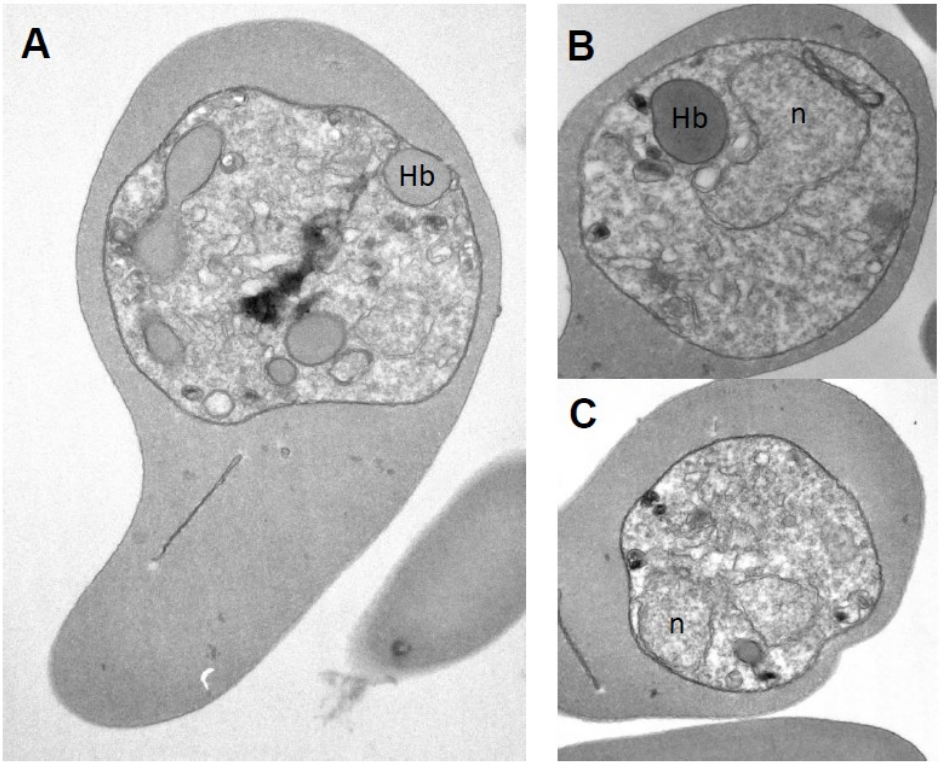

Figure 2.31 Transmission electron microscopy images of wild type *P. berghei* ANKA parasites, asexual blood stages. (A-C) Three individual wild type (WT) asexual stage parasites exhibit varying amounts of hemoglobin digestion and variations of normal parasite morphology. Nucleus (n) and hemoglobin (Hb) digestion as indicated.

First we observed that the PbHlyIII KO asexual stage parasites had clear aberrations in membrane structure and vacuole formation. While some of the phenotypes were minor with some undulating membranes and small vacuolar formations on the periphery of the parasite (Figure 2.32A), other parasites possessed large extra vacuoles either on the periphery (Figure 2.32C) or closer to the nucleus (Figure 2.32B and D). In some cases these vacuoles were seen at the juncture between two parasites (Figure 2.32E), while others completely contained the parasites (Figure 2.32F). Overall the knockouts seemed to have a loss of membrane integrity with accumulation of vacuoles and empty space in the parasite and in some cases the parasitophorous vacuole.

Our second observation was that many of the parasitized erythrocytes had drastically altered shapes resulting from either self-closure or some other mechanism, deformed by extracellular medium (Figure 2.33).

Finally we also noted that in many cases the parasitophorous vacuole seemed to be attached to the host plasma membrane and deform the erythrocyte surface along the surface of the parasite (Figure 2.34). We also found that in some cases we observed budding occurring at the erythrocyte plasma membrane surface (Figure 2.34 C and D).

Despite all of these major disturbances in parasite morphology, the PbHlyIII KO asexual blood stage parasites were successful at replicating and as stated earlier did not seem to have a defect in parasite growth rate *in vivo*. Furthermore the knockout parasites also seemed to be able to take up and degrade hemoglobin as evidenced by the presence of hemoglobin and hemozoin crystals in the parasites (Figure 2.32A, C, and E).

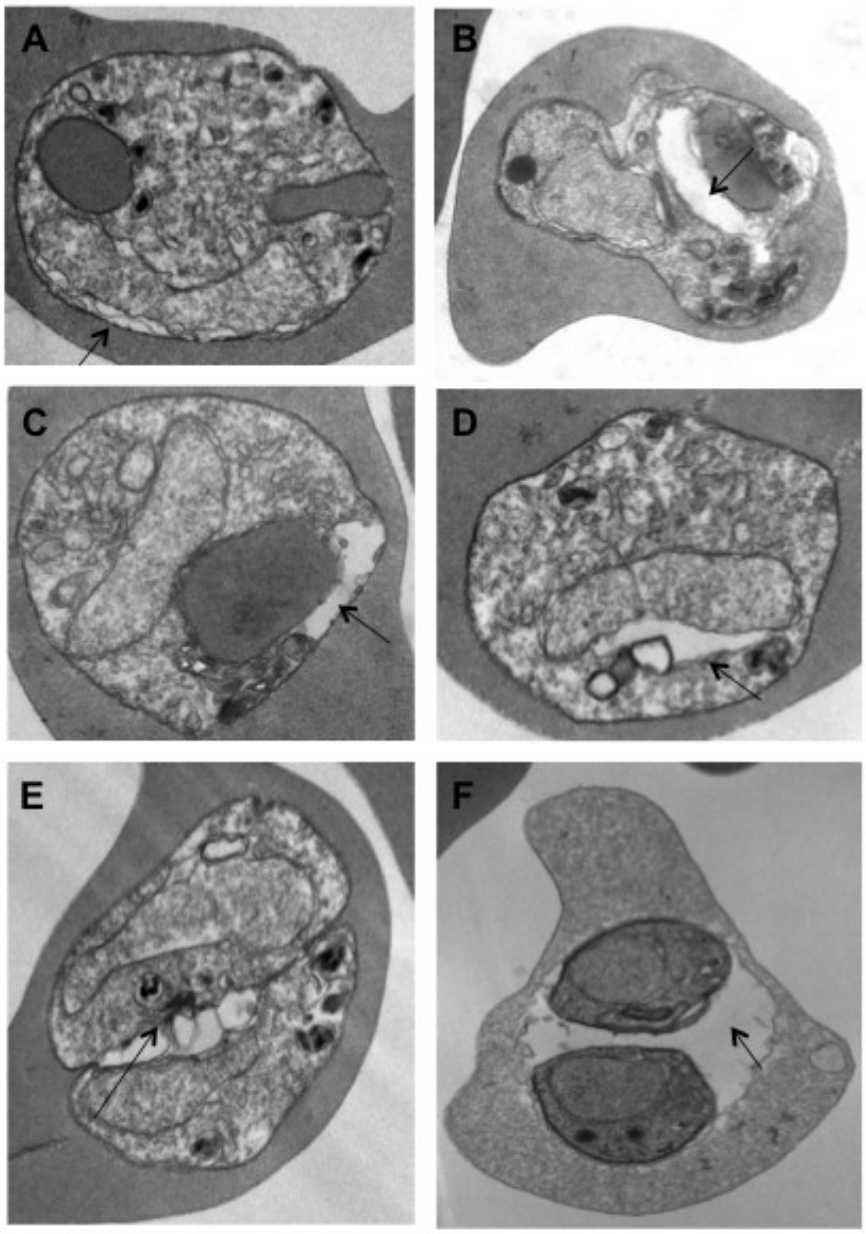

Figure 2.32 Transmission electron microscopy images of PbHlyIII KO *P. berghei* ANKA parasites depicting membrane disturbances and vacuolar aberrations (black arrows) (A) minor membrane disturbance (B) severe vacuolar aberration (C) Peripheral vacuole (D) Perinuclear vacuole (E) Vacuole between two parasites (F) Two parasites within a parasitophorous vacuole.

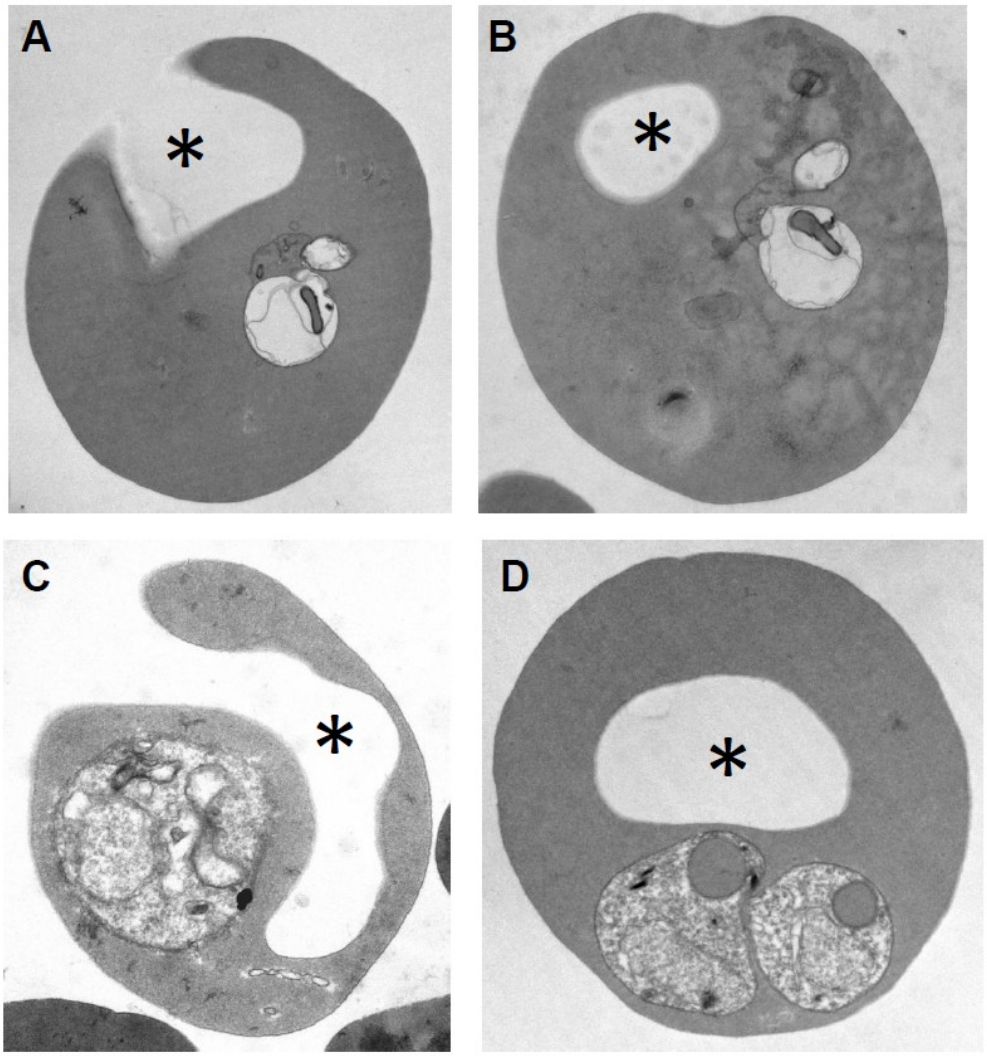

Figure 2.33 Transmission electron microscopy images of PbHlyIII KO *P. berghei* ANKA asexual blood stages depicting change in shape of erythrocyte with uptake of extracellular medium (asterix). (A and B) Serial sections of the same parasitized erythrocyte displaced by extracellular medium. (C and D) Different parasitized erythrocytes with varying levels of altered shape, displaced by extra-cellular medium.

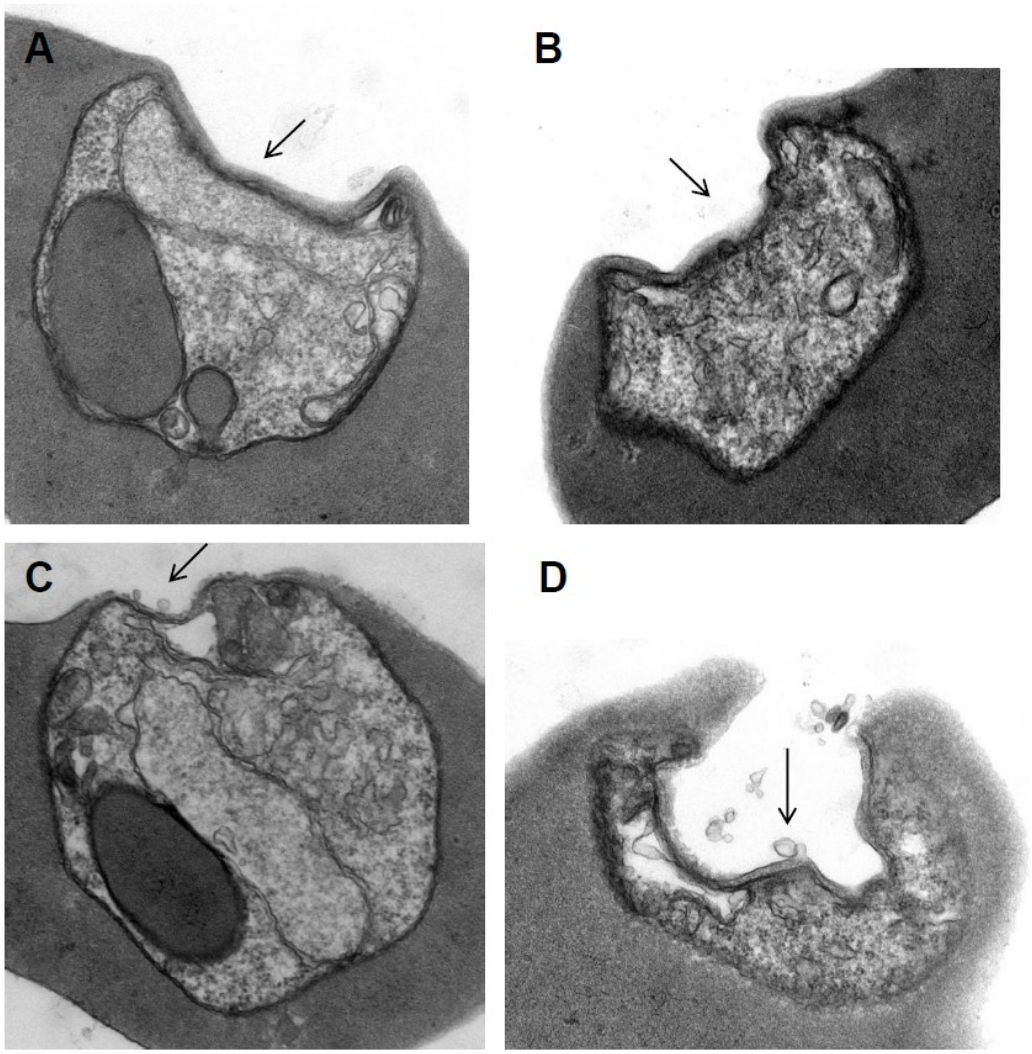

Figure 2.34 Transmission electron microscopy images of PbHlyIII KO *P. berghei* ANKA asexual blood stages with erythrocyte membrane deformed by parasitophorous vacuole or parasite and budding from the host plasma membrane. (A and B) Asexual blood stage parasites with parasitophorous vacuoles attached to and deforming the erythrocyte surface (arrows). (C and D) Asexual blood stage parasites, each clearly deforming the erythrocyte membrane with budding from the erythrocyte plasma membrane (arrows).

DISCUSSION AND CONCLUSIONS

The presence of a hemolysin like gene in *Plasmodium* was an intriguing find for our lab as we were curious why a parasite with an erythrocytic stage would encode a cytolytic protein that is similar to hemolytic proteins found in bacteria. Initial work done to characterize a recombinant *Plasmodium* hemolysin III (recPfHlyIII) in our lab revealed that recPfHlyIII was a pore-forming protein with hemolytic activity. Inhibition of recPfHlyIII was accomplished partially with a potassium channel inhibitor glibenclamide, whereas addition of sufficient size polyethylene glycol was able to completely inhibit hemolysis, while still allowing the protein to bind to the surface of erythrocytes. In a separate study a recombinant GFP tagged PfHlyIII was overexpressed in a *P. falciparum* strain, and live fluorescence microscopy supported a digestive vacuole localization for recPfHlyIII-GFP. This evidence supported our hypothesis that PfHlyIII was a functional cytolytic protein and could be a potential virulence factor in the mammalian host by damaging host erythrocytes and contributing to severe malaria anemia.

We further modified our hypothesis based on the localization results to state that soluble hemolysin in the food vacuole could be released upon parasite egress and damage bystander erythrocytes. In order to test our new hypothesis we developed the following aims: (1) confirm heterologous pore-formation in *Xenopus* oocytes, (2) characterize native hemolysin III protein expression in *Plasmodium falciparum*, and (3) determine whether the *P. berghei* HlyIII homolog can act as a virulence factor, contributing to severe malaria anemia in a mouse model of malaria.

We successfully expressed recPfHlyIII in *Xenopus* oocytes and demonstrated sensitivity of recPfHlyIII expressing oocytes to hypotonic lysis similar to those

expressing human aquaporin 1 (hAQP1), a well described water channel (77). The water injected controls were stable up to one hour, whereas hAQP1 and recPfHlyIII expressing oocytes ruptured within the first 1-15 minutes in hypotonic solution suggestive of disruption in the surface membrane resulting in sensitivity to hypotonic lysis. As further evidence for pore formation we repeated the experiment in the presence of varying sizes of the osmotic protectant polyethylene glycol and found that larger PEG molecules were able to protect the oocytes from hypotonic lysis, similar to what was found with recPfHlyIII expressed and enriched from *E. coli* (70). Based on this heterologous expression of recPfHlyIII in eukaryotic *Xenopus* oocytes, we predict that *Plasmodium* hemolysins are expressed natively as pore-forming proteins, similarly to what has been shown for bacterial hemolysins.

In order to characterize native protein expression of PfHlyIII, we expressed and purified a GST-fusion peptide with the 80 amino acid N-terminus of PfHlyIII and used this antigen to generate rabbit polyclonal antisera to PfHlyIII. Affinity purified antisera was used to probe parasite lysate and demonstrated soluble, native PfHlyIII protein expression in all asexual blood stages of *P. falciparum*. Using synchronized parasite lysates, we also demonstrated increased expression of PfHlyIII as parasites matured from ring to schizont stages. Early and middle gametocyte stages showed evidence of PfHlyIII expression, whereas later gametocyte stages did not have PfHlyIII specific bands by Western Blot. *P. falciparum* sporozoites also lacked PfHlyIII expression by Western Blot even at very high numbers. Overall we have evidence for native PfHlyIII expression in all blood stages except late stage gametocytes, suggesting an important functional role for

PfHlyIII in these stages, particularly in later schizont stages when the protein is most abundant.

Furthermore we found that PfHlyIII was not detectable in as many as 100,000 sporozoites probed by Western Blot, although it is possible that PfHlyIII is a very low abundant protein in these stages and that we were unable to detect it with our antibody in this assay. Regarding the solubility of native PfHlyIII, we found that the protein was expressed in asexual blood stages of *Plasmodium* as both a soluble and integral membrane protein as evidenced by the detection of PfHlyIII in cytosolic and membrane fractions, with release from the membrane completed with ionic detergent. Thus we have evidence to support our hypothesis that soluble PfHlyIII is present in asexual blood stages and may be released upon schizont rupture and present in patient plasma. However we were unable to specifically test malaria patient plasma samples for presence of PfHlyIII antibodies due to the high background signal of patient plasma with our MBPF80AA antigen in ELISA studies (data not shown), and further work needs to be done to demonstrate that native PfHlyIII is present in malaria patient plasma and could be available to damage nearby erythrocytes.

With evidence for soluble *Plasmodium* hemolysin expressed in asexual blood stages, we sought to find direct evidence for *Plasmodium* hemolysin contributing to severe malaria anemia through destruction of erythrocytes. Attempts to disrupt the hemolysin gene in *P. falciparum* were unsuccessful with no parasites present after fifty days of drug selection. In light of the time-consuming methods then available for gene disruption in *P. falciparum,* we turned to a mouse model of malaria *P. berghei* ANKA in Balb/c mice to try to answer our virulence question, using two separate approaches: one

involving knocking out the hemolysin homolog in *P. berghei* (PbHlyIII), and the other immunization against PbHlyIII.

Immunization of mice with a GST-tagged PbHlyIII N-terminus fusion peptide resulted in varying levels of sera response based on Western Blotting of parasite lysate with test bleed sera. In the end however, immunization against PbHlyIII resulted in little to no protection from parasitemia or anemia following challenge, with mice mounting the strongest immune response dying early with low parasitemia, likely due to sepsis or another complication resulting from the method of immunization and challenge. Weak responders survived to day 20 but developed similar anemia to GST immunized or non-immunized controls. A different route of immunization and challenge may prevent early death by reducing intraperitoneal inflammation. Furthermore using syringe emulsion techniques may provide a more stable emulsion than the vortex technique which may also result in fewer boosts required for a good immune response and less predilection for intraperitoneal inflammation (80). Once repeated we may find that a strong immune response against PbHlyIII does protect from parasitemia and even severe anemia, but this hypothesis remains to be tested.

Knocking out the *P. berghei* hemolysin homolog PbHlyIII yielded an unexpected phenotype. Rather than reducing the virulence of the parasite, PbHlyIII KO parasites were found to be more lethal than their WT counterparts, killing Balb/cmice approximately 10 days earlier than predicted, similar to what is usually seen in the experimental cerebral malaria model with C57/Bl6 mice (including some visible seizing of PbHlyIII KO *P. berghei* infected mice). While the early death phenotype precluded any anemia studies of the knockout group, the increased lethality of the parasite was

fascinating and proved difficult to interpret. Parasite growth rates as measured by both parasitemia and parasite density were the same in both WT and PbHlyIII KO infected Balb/c mice, whereas in C57/Bl6 mice, we did note a slight but significant increase in parasite growth rate that may be a result of either differential sequestration of infected erythrocytes, increased rate of invasion or perhaps an increased number of singly-infected erythrocytes. In Balb/c mice however it was particularly noted while studying the TEM images that there were many multiply-infected erythrocytes in the PbHlyIII KO infected groups, suggesting the last supposition is unlikely. Lethality in the C57/Bl6 mice was unchanged with PbHlyIII KO compared to WT *P. berghei* infection, so the increased parasite growth rate in the KO did not result in earlier mortality in these mice.

In order to determine the cause of early death in the PbHlyIII KO infected Balb/c mice, we sacrificed the mice shortly before onset of early death on day 7 post infection and processed several tissues including brain, liver, lung, spleen, heart and kidney for evidence of pathology and parasite sequestration. qPCR on these tissues supported an increased level of parasite sequestration in the spleen and in the heart (Figure 2.27), with H&E staining of spleen sections confirming the increased level of both infected and uninfected erythrocytes present in many PbHlyIII KO infected mice (Figure 2.29). We also noted severe edema, fibrosis and immune cellular infiltration in the lung in most PbHlyIII KO infected mice, but noted that many of these features were seen in the WT infected mice often as well, suggesting that lung pathology was unlikely the cause of the early death. Most interesting was the level of brain hemorrhage noted in initial studies with the PbHlyIII KO parasite, though as evidenced by Table 2.1, later studies suggested hemorrhages were not necessarily unique to the PbHlyIII KO infected mice. Furthermore

qPCR data does not support significantly increased parasite sequestration in the brain or small capillaries in the WT group, but there is evidence for some parasites sequestered in both groups, which might contribute to inflammation and hemorrhage. Regardless, the consistent findings of brainstem and cerebellum hemorrhage in the PbHlyIII KO groups warrant further study, and we hope that examining the brainstems of mice post-mortem will more clearly indicate why Balb/c mice infected with PbHlyIII KO *P. berghei* die so much earlier than those infected with WT.

The increased erythrocyte clearance and spleen pathology in the PbHlyIII KO groups is suggestive of altered deformability of the parasitized erythrocytes in the PbHlyIII KO compared to the wild type. While our original observations of the WT and PbHlyIII KO asexual stages by Giemsa film suggested some slight alterations in the number of vacuoles present, the higher resolution images produced using transmission electron microscopy revealed even greater disparities between the WT and PbHlyIII KO strains. In particular the extra vacuoles we noted by Giemsa were quite varied in shape, size and location, present as multiple small vesicles or larger vacuoles either on the periphery of the parasite, between parasites or hugging the parasite nucleus. The vacuoles appeared to be empty, devoid of hemozoin suggesting they were distinct from digestive vacuoles. The presence of digestive vacuoles with hemozoin in conjunction with hemoglobin containing vesicles in the PbHlyIII KO parasite also suggests the membrane or vacuole aberration does not affect the hemoglobin digestion pathway. Overall the morphologic changes seem to be the result of altered membrane integrity and structure, as well as alterations in the parasitophorous vacuole and its association with the erythrocyte plasma membrane.

Vesicle and membrane dynamics are quite complicated, so it is difficult to pinpoint the mediator of the membrane disruptions we see in the PbHlyIII KO parasites. However, as *Plasmodium* hemolysin is likely to function either as a pore or a receptor based on the evolutionary data available for the hemolysin III protein family, there are a few speculations we could make regarding the disruption of hemolysin being directly responsible for the morphology we see. One possibility is that hemolysin is a pore that is important for transport of some substrate involved either directly or downstream in membrane fusion or formation, perhaps directly after invasion and formation of the parasitophorous vacuole. Another possibility is that hemolysin is functioning as a receptor in the parasite and that the disruption has downstream effects on a signaling pathway such as the phosphoinositide 3-kinase pathway involved in intracellular trafficking. PAQR-2, a hemolysin III family member, is an adiponectin receptor homolog in *C. elegans* with downstream effectors involved in phosphatidylcholine biosynthesis and fatty acid elongation, suggesting PAQR-2 may play an important role in membrane fluidity. In the above model PAQR-2 appears to be important for cold adaptation, and the authors speculate PAQR-2 may function as a hydrolase (81). Yeast Izh2p is another example of a progestin receptor with regulatory roles in metabolic homeostasis, with deletion resulting in increased sensitivity to zinc levels and zinc homeostasis (66). FurthermoreIzh2p may regulate downstream pathways, perhaps through iron, zinc or phosphate homeostasis, including lipid metabolism and lipid remodeling (66).

As *Plasmodium* hemolysin does have a conserved N-terminal domain similar to the PAQR family proteins, PfHlyIII may have a similar function to PAQR-2 or Izh2p as a hormone receptor, with disruption leading to downstream disruption of lipid metabolism

or remodeling. Despite the seemingly severe morphological changes in the knockout parasite, it does not appear that loss of hemolysin results in death for asexual parasites or even gametocytes, suggesting that there are other compensatory effectors or even mutations that can overcome hemolysin disruption.

In a separate attempt to nail down the function of hemolysin and essentiality in the parasite, we attempted to follow the PbHlyIII KO through the mosquito stages and into the liver. However while we were able to observe oocyst formation in the midgut as well as minimal sporozoites in the salivary glands, there does seem to be a defect in the mosquito stage growth and development in the PbHlyIII KO parasite. Specifically the oocysts appear to be smaller and fewer in number compared to WT *P. berghei*, and the final sporozoite harvest from salivary glands is tenfold lower compared to WT. We did not rule out the possibility that sporozoites are formed but unable to invade the salivary glands efficiently. Due to the limited number of sporozoites harvested from the salivary glands, we were unable to test whether the PbHlyIII KO sporozoites were infectious to mice and could develop into liver stage and subsequent blood stage infections. Future directions will include dissecting this growth phenotype further and may help elucidate the requirement and function of *Plasmodium berghei* hemolysin III.

In conclusion we were able to clearly define the cyclical native protein expression of PfHlyIII in asexual blood stages and demonstrate the functional pore formation of recombinant PfHlyIII in a eukaryotic system. While we did not find direct evidence for a virulent role of PfHlyIII in severe malaria anemia, our data still supports this possibility, as PfHlyIII is a soluble, pore-forming protein present in asexual blood stages of *Plasmodium falciparum.* Furthermore the disruption of the *P. berghei* homolog PbHlyIII

resulted in several distinct phenotypes: early lethality in Balb/c mice that may be a result of altered deformability, nonlethal but morphologically severe membrane and parasitophorous vacuolar aberrations, and a significant growth defect in the mosquito stages yielding low numbers of salivary gland sporozoites. Further exploration of these altered phenotypes should be provide new insights as to the role of *Plasmodium* hemolysin III proteins and may also provide new insights into the eukaryotic hemolysin III family of proteins which remains largely uncharacterized.

REFERENCES

1. Warrell D a. *Severe falciparum malaria.* Trans R Soc Trop Med Hyg. 2000;94:1–90.
2. Mcelroy PD, Kuile FOTER, Lal AA, Bloland PB, Hawley WA, Oloo AJ, et al. *Effect of Plasmodium Falciparum Parasitemia Density on Hemoglobin Concentrations Among Full-Term, Normal Birth Weight Children in Western Kenya, IV*. The Asembo Bay Cohort Project. Am J Trop Med Hyg. 2000;62(4):504–12.
3. Douglas NM, Anstey NM, Buffet PA, Poespoprodjo JR, Yeo TW, White NJ, et al. *The anaemia of Plasmodium vivax malaria.* Malar J. 2012 Jan 11:135.
4. Calis JCJ, Phiri KS, Faragher EB, Brabin BJ, Bates I, Cuevas LE, et al. *Severe anemia in Malawian children*. N Engl J Med. 2008 Feb 28;358(9):888–99.
5. Cusick SE, Opoka RO, Lund TC, John CC, Polgreen LE. *Vitamin d insufficiency is common in ugandan children and is associated with severe malaria.* Carvalho LH, editor. PLoS One. Public Library of Science; 2014 Jan;9(12):e113185.
6. Orimadegun AE, Sodeinde O. *Glucose-6-phosphate dehydrogenase status and severity of malarial anaemia in Nigerian children.* J Infect Dev Ctries. 2011 Nov;5(11):792–8.
7. Foote EM, Sullivan KM, Ruth LJ, Oremo J, Sadumah I, Williams TN, et al. *Determinants of anemia among preschool children in rural, western Kenya*. Am J Trop Med Hyg. 2013 Apr;88(4):757–64.

8. Awah NW, Troye-Blomberg M, Berzins K, Gysin J. *Mechanisms of malarial anaemia: potential involvement of the Plasmodium falciparum low molecular weight rhoptry-associated proteins*. Acta Trop. 2009 Dec;112(3):295–302.

9. Layez C, Nogueira P, Combes V, Costa FTM, Juhan-Vague I, da Silva LHP, et al. *Plasmodium falciparum rhoptry protein RSP2 triggers destruction of the erythroid lineage*. Blood. American Society of Hematology; 2005 Nov 15;106(10):3632–8.

10. Buffet P a, Safeukui I, Milon G, Mercereau-Puijalon O, David PH. *Retention of erythrocytes in the spleen: a double-edged process in human malaria*. Curr Opin Hematol. 2009 May;16(3):157–64.

11. Buffet PA, Safeukui I, Deplaine G, Brousse V, Prendki V, Thellier M, et al. *The pathogenesis of Plasmodium falciparum malaria in humans: insights from splenic physiology*. Blood. 2011 Jan 13;117(2):381–92.

12. Roberts DJ, Casals-Pascual C, Weatherall DJ. *The clinical and pathophysiological features of malarial anaemia*. Curr Top Microbiol Immunol. 2005;295:137–67.

13. Jakeman GN, Saul A, Hogarth WL, Collins WE. *Anaemia of acute malaria infections in non-immune patients primarily results from destruction of uninfected erythrocytes*. Parasitology. 1999 Aug;119 Pt 2:127–33.

14. Collins We, Jeffery Gm, Roberts Jm. *A retrospective examination of anemia during infection of humans with Plasmodium Vivax*. Am J Trop Med Hyg. 2003 Apr 1;68(4):410–2.

15. Foeller M, Bobbala D, Koka S. *Suicide for survival-death of infected erythrocytes as a host mechanism to survive malaria*. Cell Physiol. 2009;133–40.

16. Kiefer CR, Snyder LM. *Oxidation and erythrocyte senescence*. Curr Opin Hematol. 2000 Mar;7(2):113–6.

17. Mohan K, Dubey ML, Ganguly NK, Mahajan RC. *Plasmodium falciparum: role of activated blood monocytes in erythrocyte membrane damage and red cell loss during malaria*. Exp Parasitol. 1995 Feb;80(1):54–63.

18. Biryukov S, Stoute JA. *Complement activation in malaria: friend or foe?* Trends Mol Med. 2014 May;20(5):293–301.

19. Odhiambo CO, Otieno W, Adhiambo C, Odera MM, Stoute JA. *Increased deposition of C3b on red cells with low CR1 and CD55 in a malaria-endemic region of western Kenya: implications for the development of severe anemia.* BMC Med. 2008 Jan;6(1):23.

20. Stoute JA. *Complement receptor 1 and malaria.* Cell Microbiol. 2011 Oct;13(10):1441–50.

21. Ekvall H, Arese P, Turrini F, Ayi K, Mannu F, Premji Z, et al. *Acute haemolysis in childhood falciparum malaria.* Trans R Soc Trop Med Hyg. 2001;95:611–7.

22. Gwamaka M, Fried M, Domingo G, Duffy PE. *Early and extensive CD55 loss from red blood cells supports a causal role in malarial anaemia.* Malar J. 2011 Jan;10:386.

23. Salmon MG, De Souza JB, Butcher GA, Playfair JH. *Premature removal of uninfected erythrocytes during malarial infection of normal and immunodeficient mice.* Clin Exp Immunol. 1997 Jun;108(3):471–6.

24. Evans KJ, Hansen DS, van Rooijen N, Buckingham LA, Schofield L. *Severe malarial anemia of low parasite burden in rodent models results from accelerated clearance of uninfected erythrocytes.* Blood. 2006 Feb 1;107(3):1192–9.

25. Safeukui I, Gomez ND, Adelani AA, Burte F, Afolabi NK, Akondy R, et al. *Malaria Induces Anemia through CD8+ T Cell-Dependent Parasite Clearance and Erythrocyte Removal in the Spleen.* MBio. 2015 Jan 27;6(1):e02493–14 – .

26. Dondorp AM, Angus BJ, Hardeman MR, Chotivanich KT, Kamdrat S, Ruangveerayuth R, et al. *Prognostic significance of reduced red blood cell deformability in severe falciparum malaria*. Am J Trop Med Hyg. 1997;57(5):507–11.

27. Chang K-H, Tam M, Stevenson MM. *Inappropriately low reticulocytosis in severe malarial anemia correlates with suppression in the development of late erythroid precursors.* Blood. American Society of Hematology; 2004 May 15;103(10):3727–35.

28. Chang K-H, Stevenson MM. *Malarial anaemia: mechanisms and implications of insufficient erythropoiesis during blood-stage malaria.* Int J Parasitol. 2004 Dec;34(13-14):1501–16.

29. Chasis JA, Mohandas N. *Erythroblastic islands: niches for erythropoiesis*. Blood. 2008 Aug 1;112(3):470–8.

30. Lamikanra AA, Brown D, Potocnik A, Casals-Pascual C, Langhorne J, Roberts DJ. *Malarial anemia: of mice and men*. Blood. American Society of Hematology; 2007 Jul 1;110(1):18–28.

31. Schwarzer E, Turrini F, Ulliers D, Giribaldi G, Ginsburg H, Arese P. *Impairment of macrophage functions after ingestion of Plasmodium falciparum-infected erythrocytes or isolated malarial pigment.* J Exp Med. 1992 Oct 1;176(4):1033–41.

32. Schwarzer E, Ludwig P, Valente E, Arese P. *15(S)-hydroxyeicosatetraenoic acid (15-HETE), a product of arachidonic acid peroxidation, is an active component of hemozoin toxicity to monocytes.* Parassitologia. 1999 Sep;41(1-3):199–202.

33. Skorokhod A, Schwarzer E, Gremo G, Arese P. *HNE produced by the malaria parasite Plasmodium falciparum generates HNE-protein adducts and decreases erythrocyte deformability. Redox Rep* . Maney Publishing; 2007 Jan 19;12(1):73–5.

34. Skorokhod OA, Caione L, Marrocco T, Migliardi G, Barrera V, Arese P, et al. *Inhibition of erythropoiesis in malaria anemia: role of hemozoin and hemozoin-generated 4-hydroxynonenal.* Blood. American Society of Hematology; 2010 Nov 18;116(20):4328–37.

35. Thawani N, Tam M, Bellemare M-J, Bohle DS, Olivier M, de Souza JB, et al. *Plasmodium products contribute to severe malarial anemia by inhibiting erythropoietin-induced proliferation of erythroid precursors*. J Infect Dis. 2014 Jan 1;209(1):140–9.

36. Ru Y-X, Mao B-Y, Zhang F, Pang T, Zhao S, Liu J, et al. Invasion of erythroblasts by Pasmodium vivax: A new mechanism contributing to malarial anemia. Ultrastruct Pathol. 2009 Oct;33(5):236–42.

37. Othoro C, Lal AA, Nahlen B, Koech D, Orago AS, Udhayakumar V. *A low interleukin-10 tumor necrosis factor-alpha ratio is associated with malaria anemia in children residing in a holoendemic malaria region in western Kenya.* J Infect Dis. 1999 Jan 1;179(1):279–82.

38. Kurtzhals J, Akanmori B. *The cytokine balance in severe malarial anemia.* J Infect. 1999;180:1997–8.

39. Boeuf PS, Loizon S, Awandare GA, Tetteh JKA, Addae MM, Adjei GO, et al. *Insights into deregulated TNF and IL-10 production in malaria: implications for understanding severe malarial anaemia.* Malar J. 2012 Jan;11:253.

40. Thuma PE, van Dijk J, Bucala R, Debebe Z, Nekhai S, Kuddo T, et al. *Distinct clinical and immunologic profiles in severe malarial anemia and cerebral malaria in Zambia*. J Infect Dis. 2011 Jan 15;203(2):211–9.

41. McGuire W, Knight JC, Hill a V, Allsopp CE, Greenwood BM, Kwiatkowski D. *Severe malarial anemia and cerebral malaria are associated with different tumor necrosis factor promoter alleles*. J Infect Dis. 1999 Jan;179(1):287–90.

42. Awandare G a, Kempaiah P, Ochiel DO, Piazza P, Keller CC, Perkins DJ. *Mechanisms of erythropoiesis inhibition by malarial pigment and malaria-induced proinflammatory mediators in an in vitro model*. Am J Hematol. 2011 Feb;86(2):155–62.

43. Perkins DJ, Were T, Davenport GC, Kempaiah P, Hittner JB, Ong'echa JM. *Severe malarial anemia: innate immunity and pathogenesis.* Int J Biol Sci. 2011 Jan;7(9):1427–42.

44. McDevitt MA, Xie J, Shanmugasundaram G, Griffith J, Liu A, McDonald C, et al. *A critical role for the host mediator macrophage migration inhibitory factor in the pathogenesis of malarial anemia.* J Exp Med. 2006 May 15;203(5):1185–96.

45. Haldar K, Mohandas N. Malaria, erythrocytic infection, and anemia. Hematology Am Soc Hematol Educ Program. 2009 Jan;87–93.

46. Awandare GA, Martinson JJ, Were T, Ouma C, Davenport GC, Ong'echa JM, et al. *MIF (macrophage migration inhibitory factor) promoter polymorphisms and susceptibility to severe malarial anemia*. J Infect Dis. 2009 Aug 15;200(4):629–37.

47. Keller CC, Ouma C, Ouma Y, Awandare GA, Davenport GC, Were T, et al. *Suppression of a novel hematopoietic mediator in children with severe malarial anemia.* Infect Immun. 2009 Sep;77(9):3864–71.

48. Cromer D, Stark J, Davenport MP. *Low red cell production may protect against severe anemia during a malaria infection--insights from modeling*. J Theor Biol. 2009 Apr 21;257(4):533–42.

49. Ekvall H. *Malaria and anemia.* Curr Opin Hematol. 2003 Mar;10(2):108–14.

50. De Oca MM, Engwerda C, Haque *A. Plasmodium berghei ANKA (PbA) infection of C57BL/6J mice: a model of severe malaria*. Methods Mol Biol. 2013 Jan;1031:203–13.

51. Carvalho LJ de M, Alves FA, Oliveira SG de, Rio do Valle R del, Fernandes AAM, Muniz JAPC, et al. *Severe anemia affects both splenectomized and non-splenectomized Plasmodium falciparum-infected Aotus infulatus monkeys*. Mem Inst Oswaldo Cruz. Fundação Oswaldo Cruz; 2003 Jul;98(5):679–86.

52. Lamb TJ, Langhorne J. *The severity of malarial anaemia in Plasmodium chabaudi infections of BALB/c mice is determined independently of the number of circulating parasites.* Malar J. 2008 Jan;7:68.

53. Egan AF. *Aotus New World monkeys: model for studying malaria-induced anemia*. Blood. American Society of Hematology; 2002 May 15;99(10):3863–6.

54. Bhakdi S, Tranum-Jensen J. *Membrane damage by pore-forming bacterial cytolysins*. Microb Pathog. 1986;1(c):5–14.

55. Los FCO, Randis TM, Aroian R V, Ratner AJ. *Role of pore-forming toxins in bacterial infectious diseases*. Microbiol Mol Biol Rev. 2013 Jun;77(2):173–207.

56. Bernheimer AW, Rudy B. *Interactions between membranes and cytolytic peptides*. Biochim Biophys Acta - Rev Biomembr. 1986 Jun;864(1):123–41.

57. Johnson B, Heuck A. *Perfringolysin O Structure and Mechanism of Pore Formation as a Paradigm for Cholesterol-Dependent Cytolysins*. MACPF/CDC Proteins-Agents of Defence, Attack. 2014. p. 63–81.

58. Goñi FM, Ostolaza H. *E. coli alpha-hemolysin: a membrane-active protein toxin*. Braz J Med Biol Res. 1998 Aug;31(8):1019–34.

59. Baida G, Kuzmin N. *Cloning and primary structure of a new hemolysin gene from Bacillus cereus*. … Biophys Acta (BBA)-Gene Struct. 1995;1264:151–4.

60. Baida G, Kuzmin N. *Mechanism of action of hemolysin III from Bacillus cereus*. Biochim Biophys Acta (BBA). 1996;1284:122–4.

61. Ramarao N, Sanchis V. *The pore-forming haemolysins of bacillus cereus: a review*. Toxins (Basel). 2013 Jun;5(6):1119–39.

62. Chen Y-C, Chang M-C, Chuang Y-C, Jeang C-L. *Characterization and virulence of hemolysin III from Vibrio vulnificus*. Curr Microbiol. 2004 Sep;49(3):175–9.

63. Tang YT, Hu T, Arterburn M, Boyle B, Bright JM, Emtage PC, et al. *PAQR proteins: a novel membrane receptor family defined by an ancient 7-transmembrane pass motif.* J Mol Evol. 2005 Sep;61(3):372–80.

64. Smith JL, Kupchak BR, Garitaonandia I, Hoang LK, Maina AS, Regalla LM, et al. *Heterologous expression of human mPRalpha, mPRbeta and mPRgamma in yeast confirms their ability to function as membrane progesterone receptors.* Steroids. 2008 Oct;73(11):1160–73.

65. Villa NY, Moussatche P, Chamberlin SG, Kumar A, Lyons TJ. *Phylogenetic and preliminary phenotypic analysis of yeast PAQR receptors: potential antifungal targets*. J Mol Evol. 2011 Oct;73(3-4):134–52.

66. Mattiazzi Ušaj M, Prelec M, Brložnik M, Primo C, Curk T, Ščančar J, et al. *Yeast Saccharomyces cerevisiae adiponectin receptor homolog Izh2 is involved in the regulation of zinc, phospholipid and pH homeostasis*. Metallomics. 2015 DOI: 10.1039/c5mt00095e

67. Dibello, Julia R, Baylin, Ana, Viali, Satupaitea, Tuitele, John Bausserman, Linda McGarvey, Stephen T. *Adiponectin and type 2 diabetes in Samoan adults*. Am J Hum Biol. 2009;Jan;21(3):389–91.

68. Zhu Y, Bond J, Thomas P. *Identification, classification, and partial characterization of genes in humans and other vertebrates homologous to a fish membrane progestin receptor*. Proc Natl Acad Sci U S A. 2003 Mar 4;100(5):2237–42.

69. Aouida M, Kim K, Shaikh AR, Pardo JM, Eppinger J, Yun D-J, et al. *A Saccharomyces cerevisiae assay system to investigate ligand/AdipoR1 interactions that lead to cellular signaling*. PLoS One. 2013 Jan;8(6):e65454.

70. Moonah S, Sanders NG, Persichetti JK, Sullivan DJ. *Erythrocyte lysis and Xenopus laevis oocyte rupture by recombinant Plasmodium falciparum hemolysin III*. Eukaryot Cell. 2014 Oct;13(10):1337–45.

71. Saitou N, Nei M. *The neighbor-joining method: a new method for reconstructing phylogenetic trees.* Mol Biol Evol. 1987 Jul;4(4):406–25.

72. Efron B, Halloran E, Holmes S. *Bootstrap confidence levels for phylogenetic trees.* Proc Natl Acad Sci U S A. 1996 Nov 12;93(23):13429–34.

73. Zuckerkandl E, Pauling L. Molecules as documents of evolutionary history. J Theor Biol [Internet]. 1965 Mar [cited 2015 Jun 16];8(2):357–66.

74. Tamura K, Stecher G, Peterson D, Filipski A, Kumar S. MEGA6: *Molecular Evolutionary Genetics Analysis version 6.0*. Mol Biol. 2013 Dec;30(12):2725–9.

75. Maier AG, Braks J a M, Waters AP, Cowman AF. *Negative selection using yeast cytosine deaminase/uracil phosphoribosyl transferase in Plasmodium falciparum for targeted gene deletion by double crossover recombination.* Mol Biochem Parasitol. 2006;150(1):118–21.

76. Janse CJ, Franke-Fayard B, Mair GR, Ramesar J, Thiel C, Engelmann S, et al. *High efficiency transfection of Plasmodium berghei facilitates novel selection procedures*. Mol Biochem Parasitol. 2006;145(1):60–70.

77. Preston G, Carroll T, Guggino W, Agre P. *Appearance of water channels in Xenopus oocytes expressing red cell CHIP28 protein*. Science (80). 1992;2–4.

78. Aurrecoechea C et al. PlasmoDB: a functional genomic database for malaria parasites. [Internet] Nucleic Acids Res. Available from: http://plasmodb.org/plasmo/

79. Thermo Fisher Scientific Inc. Custom Mouse Monoclonal Antibody Development Protocols [Internet]. 2015. Available from: http://www.pierce-antibodies.com/custom-antibodies/mouse-monoclonal-antibody-development-protocols.cfm

80. Koh YT, Higgins SA, Weber JS, Kast WM. *Immunological consequences of using three different clinical/laboratory techniques of emulsifying peptide-based vaccines in incomplete Freund's adjuvant*. J Transl Med. 2006 Jan;4:42.

81. Pilon M, Svensk E. *PAQR-2 may be a regulator of membrane fluidity during cold adaptation.* Worm. 2013;(December):29–32.

Supplementary Figures

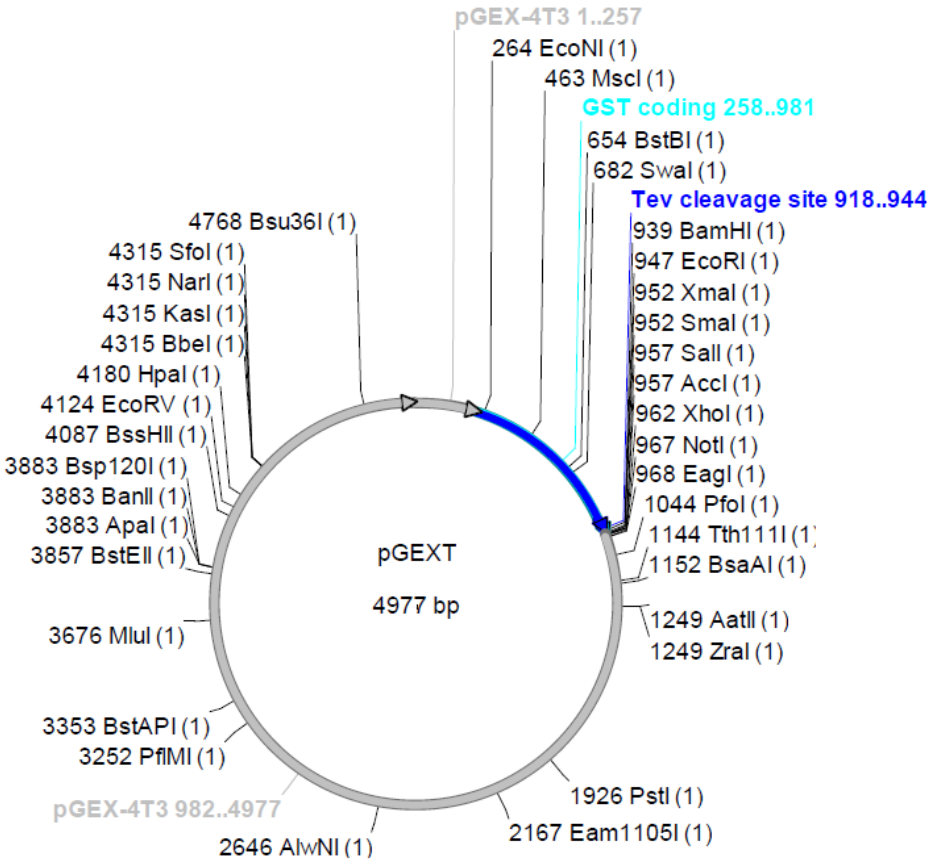

Supplementary Figure 2.1. pGEXT vector from Prigge Lab, used for GST-fusion protein production of GSTF80AA and GSTB80AA proteins with unique restriction enzyme sites designated.

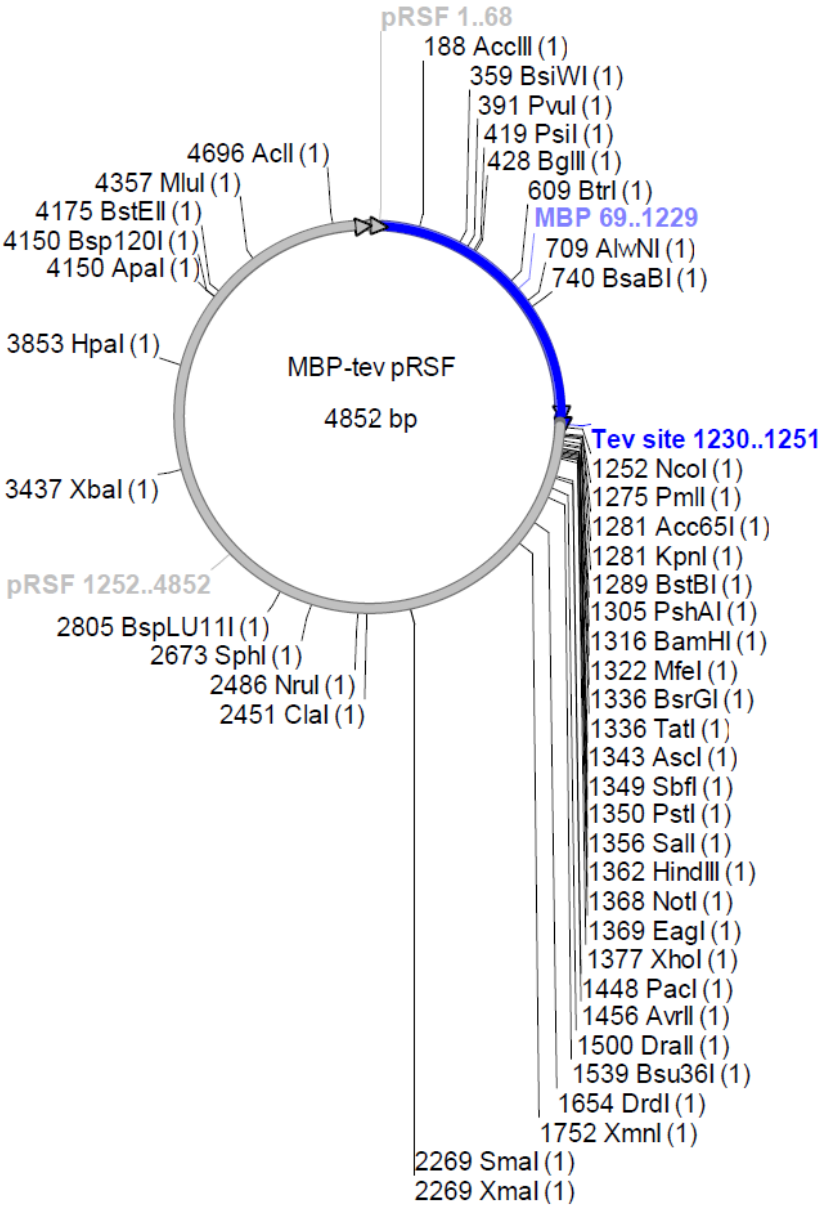

Supplementary Figure 2.2. MBP-tev pRSF from Bosch Lab, used for MBP-fusion protein production for MBPF80AA with unique restriction enzyme sites designated.

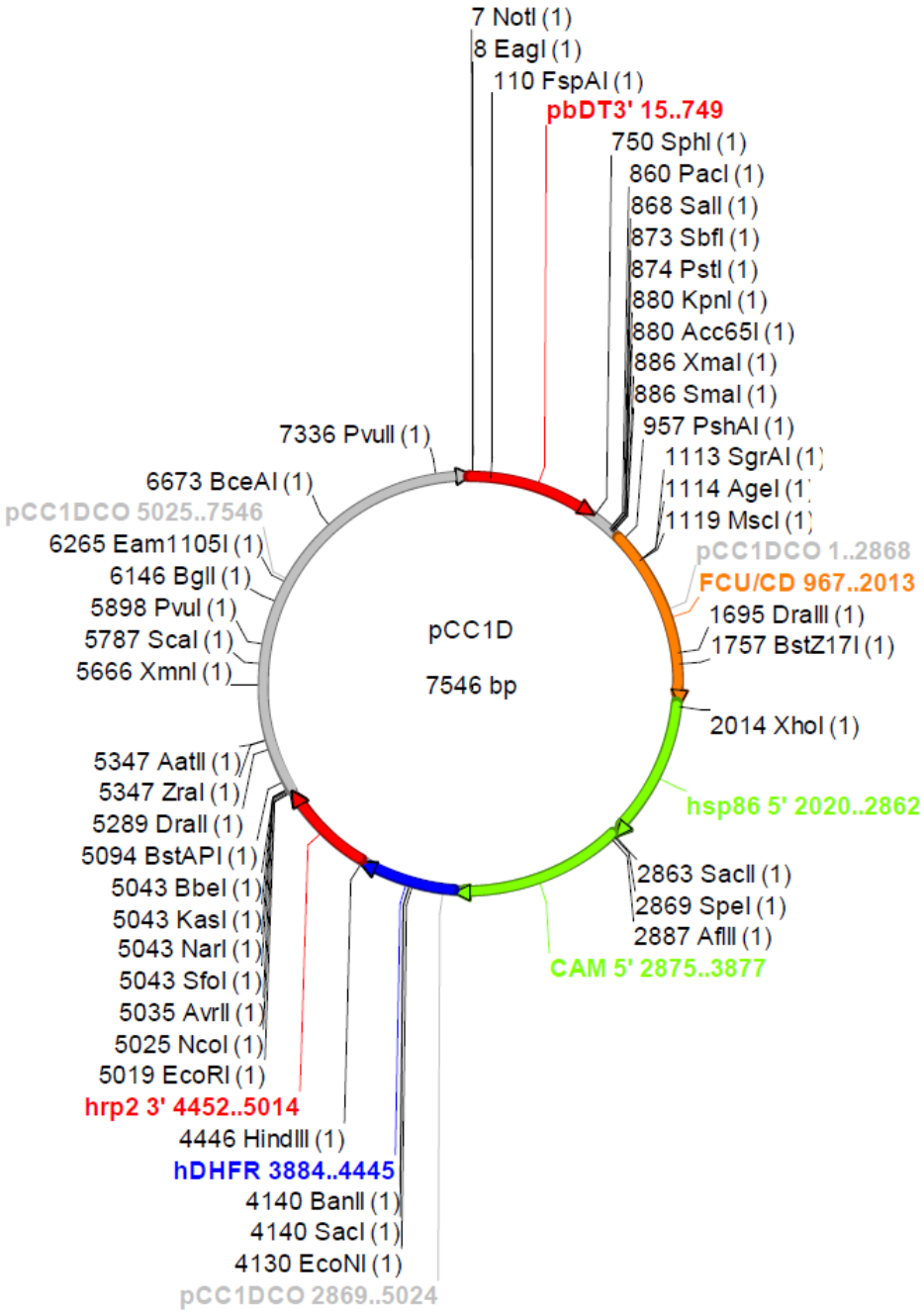

Supplementary Figure 2.3. pCC1D plasmid from Prigge Lab used for *P. falciparum* hemolysin III knockout construct with unique restriction enzyme sites designated.

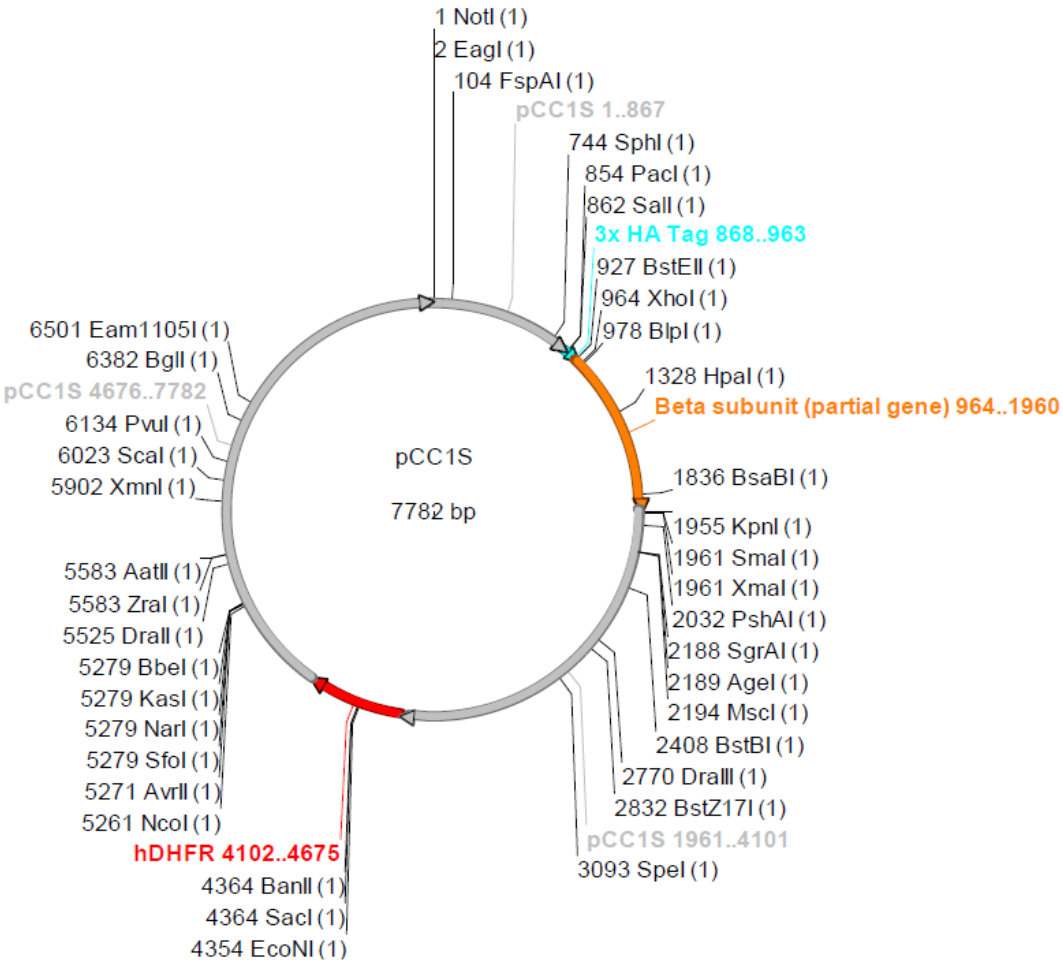

Supplementary Figure 2.4. pCC1S plasmid from Prigge Lab used for *P. falciparum* hemolysin III single crossover disruption construct with unique restriction enzyme sites designated.

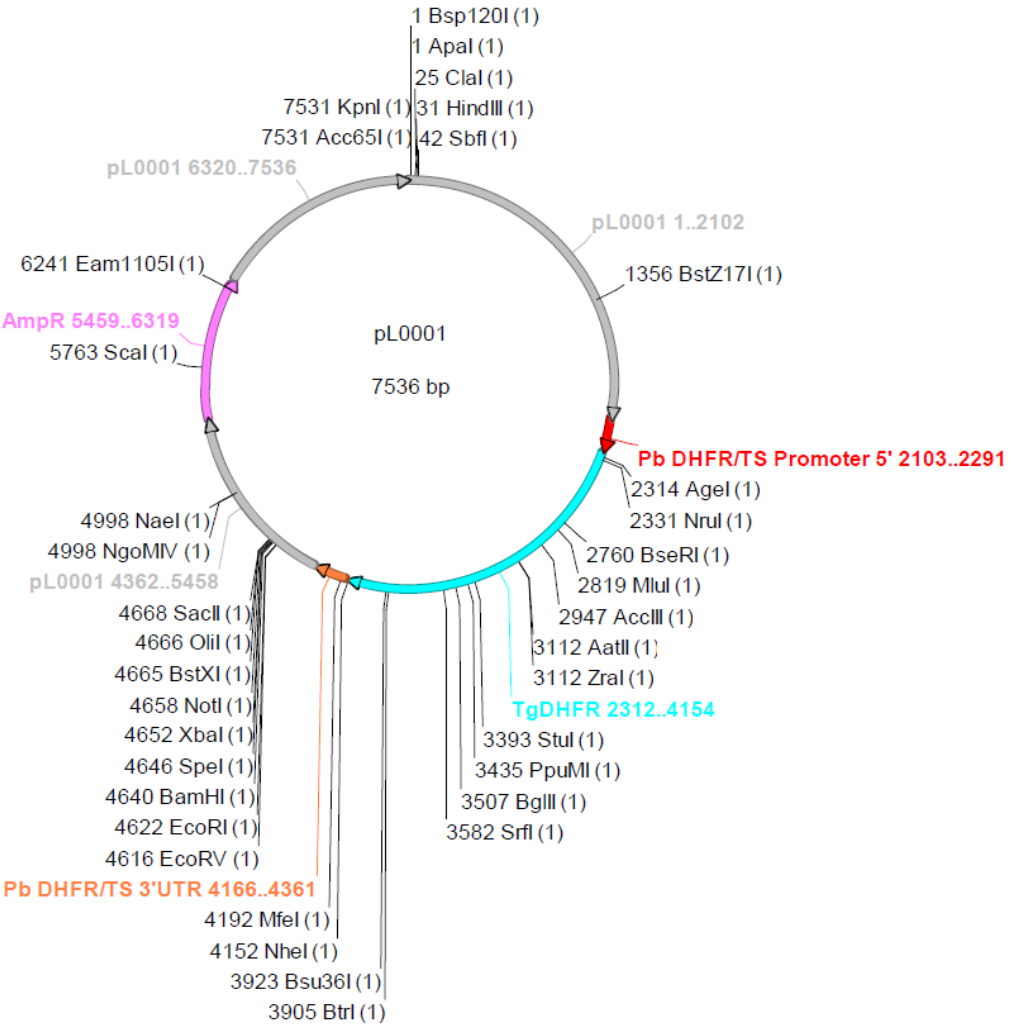

Supplementary Figure 2.5. pL0001 plasmid from Jacobs-Lorena Lab used for *P. berghei* hemolysin III knockout construct with unique restriction enzyme sites and ampicillin resistance designated.

CHAPTER 3: ANTIMALARIAL EFFICACY OF HYDROXYETHYLAPOQUININE (SN-119) AND DERIVATIVES

Adapted from previously published manuscript:

Sanders NG, Meyers DJ, Sullivan DJ. Antimalarial efficacy of hydroxyethylapoquinine (SN-119) and its derivatives. Antimicrob Agents Chemother. 2014 ;58(2):820-7. Epub 2013 Nov 18. PubMed PMID: 24247136

ABSTRACT

Hydroxethylapoquinine (HEAQ), once called hydroxyethylapocupreine, is a quinine derivative that was first synthesized in the early 1930's and proven to be effective as an antimalarial agent against bird malaria, as well as an antibacterial agent against human pneumococcal pneumonia. Strikingly, HEAQ was dosed at approximately eight grams per day in human pneumonia patients, with no toxic side effects reported due to the drug, suggesting that HEAQ is much less toxic than quinine. The advent of chloroquine and penicillin in the 1940's resulted in this drug being tabled in favor of cheaper, and in the case of penicillin, more effective compounds at the time. Later the artemisinins replaced chloroquine as the most effective antimalarial, and artemisinin-based combination therapies (ACTs) have been the standard treatment for malaria for over a decade. Unfortunately our current antimalarial arsenal has been crippled by the development of drug resistance to every major antimalarial drug class. Even the artemisinins are threatened due to the development of a delayed parasite clearance phenotype, even though there is no significant increase in the inhibitory dose that can kill 50% of the parasites (IC_{50}) reported for these compounds.

While novel antimalarial targets and new chemical classes are being explored to combat drug resistant parasites, compounds such as quinine are still relevant as they have proven efficacy against a genetically immutable target (hemozoin), and little sustained resistance in the field. The narrow therapeutic index associated with quinine and its diastereomer quinidine makes these compounds challenging for safety reasons, and less toxic derivatives would be valuable candidates for partner drugs for the artemisinins to

delay resistance and increase the longevity of the ACTs as effective antimalarials for as long as possible.

We found the historical use of HEAQ compelling, with proven efficacy against bird malaria and significantly greater tolerance at large doses in human patients than quinine. There is even one reference of Veterans returning from Korea being successfully treated with HEAQ for malaria. Here we report a novel synthesis of HEAQ from quinine, as well as three other new derivatives, the latter two based on the quinidine parent structure: hydroxyethylquinine (HEQ), hydroxyethylquinidine (HEQD), and hydroxyethylapoquinidine (HEAQD).

For my thesis we developed the following aims in order to determine whether HEAQ and derivatives would be good candidates for further antimalarial drug development: (1) Test whether the derivatives are able to inhibit heme crystallization similarly to the parent compounds which may suggest a similar mechanism of action against the malaria parasite, (2) Determine the antimalarial efficacy of all derivatives against *P. falciparum in vitro* and against *P. berghei* ANKA in a murine malaria model, and (3) Determine whether HEAQ and derivatives are less toxic than quinine and quinidine.

Quinoline compounds have been proven to inhibit heme crystallization in the parasite, and we demonstrated dose dependent inhibition of heme crystallization by all four derivatives, similar to quinine and quinidine, with HEQD having the greatest potency in the heme crystallization assay, with activity most similar to the parent compounds. We also found that the chemical property of fluorescence was maintained in

all derivatives, similar to quinine and quinidine, despite the modifications made to the side chains of the quinoline scaffold.

We tested all compounds against three strains of *P. falciparum* and found that all four derivatives inhibited the 3D7 strain with IC_{50}s less than 300 nM, about four times that of the parent drugs, while only the quinidine derivatives inhibited the chloroquine resistant (Dd2) or quinine tolerant strains (Dd2 and INDO) at appreciable levels, with IC_{50}s less than 1 μM. Similar results were seen when the compounds were tested *in vivo*, dosed orally in C57Bl/6 mice in a suppression test against *P. berghei* ANKA. HEAQ, HEQD, and HEAQD all demonstrated comparable efficacy, if less potency than parent compounds *in vivo*. Of note, the quinidine derivatives HEQD and HEAQD were equipotent with quinine and when combined with low doses of artesunate were able to cure mice and improve mouse survival better than quinidine plus artesunate.

Finally we used two measures to test the toxicity of the derivatives compared to quinine and quinidine: (1) Effect of drug exposure on mammalian cell culture viability, and (2) Human ether-à-go-go related gene (hERG) channel inhibition as a proxy for potential cardiotoxicity. In our cell culture assay we found that all derivatives showed no toxicity against human foreskin fibroblasts at 100 μM after 48 hours of incubation, and that HEQD and HEAQD were less toxic than both quinine and quinidine, with no toxicity up to 200 μM. As a perhaps more relevant measure of toxicity for the quinoline compounds, we determined the IC_{50}s of all compounds against hERG channels, suggestive of the propensity of the compounds to inhibit heart potassium channels, resulting in arrhythmias as a result of prolonged QRS/QT intervals. We found that HEQ, HEAQ and HEQD inhibited hERG channels at a much lower level than quinine (42 μM)

or quinidine (4 μM) with IC_{50}s of approximately 100 μM. HEAQD was about seven times less inhibitory than quinidine with an IC_{50} of 27 μM.

Overall we found that HEQD, one of the quinidine derivatives, was the most effective, least toxic compound we tested. This drug showed comparable antimalarial efficacy and potency to quinine, with no inhibition against hERG channels even at 100 μM, suggesting that the hydroxyethyl modification significantly decreased the likelihood of this compound to contribute to QT prolongation, while slightly decreasing the antimalarial potency of the drug. Further studies should be done to derivatize HEQD to improve the antimalarial potency particularly against drug resistant strains of the parasite, while maintaining the decreased toxicity. Further development of this compound is warranted and could result in a safer and more effective alternative to quinine for use in antimalarial therapy.

INTRODUCTION

Quinine: Discovery and Use

Cinchona bark, the source of quinine and other alkaloids, was used as early as the 17th century for treating fevers or 'ague' (1). However, it was not until 1820 that French physicians Pierre Joseph Pelletier and Joseph Caventou isolated quinine (Figure 3.1) and cinchonine from the bark, making these compounds available in a purified form (1). Following successful identification of quinine as an effective treatment for intermittent fevers, quinine became a valuable commodity and was used more often than the other alkaloids quinidine, cinchonine and cinchonidine due to the majority of obtainable Cinchona bark having a higher proportion of quinine (2).

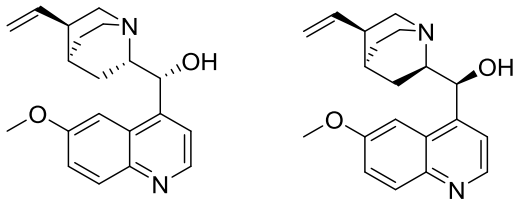

Figure 3.1 Chemical structure of diastereomers quinine (left) and quinidine (right).

Quinine was thus the first purified antimalarial drug and was the gold standard for treatment and prevention of malaria until the discovery of chloroquine in the 1940's. After chloroquine resistance developed in the late 1950's, quinine was again used as a key antimalarial until the introduction of the artemisinins in the 1980's and continues to be used to treat uncomplicated malaria in pregnant women during the first trimester, as well as severe malaria when intravenous artesunate or artemether are unavailable (2–4). Periodic reports of drug resistance to quinine do exist, mainly in Southeast Asia and

South America, but the development of resistance is slow and not sustained, classified as ‘low grade’, with no ‘high grade’ resistance noted for severe malaria cases, with treatment failures more often due to non-compliance to a treatment regimen rather than an actual increase in IC_{50} (2,3,5). Economically feasible drugs that can rapidly kill the parasite are especially crucial in light of the fact that definitive drug resistance or delayed parasite clearance has been reported for all classes of antimalarials available, including artemisinin-based combined therapies (6–9).

Though quinine and its diastereomer quinidine have proven to be effective antimalarial drugs, both compounds have narrow therapeutic indices, that is, the effective dose is very close to doses associated with toxicity. In particular, higher doses of quinine and quinidine may result in cardiotoxicity associated with delayed ventricular depolarization and in the case of quinidine, repolarization, leading to a prolonged QRS or QT interval respectively (10). Blindness is another severe adverse event associated with quinine overdose, while other side effects include tinnitus, hearing loss, headache and loss of taste sensation (3). In light of these quinine-associated toxicities, a novel compound, similar to quinine but less toxic would be ideal as either a partner drug with artemisinin-related compounds or as a replacement for other antimalarial drugs that have become ineffective due to resistance.

The Search for an Antimalarial 'As Good As or Better Than Quinine'

Many efforts have been devoted to derivitizing the cinchona alkaloid series in hopes of discovering more effective and less toxic alternatives to quinine and include the discoveries of the 4-amino and 8-amino quinolines such as chloroquine and mefloquine. The levarotatory alkaloids including cupreine, quinine and cinchonine (Figure 3.2) as well as their diastereomers (not shown) have been modified at R and R' with varied results in their antimalarial activity, none of which were particularly promising beyond a moderate chain length addition via alkylation to the R position (11).

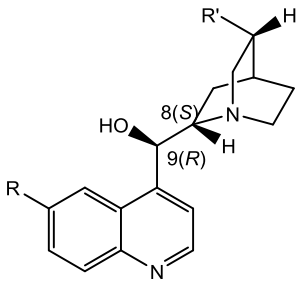

Figure 3.2 Cupreine (R=OH, R'= CH=CH2)

Dr. Robert Hegner, a dedicated scientist in the Department of Protozoology of the Johns Hopkins School of Hygiene and Public Health spent many years in the pursuit of a drug 'as good as or better than quinine', resulting in valuable insights regarding solubility and pharmacokinetic properties of various quinoline derivations (12,13). In 1939 Hegner announced in his published work that such a drug had been found, namely hydroxyethylapocupreine, or HEAQ (Figure 3.3, (13)). Hegner reported the efficacy of HEAQ in the treatment of three strains of bird malaria: *Plasmodium lophurae* (ducks), *P. relictum* (pigeons), and *P. cathemerium* (canaries). HEAQ was found to have similar

efficacy to quinine against all three strains when used at four times the dose of the parent drug, making it as effective, but less potent than quinine (13,14).

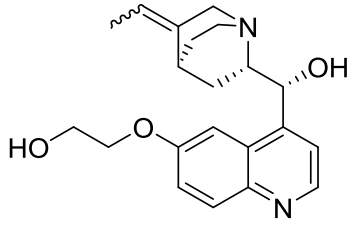

Figure 3.3 Hydroxyethylapoquinine (HEAQ), a derivative of quinine, with an isomerization of the R' group and a hydroxyethyl substitution at the R group

At the same time the bird antimalarial studies were being completed for HEAQ by Hegner's group, Dr. W. W. G. Maclachlan was treating human pneumococcal pneumonia patients with HEAQ in Pittsburg, Pennsylvania. Specifically HEAQ was used at doses of eight grams per day as an effective antibacterial compound from 1936-1939 in the treatment of over five hundred pneumonia cases, resulting in a fifty percent reduction in mortality with no visual disturbances or severe adverse effects, including atrial fibrillation, noted for the drug (15–17). At such large doses, the lack of side effects reported suggests that HEAQ is much less toxic than quinine in humans. Most intriguing is a report by Dr. Maclachlan in 1963 in which he states, "We were aware of the fact that in malaria hydroxyethylapocupreine [HEAQ] was as effective as quinine as observed in some clinical cases in Veterans from Korea and also in Venezuela, in addition to experimental studies recorded by Hegner et al" (18).

Because no formal human trials have been conducted for the use of HEAQ against *P. falciparum*, we sought to examine activity *in vitro* with human *P. falciparum* and *in vivo* with the mouse malaria model as well as the important chemical property of quinolines to inhibit hERG channels. Here we resynthesized and tested HEAQ, in addition to three novel compounds, hydroxyethylquinine (HEQ) and the diastereomers hydroxyethylquinidine (HEQD) and hydroxyethylapoquinidine (HEAQD), against *P. falciparum in vitro* as well as in a murine malaria model to determine the efficacy of these drugs compared to the parent compounds quinine and quinidine. Further characterization in regards to the mechanism of action and chemical properties of these derivatives was also conducted, along with cytotoxicity studies using human fibroblasts and hERG channel inhibition studies.

MATERIALS AND METHODS

General Information:

All reagents and solvents were used as supplied by commercial sources without further purification. All dry solvents were purchased from Aldrich as Sure Seal bottles. Reactions involving air and/or moisture sensitive reagents were carried out under an argon atmosphere using glassware that was dried under vacuum with a heat gun. The evacuated flask was then filled with argon. The reactions were monitored by thin layer chromatography using Analtech chromatography plates (silica gel GHLF, 250 microns). Visualization was performed by UV light (254 and 365 nm) and/or by staining with potassium permanganate. Flash chromatography was performed using a Grace Reveleris flash purification system and Grace silica cartridges (avg. particle size 40 um). ^{1}H (500 MHz) and ^{13}C (125 MHz) NMR spectra of compounds were obtained using a Varian Mercury spectrometer. ^{1}H NMR spectra recorded in CD_3OD were referenced to 3.310 ppm. ^{13}C NMR spectra recorded in CD_3OD were referenced to 39.15 ppm. Accurate mass determinations were recorded by the Mass Spectrometry Facility located at the University of California, Riverside.

Synthesis and Analysis of HEAQ and Derivatives

Preparation of demethyl quinine (cupreine):

Modified procedure adapted from Xu, F.; *et al* (19) and Furuya, T.; et al (20)
A 500 ml three-necked flask equipped with an argon inlet, a reflux condenser and a large magnetic stir bar (38 x 16 mm) was charged with DMF (100 ml) and 95% sodium hydride (5.92 g, 247 mmol, 8 equiv.). Ethanethiol (Stench! 18.3 ml, 247 mmol, 8 equiv.) was added drop-wise while cooling with an ice water bath. Note that after the addition of

approximately 10 ml of ethanethiol, stirring became difficult. The reaction was allowed to warm to room temperature and quinine (10.0 g, 30.8 mmol, 1 equiv.) was added in one portion. Once the reaction could be efficiently stirred, the remainder of the ethanethiol was added drop-wise at room temperature. Once the addition of ethanethiol was complete, the reaction was stirred at 100 ºC for 24 hours. The reaction mixture was cooled to ambient temperature, quenched with sat. aq. NH_4Cl and water, and the aqueous layer extracted with ethyl acetate (3 x 200 ml). The organic phase was dried with anhydrous $MgSO_4$, and approximately 300 ml of volatiles were removed by simple distillation in a well-ventilated hood (Stench!). During cooling to ambient temperature, an off-white crystalline solid formed in the still pot and was filtered via vacuum filtration to obtain 6.85 g (72% yield). Product was consistent with previously reported characterization data.[24] ^{1}H NMR (500 MHz, METHANOL-d4) δ 8.60 (d, J = 4.56 Hz, 1H), 7.91 (d, J = 9.12 Hz, 1H), 7.63 (d, J = 4.56 Hz, 1H), 7.34 (dd, J = 2.52, 9.12 Hz, 1H), 7.30 (d, J = 2.52 Hz, 1H), 5.76 (ddd, J = 7.47, 10.14, 17.29 Hz, 1H), 5.54 (d, J = 3.14 Hz, 1H), 4.99 (td, J = 1.49, 17.13 Hz, 1H), 4.92 (td, J = 1.34, 10.38 Hz, 1H), 3.68 - 3.80 (m, 1H), 3.08 - 3.20 (m, 2H), 2.68 - 2.82 (m, 2H), 2.40 (br. s., 1H), 1.85 - 1.97 (m, 2H), 1.79 - 1.85 (m, 1H), 1.56 - 1.68 (m, 1H), 1.46 (tdd, J = 3.30, 10.06, 13.20 Hz, 1H). ^{13}C NMR (126 MHz, METHANOL-d4) δ 158.1, 149.6, 147.6, 144.1, 142.4, 131.6, 128.5, 123.5, 120.0, 115.3, 105.3, 72.0, 61.1, 57.5, 44.5, 40.8, 29.2, 28.0, 21.7

Preparation of demethyl quinidine:

The same procedure for the conversion of quinine to dimethyl quinine was used for the conversion of quinidine (5.00 g, 15.4 mmol) to demethyl quinidine, but product did not crystallize. Oil was purified via flash chromatography (gradient 99% $CHCl_3$ plus

1% Et_3N to 10% MeOH/89% $CHCl_3$ plus 1% Et_3N) to obtain 3.47 g of a yellow glass. This material contained approximately 10% quinidine and was carried on to the next step without further purification.

Preparation of hydroxyethylquinine (HEAQ) and hydroxylethylquinidine (HEAQD) was carried out as described by Carlson, W.W.; et al (21).

Preparation of HEAQ

To a single-necked 50 ml RBF equipped with a reflux condenser was added ethylene carbonate (5.25 g, 59.6 mmol, 20.0 equiv.), potassium carbonate (824 mg, 5.96 mmol, 2.00 equiv.), demethyl quinine **2** (926 mg, 2.98 mmol, 1.00 equiv.) and 5 ml anhydrous *tert*-butanol. The reaction was placed in a preheated oil bath (95 ºC) for 1 h. The reaction was then poured while still hot onto ice and approximately 10-20 ml of 5 M aq. NaOH. The reaction was extracted with dichloromethane and volatiles removed to obtain a brown oil. This material was purified via flash chromatography (gradient 99% $CHCl_3$ plus 1% Et_3N to 10% MeOH/89% $CHCl_3$ plus 1% Et_3N) to obtain 854 mg of a brown glass. The brown glass was dissolved in ca. 5 ml of hot 95% EtOH, allowed to cool to ambient temperature, and then placed in a -20 ºC freezer. Pink-tan crystals formed (726 mg) and were collected by vacuum filtration. ^{1}H NMR (500 MHz, METHANOL-d4) δ 8.66 (d, J = 4.56 Hz, 1H), 7.96 (d, J = 9.12 Hz, 1H), 7.68 (d, J = 4.56 Hz, 1H), 7.42 - 7.51 (m, 2H), 5.76 (ddd, J = 7.62, 10.14, 17.29 Hz, 1H), 5.58 (d, J = 3.14 Hz, 1H), 4.97 (td, J = 1.49, 17.13 Hz, 1H), 4.90 (td, J = 1.34, 10.37 Hz, 1H), 4.20 - 4.29 (m, 2H), 3.93 - 4.01 (m, 2H), 3.69 (dddd, J = 2.36, 5.03, 10.65, 13.24 Hz, 1H), 3.06 - 3.17 (m, 2H), 2.64 - 2.78 (m, 2H), 2.36 (br. s., 1H), 1.83 - 1.96 (m, 2H), 1.76 - 1.83 (m, 1H), 1.54 - 1.65 (m, 1H), 1.46 (tdd, J = 3.22, 9.96, 13.15 Hz, 1H). ^{13}C NMR (126 MHz, METHANOL-d4) δ

159.1, 150.7, 148.3, 144.9, 142.8, 131.6, 128.2, 123.8, 120.2, 115.1, 103.4, 72.3, 71.4, 61.7, 61.2, 57.7, 44.3, 41.0, 29.3, 28.3, 21.8. HRMS (*m/z*): [MH^+] calculated for $C_{21}H_{27}N_2O_3$ 355.2016, found 355.2012.

Preparation of HEAQD

To a single-necked 100 ml RBF equipped with a reflux condenser was added ethylene carbonate (19.7 g, 224 mmol, 20.0 equiv.), potassium carbonate (3.09 g, 22.4 mmol, 2.00 equiv.), crude demethyl quinidine (3.47 g, 11.2 mmol, 1.00 equiv.) and 18.6 ml anhydrous *tert*-butanol. The reaction was placed in a preheated oil bath (95 ºC) for 3 h. The reaction was then poured while still hot onto ice and 10-20 ml of 5 M aq. NaOH. The reaction was extracted with dichloromethane to obtain a brown oil which was purified via flash chromotography (gradient 99% $CHCl_3$ plus 1% Et_3N to 10% MeOH/89% $CHCl_3$ plus 1% Et_3N) to obtain a reddish-orange glass. This material was crystallized from hot ethyl acetate to obtain 1.79 g of an off-white crystalline solid. ^{1}H NMR (500 MHz, METHANOL-d4) δ 8.66 (d, J = 4.56 Hz, 1H), 7.95 (d, J = 9.12 Hz, 1H), 7.69 (d, J = 4.56 Hz, 1H), 7.41 - 7.48 (m, 2H), 6.14 - 6.21 (m, 1H), 5.63 (d, J = 3.14 Hz, 1H), 5.05 - 5.14 (m, 2H), 4.20 - 4.27 (m, 2H), 3.96 (t, J = 4.72 Hz, 2H), 3.56 (ddd, J = 2.12, 7.78, 13.52 Hz, 1H), 3.05 (dt, J = 2.59, 9.08 Hz, 1H), 2.88 - 2.95 (m, 2H), 2.77 - 2.86 (m, 1H), 2.20 - 2.35 (m, 2H), 1.73 (br. s., 1H), 1.53 - 1.64 (m, 2H), 1.08 (ddd, J = 4.09, 9.43, 13.52 Hz, 1H). ^{13}C NMR (126 MHz, METHANOL-d4) δ 159.0, 150.9, 148.3, 144.9, 142.0, 131.5, 128.2, 123.7, 120.1, 115.2, 103.3, 72.6, 71.4, 61.7, 60.9, 51.0, 50.5, 41.6, 29.9, 27.4, 21.3. HRMS (*m/z*): [MH^+] calculated for $C_{21}H_{27}N_2O_3$ 355.2016, found 355.2022.

General procedure for the preparation of HEAQ or HEAQD was carried out as described by Portlock, D.E.; *et al* (22) (analytical scale double bond isomerization):

HEAQ

To a solution of HEQ (250.0 mg, 0.705 mmol, 1.00 equiv.), 12 ml of 50% aq. ethanol and 0.59 ml of conc. HCl (7.05 mmol, 10.0 equiv.) was added 12.5 mg of 5 wt% of Rhodium catalyst on activated carbon. The mixture was heated to reflux for 24 hrs. After allowing the reaction to cool to ambient temperature, the reaction was vacuum filtered through celite, and the volatiles of the filtrate were removed *in vacuo*. The residue was taken up in water, and the pH was made basic with conc. NH_4OH. The resulting white precipitate was vacuum filtered and dried under high vacuum to obtain 192 mg (76%) of a white amorphous solid. ^{1}H NMR (500 MHz, METHANOL-d4) δ 8.66 (d, J = 4.56 Hz, 1H), 7.95 (d, J = 8.80 Hz, 1H), 7.68 (d, J = 4.56 Hz, 1H), 7.36 - 7.58 (m, 2H), 5.60 - 5.72 (m, 1H), 5.08 - 5.28 (m, 1H), 4.15 - 4.39 (m, 2H), 3.89 - 4.06 (m, 2H), 3.69 - 3.87 (m, 1H), 3.38 - 3.59 (m, 2H), 3.02 - 3.15 (m, 1H), 2.68 - 2.87 (m, 1H), 2.35 (br. s., 1H), 2.07 - 2.19 (m, 1H), 1.83 - 1.98 (m, 1H), 1.56 - 1.71 (m, 1H), 1.53 (d, J = 6.76 Hz, 1H), 1.47 (d, J = 6.76 Hz, 2H), 1.16 - 1.38 (m, 1H). ^{13}C NMR (126 MHz, METHANOL-d4) δ 159.1, 150.8, 148.3, 144.9, 141.5, 140.4, 131.5, 128.1, 123.7, 120.1, 115.9, 115.7, 103.4, 103.4, 72.3, 71.4, 71.4, 62.0, 61.7, 61.7, 59.9, 57.6, 45.0, 45.0, 34.7, 28.6, 28.4, 27.5, 27.3, 27.2, 12.9, 12.6. HRMS (*m/z*): [MH^+] calculated for $C_{21}H_{27}N_2O_3$ 355.2016, found 355.2017.

HEAQD:

The same procedure was used for HEQD to obtain 264 mg (88%) of a white amorphous solid. ^{1}H NMR (500 MHz, METHANOL-d4) δ 8.65 (d, J = 4.56 Hz, 1H),

7.95 (d, J = 9.59 Hz, 1H), 7.59 - 7.73 (m, 1H), 7.39 - 7.53 (m, 2H), 5.52 - 5.72 (m, 1H), 5.09 - 5.32 (m, 1H), 4.17 - 4.40 (m, 3H), 3.36 (d, J = 17.13 Hz, 1H), 3.14 - 3.28 (m, 1H), 2.88 - 3.04 (m, 1H), 2.70 - 2.88 (m, 1H), 2.35 (br. s., 1H), 1.98 - 2.13 (m, 1H), 1.58 - 1.71 (m, 3H), 1.55 (d, J = 6.76 Hz, 3H), 1.32 - 1.50 (m, 1H). ^{13}C NMR (126 MHz, METHANOL-d4) δ 159.0, 159.0, 150.7, 150.7, 148.3, 144.9, 144.9, 142.5, 141.4, 131.5, 128.2, 128.2, 123.8, 123.7, 120.2, 120.1, 114.3, 114.0, 103.4, 103.3, 72.6, 72.5, 71.4, 71.4, 61.7, 60.7, 60.7, 53.3, 52.2, 51.8, 51.0, 34.9, 28.2, 28.0, 27.4, 27.4, 27.0, 12.9, 12.6. HRMS (*m/z*): [MH^+] calculated for $C_{21}H_{27}N_2O_3$ 355.2016, found 355.2029.

Heme Crystallization Inhibition Assay

The heme extension assay was designed to mimic hemozoin crystal formation in the parasite digestive vacuole, using acidic pH and lipids to initiate crystallization of monomeric heme. Drug dilutions were made from DMSO or water 10 mM stocks with 100 mM sodium acetate, pH 4.8 and aliquotted in a 96 well plate (costar 3595) in triplicate, with five serial, two-fold dilutions per drug. Heme stock (10 mM) was made in DMSO and was diluted to 50 µM with 100 mM sodium acetate, pH 4.8. 10 mM 1-Monooleoyl-rac-glycerol (MOG) stock was made in ethanol and sonicated before addition to 50 µM heme stock to make 25 µM MOG, 50 µM heme in 100 mM sodium acetate, pH 4.8. The 25 µM MOG/50 µM heme solution was sonicated and added to the assay plate, 100 µL/well. The plates were incubated at 37°C for two hours to allow crystallization, followed by addition of 100 µL 100 mM sodium bicarbonate pH 9.1 to solubilize any remaining monomeric heme. After an incubation of one hour at room temperature, the amount of solubilized monomeric heme was determined by measuring absorbance at 405 nm and calculating the nanomoles of heme based on a previously

determined standard curve. Finally, 20 µL of 1 M sodium hydroxide was added to the plates to dissolve any crystals that formed, and absorbance was read at 405nm to determine the total amount of heme present in each well. Data was exported to Microsoft Excel and inhibition of heme crystallization was determined as a function of the total nanomoles of monomeric heme minus the unincorporated heme, divided by the total nanomoles of heme crystal formed in the no drug control.

Fluorescence Determination

To verify that the four quinoline derivatives retained fluorescent chemical properties similar to quinine and quinidine, 1 M drug stocks of quinine, quinidine, HEAQ and HEAQD were made in 1 M sulfuric acid. The solutions were diluted 1:100 in distilled water and five dilutions of these stocks were made using 0.05 M sulfuric acid. The fluorescence of these compounds was determined at 350 and 450 nm.

72-hour SYBR Green I Parasite Inhibition Assay

A 72-hour SYBR Green I assay was used to determine the sensitivity of three strains of *P. falciparum* (3D7, INDO, Dd2 obtained from Malaria Research Reference Reagent Resource) to quinine, quinidine, ART, CQ, and derivatives HEQ, HEAQ, HEQD and HEAQD. Drug stocks were prepared at 10 mM concentrations in DMSO or water, filter-sterilized, and stored at -20°C. Dilutions were made in RPMI 1640 medium to the appropriate starting concentration, followed by serial two-fold dilutions to generate 5-10 concentrations for each drug. Drugs (10 µL) were aliquotted in triplicate into 96-well plates (Costar #3595) at ten times the final concentration. *P. falciparum* cultures were synchronized and diluted to 2% ring stage and adjusted to1% hematocrit with uninfected erythrocytes. The cultures (90 µL) were then added to the assay plates and the plates

were incubated in a gassed chamber at 37°C for 72-hours until no drug control parasitemia reached between 10-15% (late trophozoite or schizont stages). Assay plates were frozen at -80°C for at least one hour or overnight, followed by thawing at 37°C for 1-2 hours. Immediately after the freeze-thaw, 100 µL of 2X SYBR Green I in lysis buffer (Tris 20 mM, pH 7.5, EDTA 5 mM, Saponin .008% wt/vol, Triton X-100 .08% vol/vol) was added to each well for a total volume of 200 µl/well and mixed by pipetting up and down. The plates were allowed to incubate, protected from light, for at least one hour. Fluorescence was measured at 485 and 535 nm using an HTS 7000 Plus BioAssay reader, adjusting the gain between 80-90 for optimal reads. Data was exported to Microsoft Excel, where background fluorescence from the positive controls (1 mM chloroquine) was subtracted from each sample and percent inhibitions were calculated by dividing the sample fluorescence by the no drug controls and multiplying by one hundred. IC_{50}'s were calculated as the concentration of drug required to inhibit 50% of the parasite growth in the no drug control. At least three replicates were completed for each strain of *P. falciparum* and each drug unless otherwise noted.

Murine Malaria Model

We obtained fifty-five C57/Bl6 mice, 5 weeks old, and weighing between 15-23 g from Jackson Labs for our experiment (n=5 mice per group, 12 groups; 4 mice were used in the artesunate alone group). Mice were kept in Johns Hopkins Bloomberg School of Public Health mouse facility according to the ACUC animal protocol number MO09H401. Mice were infected intraperitoneally with *Plasmodium berghei* ANKA ($1x10^7$ infected erythrocytes) and drugs were administered orally twice a day using sterile plastic feeding tubes (Instech Solomon Scientific FTP 2038) for five days beginning

twenty-four hours post infection. All quinoline salts were dissolved in distilled water (8 mg/ml or 2 mg/ml) and artesunate was dissolved in 100% ethanol (100 mg/ml) and diluted 1:100 in distilled water. The effects of compounds on parasite levels and mouse survival were determined by measuring weekly parasitemia levels by Giemsa-stained blood smears and checking mouse survival daily for up to thirty days.

Human Ether-a-go-go (hERG) channel inhibition Ionworks patch clamp assay

hERG channels were stably expressed in Chinese hamster ovary (CHO) cells which were held at -70 mV and hERG currents were evoked by two voltage pulses. During the first pulse, cells were depolarized to +40 mV for 2 s and hyperpolarized to -30 mV for 2 s. This was repeated after a 3 s holding at -70 mV. The difference of tail currents at the second pulse between pre-compound and post-compound addition was used to measure compound activity, with dofetilide and buffer as positive and negative controls respectively. Compounds were dissolved in DMSO and diluted 1:3 in an 8-point gradient with the maximum concentration at 100 μM. In order to be classified as a hERG inhibitor, the compounds caused more than three standard deviations of reduction in hERG currents. Dofetilide was used as a control

48-hour Alamar Blue Assay with Human Foreskin Fibroblasts

Human Foreskin Fibroblasts (ATCC CRL-1635) were grown and harvested at log phase (Day 3 after passage). Cells were plated at 10,000 cells per well in 200 μL of MEM supplemented with 10% FBS, 1% penicillin/streptomycin, and 1% L-glutamine in a 96 well plate (costar 3595) and allowed to incubate for one day at 37°C, 5% CO_2 until cells again reached log phase. After 24 hrs, 100 μL MEM was removed and replaced with fresh media. After another 24 hr-incubation, 150 μL medium was removed from wells,

and 150 µL drug dilutions made in MEM from 10 mM stocks were added to the assay plate in triplicate, with four two-fold serial dilutions of drug. Plates were incubated for two days at 37°C, 5% CO_2. After 48 hrs, 20 µL of Alamar blue was added to each well, including a no drug control as well as a blank well with media only. Sample fluorescence was read on an HTS 700 Plus Bio Assay Reader at 550 and 595 nm and data was exported to Microsoft Excel. Cytotoxicity of drugs was calculated as the percentage of the no drug growth control after 48 hours.

RESULTS

Synthesis and Analysis of HEAQ and Derivatives

We modified the original synthetic approach of Butler and Cretcher in 1937 and 1938 to prepare HEAQ from quinine and HEAQD from quinidine (Figure 3.4 (23,24)). Per Xu, F et al., 2010 and Furuya, T et al., 2009, quinine (QN) underwent demethylation in the presence of sodium ethanethiolate to form cupreine (19,20). Formation of the hydroxyethyl ether was accomplished by reacting cupreine with ethylene carbonate and potassium carbonate, yielding HEQ according to Carlson, W.W. et al., 1947 (21). Finally, rhodium catalyzed positional isomerization of the terminal alkene of HEQ resulted in the final product, HEAQ (E, Z) as a mixture of *E* and *Z* geometric isomers. A similar approach was used to produce HEQD and HEAQD (E, Z), using quinidine (QND) as the parent compound. The crystalline alkaloids of HEAQ, HEQD and HEAQD were initially obtained from solution as free bases and later converted to hydrochloride salts for use in animal studies.

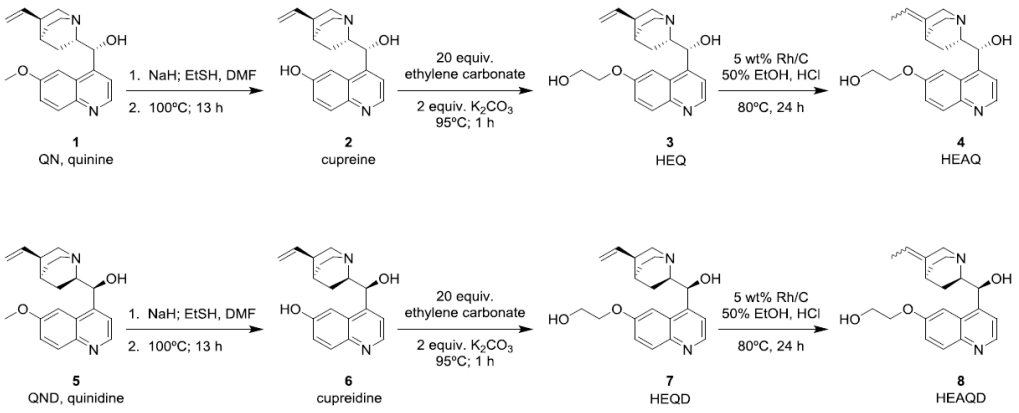

Figure 3.4 Scheme for synthesis of derivatives HEQ, HEAQ, HEQD, and HEAQD

Heme Crystal Inhibition and Fluorescence

Antimalarial quinolines accumulate in the parasite digestive vacuole and are thought to inhibit *Plasmodium* growth by forming an intermolecular hydrogen bond with heme, disrupting formation of the hemozoin crystals resulting in the buildup of free heme which can become oxidized and then is toxic to the parasite (25–27). All derivatives were found to inhibit heme crystallization in the presence of lipid at pH 4.6 similarly to quinine and quinidine (Figure 3.5), but only HEQD appreciably inhibited heme to the same extent as quinine and quinidine *in vitro*.

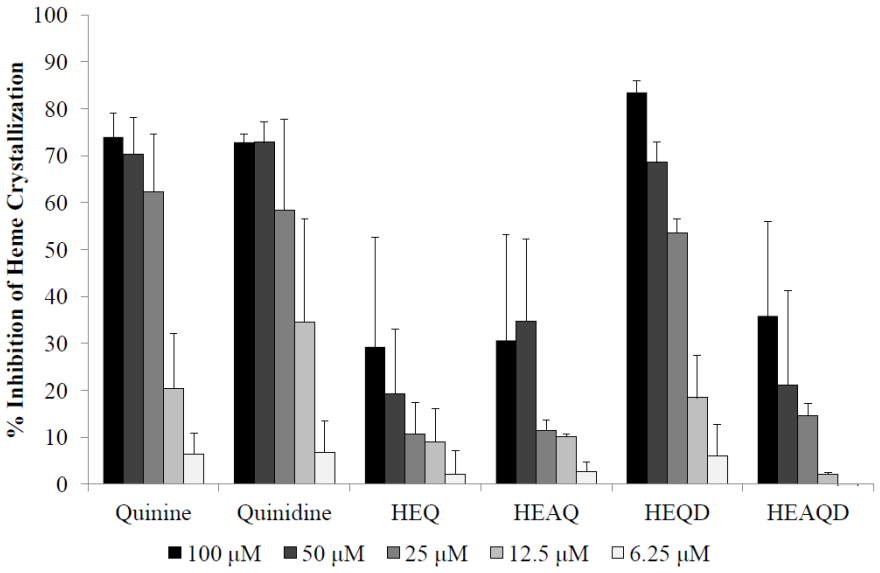

Figure 3.5 Quinine, quinidine and derivatives in inhibit heme crystallization after 16 hours. Two to five independent experiments were completed for each compound with each concentration in triplicate, reported with corresponding standard error of the mean. Mean IC_{50} values calculated for all compounds in the order listed above were 16.3, 16.0, 208, 59.3, 24.0, and 155 µM respectively.

Quinine's inherent fluorescent properties have been well-described, and in fact quinine is often used as a fluorescent standard (28,29). We wanted to determine whether our modifications in any way altered the fluorescent properties of our four quinoline derivatives. We found all four derivatives to fluoresce in a dose-dependent manner similarly to the parent compounds (Figure 3.6).

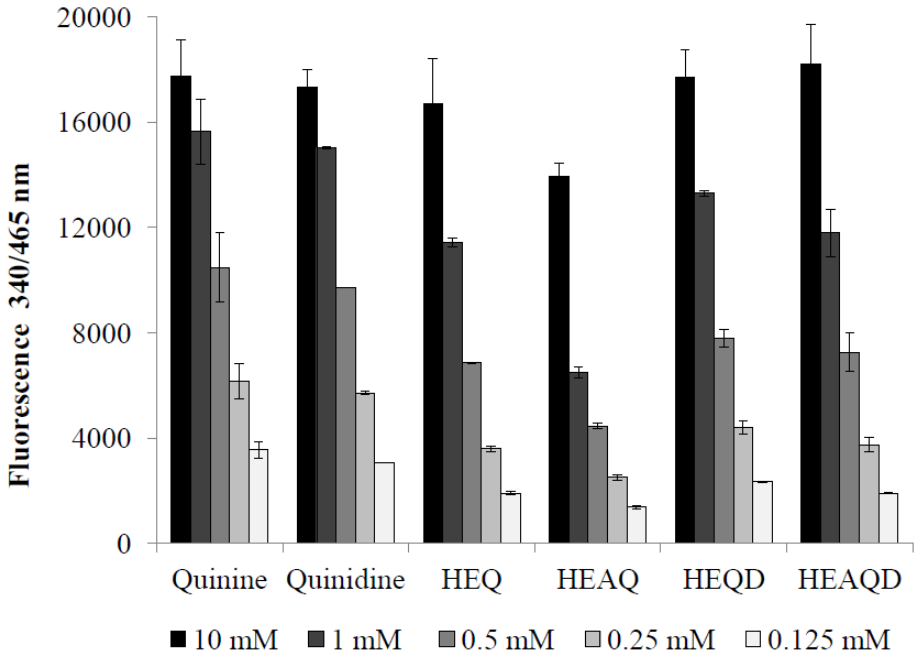

Figure 3.6 Fluorescence of quinoline parent compounds and derivatives in 50 mM sulfuric acid.

In vitro Antimalarial Efficacy against *P. falciparum*

Quinoline derivatives were evaluated for antimalarial efficacy against three strains of *Plasmodium falciparum* in a standard 72-hour SYBR green assay with results shown in Table 1. All derivatives were effective at inhibiting a quinine-sensitive strain, 3D7, at less than 300 nM, with an IC_{50} approximately three to four times higher than the parent compound, quinine or quinidine. Of note, the quinidine derivatives, HEQD and HEAQD were the most active against *P. falciparum,* with HEQD (111 nM) comparable with quinine (56 nM). Against the quinine-tolerant strains INDO and Dd2, all quinoline derivatives exhibited elevated IC_{50}s, with HEAQ and HEAQD exhibiting IC_{50}s five to nine times higher than quinine and quinidine. Importantly, the quinidine derivatives HEQD and HEAQD demonstrated efficacy against quinine these strains around 500 nM with the exception of HEQD against INDO, within the acceptable range of drug sensitivity for quinine and quinidine. Artemisinin was used as a control and consistently inhibited all three strains at low nanomolar concentrations.

Table 3.1: The average IC_{50} (nM) of quinine and quinidine derivatives against three strains of *P. falciparum* were determined using a 72-hour SYBR green assay.

	Mean IC_{50} (nM, SEM)		
Compound	3D7	INDO	Dd2
Quinine	56 (6)	263 (25)	92 (10)
HEQ	258 (33)	7100 (276)	2800 (363)
HEAQ	255 (29)	3470 (429)	1133 (133)
HEAQ HCl salt	240 (77)	--	1250 (189)
Quinidine	24 (2	153 (279)	43 (1)
HEQD	111 (22)	1875 (427)	313 (13)*
HEAQD	168 (25)	725 (170)	333 (44)
HEAQD HCl Salt	148 (55)	--	233 (17)
Artemisinin	8.3 (1)	5.1 (1)	5.5 (1)

Three or more biological replicates were completed for all compounds unless otherwise noted, with each compound in triplicate per experiment, reported with corresponding standard error of the mean (SEM). * Two independent experiments were completed for this compound. -- No data for these compounds.

In vivo Antimalarial Efficacy against *P. berghei* ANKA

In order to see how the derivatives would perform *in* vivo, we next evaluated the antimalarial efficacies of HEAQ, HEQD, and HEAQD in a murine malaria model. Fifty-five C57/Bl6 mice were infected intraperitoneally with *Plasmodium berghei* ANKA ($1x10^7$ infected erythrocytes) and compounds were administered orally twice a day for five days beginning twenty-four hours post infection. Parasitemia was reduced by all derivatives except HEAQ 20 mg/kg at 3 days post drug administration (Figure 3.7). Quinine, compound HEAQ, and HEAQ in combination with artesunate all improved mouse survival, but were unable to cure the mice after five days of dosing (Figure 3.8, A and C). However, HEAQ at 80 mg/kg alone or with artesunate did significantly decrease parasitemia compared to the no drug control and was comparable to quinine at 20 mg/kg (Figure 3.7). Quinidine, HEQD, HEAQD, HEQD plus artesunate and HEAQD plus artesunate all significantly decreased parasitemia by day three post infection (Figure 3.7A), but only 80 mg/kg HEAQD plus artesunate and 20 mg/kg HEQD plus artesunate were able to successfully clear parasitemia through day six (3.7B) and successfully cured three mice (Figure 3.8C). Artesunate alone at 10 mg/kg was unable to cure mice or allow them to survive until day 30.

Figure 3.7 Dose dependent clearance of P. berghei ANKA by compounds quinine (QN), HEAQ, quinidine (QND), HEQD and HEAQD, alone and in combination with artesunate (AS 10 mg/kg) in C57/Bl6 mice. Percent parasitemia was calculated as the percent of infected RBCS out of 500 for ≥1% parasitemia, and out of 10,000 for <1% parasitemia, graphed with standard error of the mean. Compounds listed first, dosages following (e.g. QN 20 mg/kg). (A) Day 3 parasitemia, after 2 days of dosing. (B) Day 6 parasitemia, one day after the final dose was administered. (C) Day 13 parasitemia, one week after the final dose was administered.

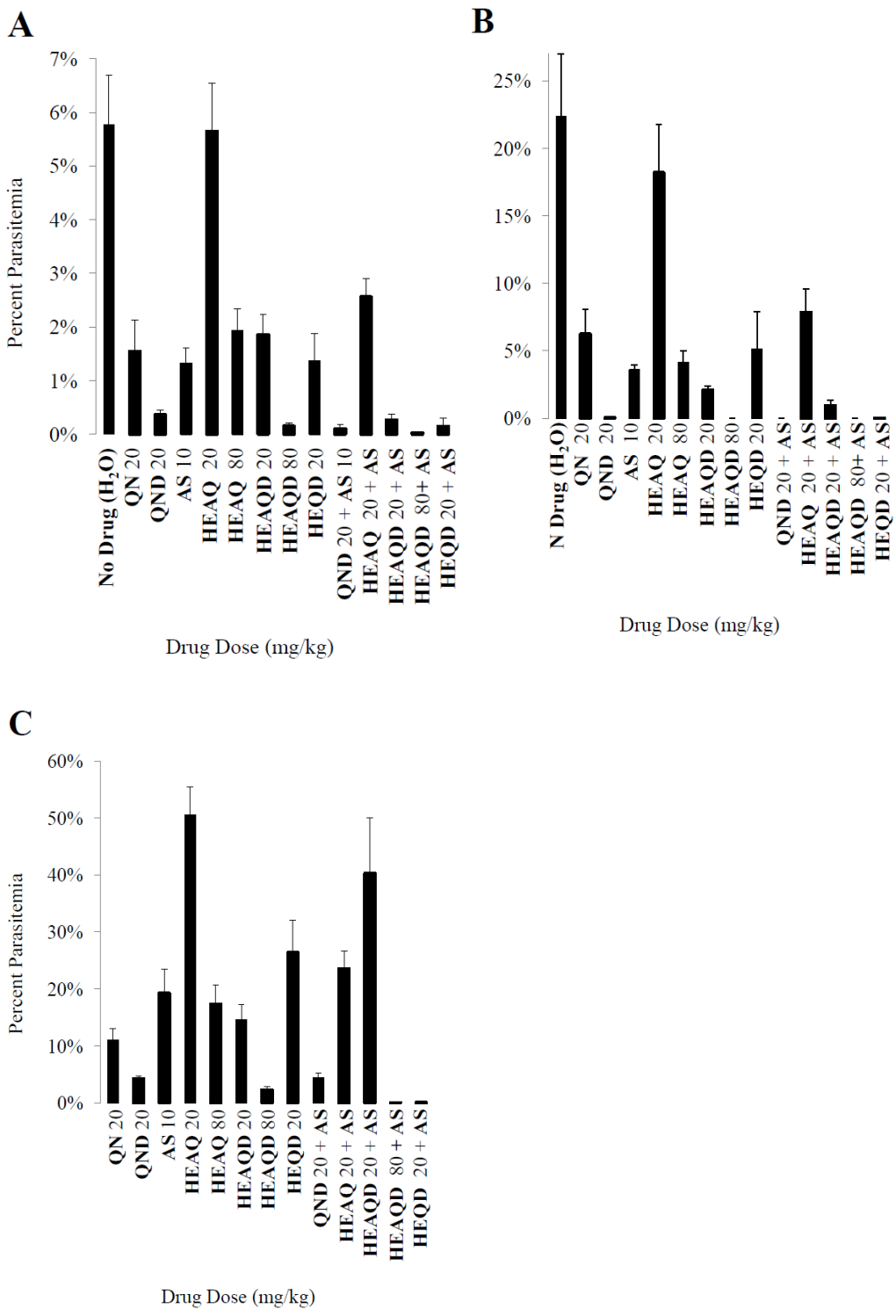
A
Percent Parasitemia
7%
6%
5%
4%
3%
2%
1%
0%
No Drug (H2O)
QN 20
QND 20
AS 10
HEAQ 20
HEAQ 80
HEAQD 20
HEAQD 80
HEQD 20
QND 20 + AS 10
HEAQ 20 + AS
HEAQD 20 + AS
HEAQD 80+ AS
HEQD 20 + AS
Drug Dose (mg/kg)
B
25%
20%
15%
10%
5%
0%
N Drug (H2O)
QN 20
QND 20
AS 10
HEAQ 20
HEAQ 80
HEAQD 20
HEAQD 80
HEQD 20
QND 20 + AS
HEAQ 20 + AS
HEAQD 20 + AS
HEAQD 80+ AS
HEQD 20 + AS
Drug Dose (mg/kg)
C
Percent Parasitemia
60%
50%
40%
30%
20%
10%
0%
QN 20
QND 20
AS 10
HEAQ 20
HEAQ 80
HEAQD 20
HEAQD 80
HEQD 20
QND 20 + AS
HEAQ 20 + AS
HEAQD 20 + AS
HEAQD 80 + AS
HEQD 20 + AS
Drug Dose (mg/kg)

Figure 3.8 Dose dependent survival of C57/Bl6 mice infected with *P. berghei* ANKA after treatment with QN, HEAQ, QND, HEQD and HEAQD, alone or in combination with AS (10 mg/kg). (A) HEAQ at either 20 mg/kg or at 80 mg/kg was comparable to quinine in survival with all mice dying between day 20 and 25 (B) HEAQD and HEQD were comparable to quinidine with mice surviving to day 20-25 as with quinine and HEAQ. Despite 80 mg/kg of HEAQD having a lower parasitemia on day 16 these mice had a surge in parasitemia and died quickly compared to the lower dose of 20 mg/kg HEAQD. (C In combination with AS, 20 mg/kg of HEQD was comparable to 80 mg/kg of HEAQD clearing 3 of 5 mice completely parasites, as well as 3 (HEQD) or 4 (HEAQD) of 5 mice survive until Day 30. Quinidine at 20 mg/kg allowed only 1 of 5 mice live until day 30 but did not clear parasites.

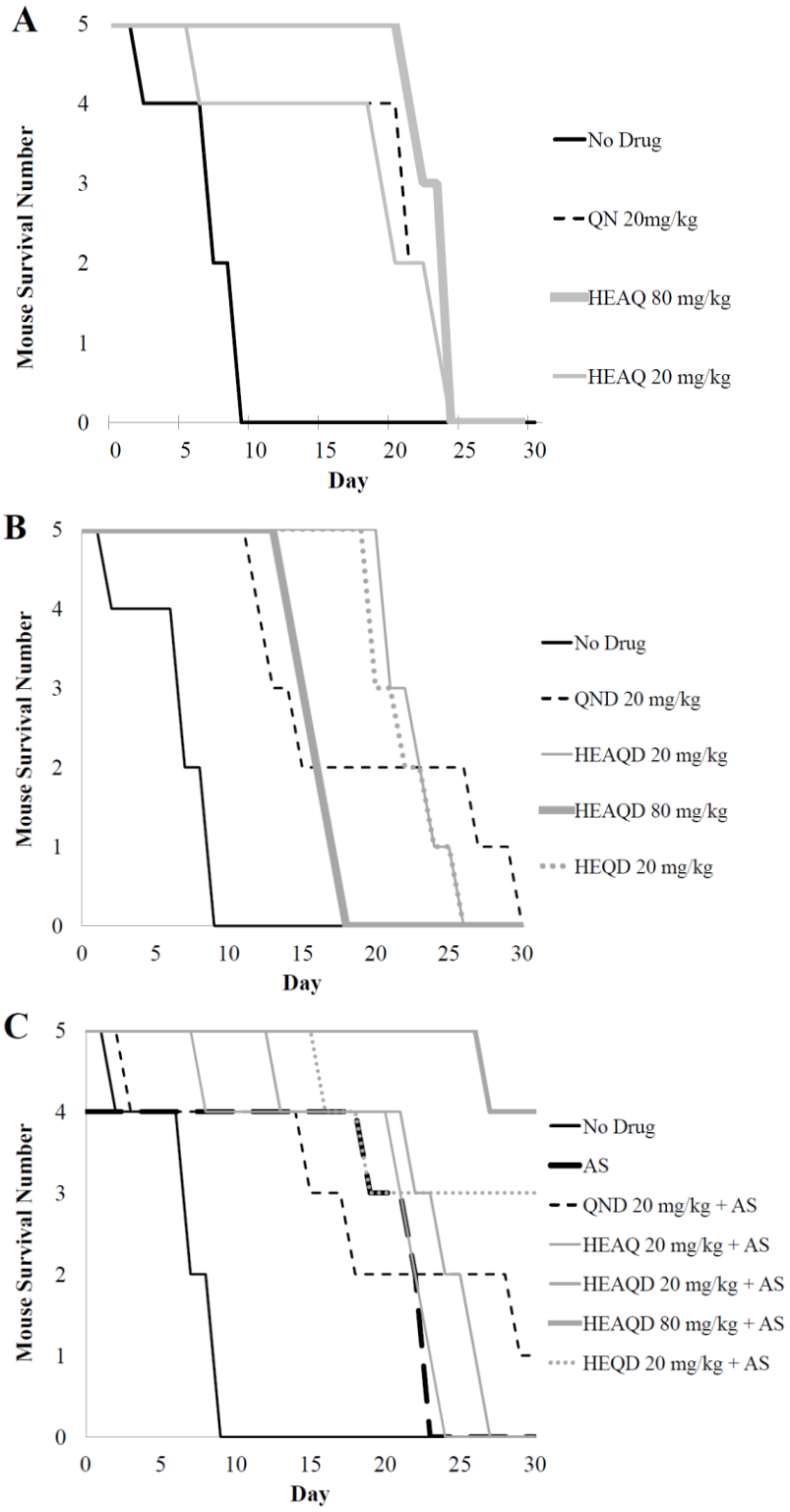
A
Mouse Survival Number
Day
No Drug
QN 20mg/kg
HEAQ 80 mg/kg
HEAQ 20 mg/kg
B
Mouse Survival Number
Day
No Drug
QND 20 mg/kg
HEAQD 20 mg/kg
HEAQD 80 mg/kg
HEQD 20 mg/kg
C
Mouse Survival Number
Day
No Drug
AS
QND 20 mg/kg + AS
HEAQ 20 mg/kg + AS
HEAQD 20 mg/kg + AS
HEAQD 80 mg/kg + AS
HEQD 20 mg/kg + AS

Toxicity Studies: hERG Channel Inhibition and Cell Viability

The most compelling evidence reported for HEAQ, besides its antimalarial efficacy, is the decreased toxicity associated with its historic human use compared to other quinine derivatives. An important clinical adverse drug reaction of the quinoline class is prolongation of the QRS heart interval associated with inhibition of the hERG channel. hERG inhibition studies were conducted using Chinese hamster ovary (CHO) cells expressing hERG channels and Ionworks automatic patch clamp to determine hERG IC_{50}s for HEQ, HEAQ, HEQD and HEAQD compared to the parent compounds (Table 2, Figure 3.9). Strikingly, compounds HEQ, HEAQ, and HEAQD demonstrated IC_{50}s of approximately 100 uM compared to 42.2 μM for quinine, while compound HEAQD was seven times less inhibitory than the parent, inhibiting 50% of the CHO hERG channels at 27 μM compared to 4 μM quinidine.

Table 3.2: hERG channel inhibition by quinine, quinidine and derivatives. hERG channels were expressed in Chinese hamster ovary (CHO) cells using the Ionworks patch clamp assay. Reported IC_{50} values (10,30).

Compound	IC_{50} (μM)	SD	Reported IC_{50} (μM)	Hill	SD	% at max conc	hERG Inhibitor?
Dofetilide	0.05	0.01	0.1	2.27	0.79	-100	Yes
Quinine	42.2	7.41	57.0	1.30	0.30	-83.4	Yes
HEQ	>100	--	-	--	--	-35.2	No
HEAQ	109	20.9	-	1.80	0.83	-49.4	Yes
Quinidine	3.95	0.75	4.60	0.96	0.18	-95.8	Yes
HEQD	94.3	8.12	-	4.00	0.00	-70.1	Yes
HEAQD	27.3	7.57	-	3.00	0.00	-87.0	Yes

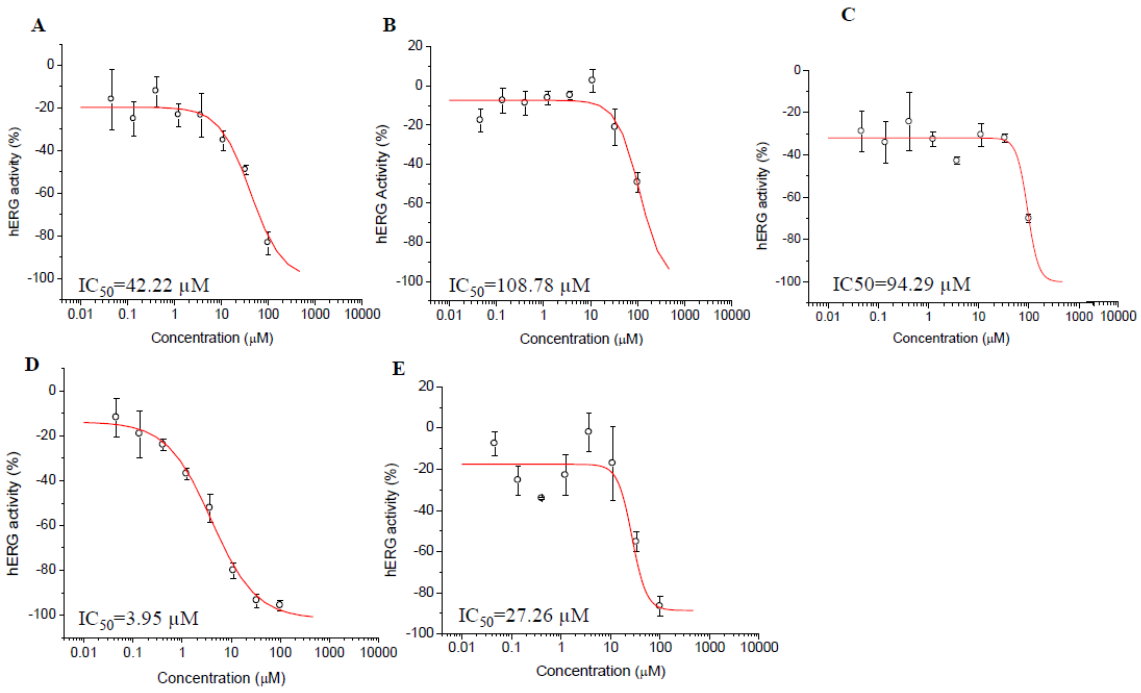

Figure 3.9 IC_{50} concentrations were determined for parent compounds and derivatives against hERG channels expressed in CHO cells as measured by the Ionworks patch clamp assay. Representative graphs of quinine (A), HEAQ (B), quinidine (C) HEAQD (D) and (E) HEQD are pictured above. Compounds were tested in quadruplicate in a 8-point gradient with a maximum concentration of 100 µM with serial 1:3 dilutions.

In vitro cell toxicity studies were also completed by observing the effects of different concentrations of quinine, quinidine, HEAQ, HEQD or HEAQD on human foreskin fibroblasts using a 48-hour Alamar blue assay to determine cell viability. While all compounds showed no toxicity at 100 µM, quinine had an LD_{50} of ~200 µM, with quinidine, HEAQ and HEAQD showing no toxicity at this concentration (Figure 3.10).

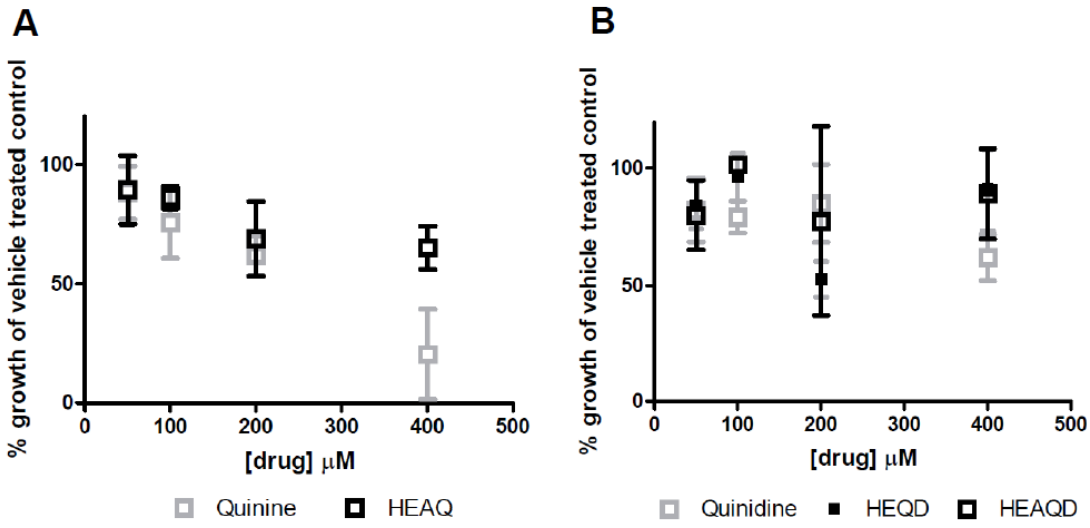

Figure 3.10 Dose dependent cytotoxicity of (A) HEAQ and (B) HEQD and HEAQD compared to quinine and quinidine against human foreskin fibroblasts, using Alamar blue fluorescence as a measure of cell viability and metabolic activity. Results are recorded as a percentage of the vehicle (DMSO) treated growth control.

DISCUSSION AND CONCLUSIONS

Antimalarial drug resistance continues to threaten global public health measures to treat, contain and eventually eliminate malaria. HEAQ and derivatives HEQ, HEQD, and HEAQD may provide less toxic alternatives to quinine or quinidine, which continue to be effective malaria drugs, but have toxicity due to narrow therapeutic indices. Building on research that began in the 1930's but was not pursued due to the discovery of chloroquine and other effective antimalarials, we sought to determine whether HEAQ and three derivatives would be effective against *P. falciparum* in an era of increasing antimalarial drug resistance and also to investigate inhibition of hERG which has been associated with prolongation of the Q-T interval. We were successful in synthesizing HEAQ as well as the novel diastereomer HEAQD, and also produced intermediates without the isomerized vinyl group, HEQ and HEQD**.** We demonstrated all compounds inhibit heme crystallization and retain fluorescent properties similar to the parent compounds, supporting the inhibition of hemozoin formation as a likely mechanism of action of the derivatives.

Our *in vitro* and *in vivo* antimalarial results correspond with the data previously reported by Hegner et al (1941) for the activity of HEAQ against three strains of bird malaria, with the quinine and quinidine derivatives displaying decreased activity per mg/kg but at higher doses comparable action to the parent compounds (14). Specifically, here all derivatives showed decreased activity *in vitro* against clones 3D7, Indo and Dd2, but were equally effective at controlling parasitemia in the *in vivo* model at the higher dose of 80 mg/kg. Overall, compound HEQD and to a lesser extent HEAQD showed the greatest activity in the *in vivo* model when combined with artesunate with no adverse side

effects observable in the mice, making it a potential alternative to quinine or quinidine as an antimalarial drug.

The reported hERG channel inhibition data suggests that all four derivatives are less prone to QT prolongation than the parent compounds quinine or quinidine, with HEQ, HEAQ, and HEQD inhibiting 50% of hERG channels at approximately 100 μM, twice the IC_{50} of quinine (42 μM). Interestingly, the intermediates HEQ and HEQD exhibited less hERG channel inhibition than the final products HEAQ and HEAQD. Cretcher and Renfrew (1941) previously commented on the effect of the resulting modifications on anti-pneumococcal activity, stating that "greater antipneumococcic action appears to be associated with the ethylidene group" (31). While we did not observe increased malaria activity with the ethylidene or isomerized vinyl group group, we did observe a decrease in hERG channel inhibition associated with the hydroxyethyl substitution, suggesting that this modification and not isomerization of the vinyl group can be credited for the great reduction in potassium channel inhibition**.** Our HFF cell line cytotoxicity data also agrees with previous studies on cell lines conducted by Kominos and Machlachlan (1963), with HEAQ and HEAQD showing overall less toxicity compared to quinine and quinidine (18). In addition, the quinidine derivatives HEQD and HEAQD showed no toxicity against HFFs at up to 200 μM for 48 hours. It is possible that metabolism of HEAQ and other derivatives is different from the parent compounds and that the lack of a toxic metabolite such as quinone species is the reason for the decreased toxicity of the hydroethyl substituted quinolines.

Our data suggests that modifications of the methoxy side chain (R, Figure 3.2) with hydroxylated alkyl groups may be effective at decreasing cardiotoxic events

associated with quinine and quinidine in addition to the decrease in quinine-associated toxicities such as eye damage in dogs which decreased with hydroxylalkylation of R as mentioned in other studies (24,31). Interestingly, avian antimalarial potency increased with increasing lengths of the alkylated side chain up to four to five carbons, but beyond five carbons decreased potency (32). In recent studies on *P. falciparum*, substitutions at the R' group with aromatic groups resulted in increased sensitivity against quinine-resistant strains in some cases, while most resulted in decreased potency compared to parent compounds including quinine, cinchonine, quinidine and cinchonidine (33). When the R' group was reduced to the dihydro group (optochin and others) a slight decrease in potency was noted. Compound SN-8707 has the dihydro R' group as well as a hydroxyethyl R group with a reported quinine ratio of 0.6 in *P. lophurae*, which is more potent than our reported derivatives (~0.2-0.25, see Supplementary Table 1). Toxicity studies of SN-8707 and the quinidine derivative may provide more insight into the role of these modifications in decreasing cardiotoxicity as well as other quinine-associated toxicities.

REFERENCES

1. Meshnick S, Dobson M. *The history of antimalarial drugs*. In: P. J. Rosenthal, editor. Antimalarial Chemotherapy: Mechanisms of Action, Resistance, and New Directions in Drug Discovery. Totowa, NJ: Humana Press Inc.; 2001. p. 15–26.
2. Achan J, Talisuna AO, Erhart A, Yeka A, Tibenderana JK, Baliraine FN, Rosenthal PJ DU. *Quinine, an old anti-malarial drug in a modern world: role in the treatment of malaria*. Malar J. BioMed Central Ltd; 2011 Jan;10(144):1–12.
3. Sullivan DJ. *Cinchona alkaloids: quinine and quinidine*. In: Staines HM, Krishna S, editors. Treatment and prevention of malaria. 2012. p. 45–68.
4. Organization WH. WHO | *Guidelines for the treatment of malaria.* Third edition. World Health Organization; Available from: http://www.who.int/malaria/publications/atoz/9789241549127/en/
5. Griffith KS, Lewis LS, Mali S PM. *Treatment of Malaria in the United States: A Systematic Review*. J Am Med Assoc. 2007;297(20):2264–77.
6. Sridaran S, Mcclintock SK, Syphard LM, Herman KM, Barnwell JW. *Anti-folate drug resistance in Africa : meta-analysis of reported dihydrofolate reductase (dhfr) and dihydropteroate synthase (dhps) mutant genotype frequencies in African Plasmodium falciparum parasite populations*. Malar J. 2010;9(247):1–22.
7. Parija SC, Praharaj I. *Drug resistance in malaria*. Indian J Med Microbiol. 2011;29(3):243–8.
8. O'Brien C, Henrich PP, Passi N, Fidock DA. *Recent clinical and molecular insights into emerging artemisinin resistance in Plasmodium falciparum*. Curr Opin Infect Dis. 2012;24(6):570–7.

9. Frosch AEP, Venkatesan M, Laufer MK. *Patterns of chloroquine use and resistance in sub-Saharan Africa: a systematic review of household survey and molecular data*. Malar J. BioMed Central Ltd; 2011 Jan;10(1):116.

10. White NJ. *Cardiotoxicity of antimalarial drugs*. Lancet Infect Dis. 2007;7(8):549–58.

11. Goodson JA, Henry TA, Macfie JWS. XCVIII . *The action of the cinchona and certain other alkaloids in bird malaria.* Biochem J. 1930;24:874–90.

12. Hegner R, Shaw EH, Manwell RD. *Methods and results of experiments on the effects of drugs on bird malaria*. Am J Hygeine. 1928;564–82.

13. Hegner R, West E, Dobler M. *A new drug effective against bird malaria*. Am J Epidemiol. 1939;(33-Section C):101–11.

14. Hegner R, West E, Dobler M. *Further studies of hydroxyethylapocupreine against bird malaria*. Am J Hygeine. 1941;132–9.

15. Maclachlan WWG, Johnston JM, Bracken MM, Crum GE. *The treatment of pneumococcic pneumonia by hydroxyethylapocupreine*. Am J Med Sci. 1939;197(1):31–8.

16. Maclachlan WW., Johnston JM, Bracken MM, Pierce LS. *A comparison of the mortality in pneumococcic pneumonia treated by hydroxyethylapocupreine and by sulfapyradine.* Am J Med Sci. 1941;201(3):367–74.

17. Maclachlan WWG, Bracken MM, Bailey WRJ. *Prognosis of pneumonia*. Am J Med Sci. 1949;217(4):438–44.

18. Kominos S, Maclachlan WWG. *The cytotoxic effect of quinine, quinidine and hydroxyethylapocupreine upon mammalian cell cultures*. Am J Med Sci. 1963;245(5):89–92.

19. Xu F, Corley E, Zacuto M, Conlon D a, Pipik B, Humphrey G, et al. *Asymmetric synthesis of a potent, aminopiperidine-fused imidazopyridine dipeptidyl peptidase IV inhibitor.* J Org Chem. 2010 Mar 5;75(5):1343–53.

20. Furuya T, Strom AE, Ritter T. *Silver-Mediated Fluorination of Functionalized Aryl Stannanes*. J Am Chem Soc. 2009;131(5):1662–3.

21. Carlson WW, Cretcher LH. *Hydroxylalkylation with cyclic alkylene esters. I. Synthesis of Hydroxyethylapocupreine.* J Am Chem Soc. 1947;69(I):1952–6.

22. Portlock DE, Naskar D, West L, Seibel WL, Gu T, Krauss HJ, et al. *Positional isomerization of quinine and quinidine via rhodium on alumina catalysis: practical one-step synthesis of Δ3,10-isoquinine and Δ3,10-isoquinidine.* Tetrahedron Lett [Internet]. 2003 Jul [cited ;44(28):5365–8.

23. Butler CL, Renfew AG. Cinchona alkaloids in pneumonia. VI. *A New method for the hydroxylation of phenolic cinchona alkaloids.* J Am Chem Soc. 1938;60:1472–5.

24. Butler CL, Hostler M, Cretcher L. *Cinchona Alkaloids in Pneumonia. V. Alkyl ethers of apocupreine*. J Am Chem Soc. 1937;445(5):5–6.

25. Warhurst DC, Craig JC, Adagu IS, Meyer DJ, Lee SY. *The relationship of physico-chemical properties and structure to the differential antiplasmodial activity of the cinchona alkaloids*. Malar J. 2003 Sep 1;2(Cd):26.

26. De Villiers K a, Marques HM, Egan TJ. *The crystal structure of halofantrine-ferriprotoporphyrin IX and the mechanism of action of arylmethanol antimalarials*. J Inorg Biochem. 2008 Aug;102(8):1660–7.

27. De Villiers K a, Gildenhuys J, le Roex T. *Iron(III) protoporphyrin IX complexes of the antimalarial Cinchona alkaloids quinine and quinidine*. ACS Chem Biol. 2012 Apr 20;7(4):666–71.

28. Fletcher A. *Quinine sulfate as a fluorescence quantum yield standard*. Photochem Photobiol. 1969;9:439–44.

29. GILL J. *The fluorescence excitation spectrum of quinine bisulfate*. Photochem Photobiol. 1969;9:313–22.

30. Weerapura M, Hébert TE, Nattel S. *Dofetilide block involves interactions with open and inactivated states of HERG channels*. Pflugers Arch. 2002. Mar;443(4):520–31.

31. Renfew AG, Cretcher LH. *Structure and antipneumococcic activity in the cinchona series.* Chem Rev. 1941;30(1):49–68.

32. Buttle GAH, Henry TA, Solomon W, Trevan JW, Gibbs EM. *The action of the cinchona and certain other alkaloids in bird malaria.* Biochem J. 1938;32(1):47–58.

33. Dinio T, Gorka AP, McGinniss A, Roepe PD, Morgan JB. *Investigating the activity of quinine analogues versus chloroquine resistant Plasmodium falciparum*. Bioorg Med Chem. Elsevier Ltd; 2012 May 15;20(10):3292–7

Supplementary Table 3.1. List of quinoline compounds with associated quinine ratios and *P. falciparum* inhibition in literature and collaborative drug discovery database with ≥ 70% similarity to cupreine, quinine and HEAQ (32). Compounds with a quinine ratio greater than one are more potent than quinine. See Figure 3.2 in manuscript for R and R' designations on quinoline structure.

Compound		**R**	**R'**	**Quinine ratio, s*train***		***P. falc* % inhibition at 10uM**			***P. falc* EC_{50} (nM)**
Levarotatory						W2	3D7	Dd2	3D7
Cinchonine, CDD-10723, CDD-1522, SN-1030	8S, 9R	H	CH-CH=CH2	2.5, 1, 2	*P. gallinaceum*	100	100		183
Cupreine, CDD-1007918	8S, 9R	OH	CH-CH=CH2						404
Dihydrocupreine	8S, 9R	OH	CH2-CH3	0.92	*P. inconstans*		99	2	640
Apocupreine, CDD-1002621, CDD-1012793, CDD-1002726	8S, 9R	OH	C=CH-CH3				99,98	11, -2	490
Quinine, CDD-993709, CDD-14859, CDD-10961	8S, 9R	OCH3	CH-CH=CH2				100	99	100, 150
Dihydroquinine *methyl*, CDD-	8S, 9R	OCH3	CH2-CH3	1.35, 1	*P. inconstans*, *P. lophurae*		100	62, 51	30, 39, 230

995445, CDD-10887, SN-3094, CDD-1006404, CDD-1013193									
CDD-995897	8S, 9?	OCH3	CH2-CH3				100	98	140
Optochin *ethyl* CDD-993708	8S, 9R	O-CH2-CH3	CH2-CH3	1.05	*P. inconstans*		98	99	110
propyl, CDD-995898	8S, 9R	O-CH2-CH2-CH3	CH2-CH3	1.49	*P. inconstans*		100	57	430
n-Butyl	8S, 9R	O-CH2-(CH2)2-CH3	CH2-CH3	1.87	*P. inconstans*				
n-Hexyl	8S, 9R	O-CH2-(CH2)4-CH3	CH2-CH3	1.5	*P. inconstans*				
n-Octyl	8S, 9R	O-CH2-(CH2)6-CH3	CH2-CH3	1.43	*P. inconstans*				
n-Decyl	8S, 9R	O-CH2-(CH2)8-CH3	CH2-CH3	1.6	*P. inconstans*				
Apoquinine, isoquinine, CDD-1002719, CDD-1002729	8S, 9R	OCH3	C=CH-CH3	0.98	*P. inconstans*		102, 99, 99	45, 61	220, 200, 320
ethyl	8S, 9R	O-CH2-CH3	C=CH-CH3	1.18	*P. inconstans*				

propyl	8S, 9R	O-CH2-CH2-CH3	C=CH-CH3	1.23	*P. inconstans*				
n-Butyl	8S, 9R	O-CH2-(CH2)2-CH3	C=CH-CH3	1.1	*P. inconstans*				
n-Hexyl	8S, 9R	O-CH2-(CH2)4-CH3	C=CH-CH3	1.72	*P. inconstans*				
n-Octyl	8S, 9R	O-CH2-(CH2)6-CH3	C=CH-CH3	1.6	*P. inconstans*				
n-Decyl	8S, 9R	O-CH2-(CH2)8-CH3	C=CH-CH3	1.18	*P. inconstans*				
Epiquinine	8S, 9S	OCH3	CH-CH=CH2	<1.5	*P. gallinaceum*				
Hydroxyethyl-quinine, 3	8S, 9R	O-CH2-CH2-OH	CH-CH=CH2				100		250
Hydroxyethyl-apoquinine 4, SN-119	8S, 9R	O-CH2-CH2-OH	C=CH-CH3	0.2	*P. gallinaceum, lophurae, cathemerium*		100		250
Hydroxyethyl-dihydroquinine, CDD-10919, SN-8707	8S, 9R	O-CH2-CH2-OH	CH2-CH3	0.6	*P. lophurae*				
CDD-10937, SN-3133	8S, 9R	O-CH2-CH2-S-CH2-CH3	C=CH-CH3	0.3	*P. lophurae*				
CDD-10923,	8S, 9R	O-CH2-CH2-	C=CH-CH3	0.4	*P. lophurae*				

SN-3134		O-CH2-CH3							
CDD-10872, SN-7723	8S, 9R	OCH3	H	0.8	*P. lophurae*				
CDD-11251, SN-3135	8S, 9R	NH-CH2-CH2-OH	C=CH-CH3	0.4	*P. lophurae*				
CDD-10922, SN-7325	8S, 9R	CH2-CH2-O-CH3	C=CH-CH3	0.2	*P. lophurae*				
CDD-10921, SN-7326	8S, 9R	O-CH2 (OH)-CH2-OH	C=CH-CH3	0.2	*P. lophurae*				
CDD-10920, SN-8706	8S, 9R	CH (CH2-OH)2	C=CH-CH3	0.08	*P. lophurae*				
CDD-1012800, CDD-1002688	8S, 9R	C≡N	CH2-CH3				100	55	150
CDD-1005755	8S, 9R	Cl	CH2-CH3				100	98	120

Dextrarotatory									
Cinchonidine CDD-10724, CDD-994062	8R, 9S	H	CH-CH=CH2	1, 0.6, 0.4	*P. gallinaceum*		100		95
Dihydrocinchonidine, SN-3704, CDD-10725, CDD-995699	8R, 9S	H	CH2-CH3	2	*P. lophurae*		98	20	
CDD-14079	8R, 9R	H	CH-CH=CH2			100	100		
Dihydrocupreidine, SN-15293, CDD-10853	8R, 9S	OH	CH2-CH3	0.68	*P. inconstans*				
Dihydroepicupreidine CDD-996493, CDD-1012492	8R, 9R	OH	CH2-CH3				94	-4	1000
Apocupreidine	8R, 9S	OH	C=CH-CH3				98	-1	250
Quinidine, CDD-10884, CDD-14859, CDD-1010673	8R, 9S	OCH3	CH-CH=CH2	1.5, 1	*P. gallinaceum*	68 (W2)	60, 98	95	9.5
Dihydroquinidine *methyl*, CDD-	8R, 9S	OCH3	CH2-CH3	0.81	*P. inconstans*	100 (W2)	100	95	103, 120

14080, CDD-1008089, CDD-995421									
ethyl	8R, 9S	O-CH2-CH3	CH2-CH3	0.98	*P. inconstans*				
Apoquinidine	8R, 9S	OCH3	C=CH-CH3	1	*P. inconstans*				
Epiquinidine, CDD-10886, CDD-14860	8R, 9R	OCH3	CH-CH=CH2	< 1.5, .04, .06	*P. gallinaceum, lophurae*	100 (W2)	100		
Hydroxyethyl-quinidine, 7	8R, 9S	O-CH2-CH2-OH	CH-CH=CH2				100		110
Hydroxethyl-apoquinidine, 8	8R, 9S	O-CH2-CH2-OH	C=CH-CH3				100		170
CDD-1008629, CDD-1013570	8R, 9S	OCH3	OH, CH-CH=CH2						105
CDD-1009849	8R, 9S	OCH3	CH2-CH3						32
CDD-10873, SN-5860	8R, 9S	OCH3	H	0.4	*P. lophurae*				
QN - 1-16 CN - 1-4 QD - 1-4 CD – 1-4	8S, 9R 8R, 9S	OCH3	Aromatic substitutions (33)						66-500+ (HB3) 146-500+ (Dd2)

CHAPTER 4: DEVELOPING A GAMETOCYTOCIDAL ASSAY AND DISCOVERY OF NOVEL TRANSMISSION BLOCKING COMPOUNDS

Adapted from previously published manuscript:

Sanders NG, Sullivan DJ, Mlambo G, Dimopoulos G, Tripathi AK. Gametocytocidal screen identifies novel chemical classes with *Plasmodium falciparum* transmission blocking activity. PLoS One. 2014 Aug 26;9(8):e105817. PubMed ID PMID: 25157792

ABSTRACT

The goal of malaria elimination is only going to be possible if there are sufficient tools to block the transmission cycle between the mosquito vector and human host. While vector control has been shown to be effective and essential for elimination of malaria in a variety of geographical regions, drugs that can kill gametocytes and block transmission are essential to destroy the gametocyte reservoir present in asymptomatic individuals that continues to go unchallenged in many endemic settings. However, screening for such compounds has proven challenging as current assays for transmission blocking drugs have limitations including a requirement for transgenic parasites, multiple or lengthy incubation steps making them not amenable for high throughput settings, or requirement for very high parasitemia gametocyte cultures for sufficient signal to noise ratio.

We set out to develop a high-throughput assay that would address some of these challenges, with a goal to use affordable reagents and instrumentation, minimal incubation steps and facilitate the use of any strain of *P. falciparum*, including field strains. We made use of the SYBR Green I nucleic acid dye that preferentially binds to double-stranded DNA and found that in combination with a background suppressor obtained from CyQUANT, we were able to detect only live gametocytes with intact membranes as the background suppressor quenched the fluorescence of any dead or permeabilized cells. By adding exflagellation media to drug-treated gametocyte cultures we were able to increase the DNA content of the male gametes to further boost the signal in our assay. Using this unique combination of reagents, we developed a live-dead assay

for *P. falciparum* gametocytes that we adapted for high throughput screening for discovery of novel transmission blocking drugs.

For this project my aims included: (1) Optimizing and validating the assay, comparing results with Giemsa stained blood films, the gold standard for determining gametocyte viability, (2) Screening large compound libraries for discovery of novel transmission blocking compounds, and (3) IC_{50} determination for top hits and validation for transmission blocking activity using membrane feeding assays.

After optimizing conditions for the assay we were able to demonstrate a strong correlation between gametocyte number and SYBR Green I fluorescence with a strong signal to noise ratio using between 5-10% gametocyte cultures with exflagellation media and addition of the background suppressor.

Using our optimized assay we first screened the Johns Hopkins Clinical Compound Library version 1.3 of approximately 1,500 FDA approved drugs and obtained 25 hits with IC_{50} values less than 20 μM. We further validated these compounds with Giemsa-stained blood films to confirm gametocyte killing, and also performed membrane feeding assays with some of the top hits to validate their transmission blocking activity. Pyrvinium pamoate was our most effective compound, with 100% gametocyte killing at 4 μM and 100% inhibition of oocyst development in mosquito midguts at 5 μM. In addition we discovered a novel class of compounds, quaternary ammonium compounds, all of which had gametocytocidal activity and IC_{50}s less than 10 μM, as well as other interesting classes such as antidepressants, antineoplastics, and anthelminthic compounds.

We were also interested in testing compounds with known activity against asexual stages of the parasite, so we requested the Medicines for Malaria Venture malaria box of 400 compounds with a combination of drug-like and probe-like molecules. Using our assay we identified eighteen compounds with high efficacy against gametocytes with IC_{50}s less than 10 μM. The majority of these compounds shared a similar pharmacophore, an acridine-like structure with three fused benzene rings and a central nitrogen, with varied side chains, one similar to chloroquine. We validated our hits by comparing our results with several other gametocytocidal assays that were developed around the same time as ours and screened the malaria box, and found that all of our hits were shared among at least one of the other three assays with three distinctive reporters/targets including alamar blue, confocal microscopy based on gametocyte specific proteins, and luciferase.

Overall we were able to develop a robust gametocytocidal assay and identify several new classes of potential transmission-blocking compounds. Future directions include target validation and determining the mechanism of action of some of the novel drug classes identified in our study, as well as exploring other derivatives within the new classes.

INTRODUCTION

Malaria Elimination Requires Drugs to Block Transmission

Malaria is a historically relentless public health problem and continues in the present day to contribute to severe morbidity and mortality worldwide, impeding development in many of the world's poorest countries. *Plasmodium falciparum* malaria is associated with the highest fatality rates, resulting in an estimated 200 million cases and more than one million deaths in 2012 (1). Efforts to control, eliminate, and ultimately eradicate this disease have only been partially successful, with failure due in large part to the development of compound resistance in both the *Anopheles* mosquito vector, as well as the parasite (2,3). Sustainable interventions and control measures have also posed a challenge, and a multi-faceted strategy targeting both transmission and disease is necessary if there is any hope of controlling this devastating disease (2–4).

Of particular interest is the discovery of new chemical entities and classes targeting the sexual stage of the parasite, gametocytes, which are responsible for transmission back to the mosquito vector. To this end, a variety of assays have been developed, each utilizing different measures of parasite viability including alamar blue to detect metabolic activity, detection of parasite proteins such as lactate dehydrogenase, or bioluminescence of viable transgenic parasites (5–11). While the reported assays are more high-throughput than the gold standard of counting Giemsa-stained blood films, they still have limitations including the requirement for transgenic parasites or multiple incubation and transfer steps.

Here we describe a simple assay using the SYBR-green I DNA probe along with a background suppressor to assay for live gametocytes. To achieve robust signal to noise ratio we use a combination of exflagellation, to increase DNA content from viable male gametocytes, and background suppressor to mask the signals from drug killed gametocytes. Incubation time after drug treatment is minimal with no transfer or centrifugation steps and can be easily adapted to higher throughput formats such as 384 or 1536-well plates. In addition, this assay does not require transgenic parasites and thus could be used to screen field isolates. After validating the assay, we screened an FDA-approved library of 1584 compounds as well as the MMV malaria box of 400 confirmed antimalarials that are active against asexual blood stages in *P. falciparum*. We report the results of both drug screens, with particular emphasis on the novel classes of active compounds identified by the assay: quaternary ammonium compounds and acridine-like compounds.

MATERIALS AND METHODS

Ethics Statement

This study was carried out in strict accordance with the recommendations in the Guide for the Care and Use of Laboratory Animals of the National Institutes of Health. Mice were only used for mosquito rearing as a blood source according to approved protocol. The protocol was approved by the Animal Care and Use Committee of the Johns Hopkins University (ACUC MO14H114).

P. falciparum gametocyte cultivation:

The *P. falciparum* NF54 strain was cultured according to the method described by Trager and Jenson with minor modifications. Briefly parasites were cultured using O^+ human erythrocytes at 4% hematocrit in parasite culture medium (RPMI 1640 supplemented with 25 mM HEPES, 10 mM Glutamine, 0.074 mM hypoxanthine and 10% O^+ human serum). Cultures were maintained under standard conditions of 37°C in a candle jar made of glass desiccators. Gametocyte cultures were initiated at 0.5% mixed stage parasitemia from low passage stock and cultures were maintained up to day 15 with daily media changes. To achieve greater level of asexual parasitemia before gametocytogenesis, hematocrit was reduced to 2% between days 3 to 6. After day 6 hematocrit was brought back to approximately 4%. To block reinvasion of remaining asexual parasites and obtain pure and near synchronous gametocytes, cultures were treated with 50 mM *N*-acetyl-D-glucosamine (NAG) for 72 hours between days 8 to 11.

Development and optimization of gametocytocidal assay:

To determine the effect of drugs on mature gametocytes we developed a SYBR Green I based DNA quantification assay. Because gametocytes do not multiply, our assay utilizes increase in DNA content after exflagellation and Cyquant background suppressor dye (Life Technologies, Grand Island, NY, USA) which blocks DNA fluorescence from dead gametocytes to achieve a robust signal to noise ratio. For assay optimization mature gametocytes were enriched using Percoll density gradient centrifugation. Enriched gametocytes were plated in 96 well plates and serially diluted with uninfected 1% hematocrit erythrocytes or media alone to obtain serial gametocytemia values or gametocyte numbers respectively. Triplicate wells of each parasite dilution were either treated with 10 μM pyrvinium pamoate or 0.1% DMSO (vehicle control) for 48 hrs at 37^{o}C in candle jar as described above. After drug exposure, 11 μl of 10x exflagellation medium (RPMI 1640 with 200 mM HEPES, 40 mM sodium bicarbonate, 100 mM glucose pH 8.0) was added and plates were incubated at room temperature for 30 min.

Next 11 μl of 10x Cyquant direct background suppressor and SYBR Green I in PBS was added per well and plate was incubated at room temperature for 2 hrs. After addition of detection reagents plates were protected from light. Fluorescence was then measured at excitation and emission wavelengths of 485 and 535 in a plate reader (HTS7000 Perkin Elmer). To achieve consistent reads, special care was taken to not disturb the settled layer of gametocyte infected erythrocytes for consistent readings, during addition of reagents, incubations and detection plates

Screening of JHU FDA approved compound library:

The Johns Hopkins University Clinical Compound Library version 1.3 is comprised of more than 1500 drugs, which are approved by the FDA for treatments of different diseases or medical conditions. The JHU drug library is stocked in 96 well plates at 10 mM in 100% DMSO. In order to achieve dispensable concentration we diluted compounds in incomplete RPMI to new master plates at 400 µM. We dispensed 5 µl of Compound library to the 96-well plates, to a final compound concentration of 20 µM and DMSO concentration of 0.1%. Each compound was dispensed in duplicate plates to get two replicates of inhibition data. Columns 1 and 12 of each plate were used as in-plate controls and contained 0.1% DMSO (negative control, 0% inhibition) and 20 µM clotrimazole (positive control, ~70% inhibition), respectively. Ninety-five µl per well of day 15 pure gametocyte cultures at approximately 3-5% gametocytemia were then added to the compound containing plates at 1% hematocrit. Plates were incubated for up to 48 hrs at 37°C in microaerophilic conditions of a candle jar. After 48 hrs of drug treatment, gametogenesis was induced by adding 11 µl per well of 10x exflagellation media and incubation for 30min at room temperature. Next 11 µl per well of 10x Cyquant direct background suppressor and SYBR Green I (Life Technologies, Grand Island, NY, USA) in PBS was added to the plates and further incubated at room temperature for 2 hrs in the dark. Plates were then read at excitation and emission wavelengths of 485 and 535 nm respectively and raw data was transferred to Microsoft Excel. Fluorescence signals from both negative (0.1% DMSO) and positive (clotrimazole) wells were used for quality control of the assay and to determine percent inhibition by each compound. Compounds

which showed values between positive and negative controls and where duplicate data were in concert, was considered a hit. All the hits from the primary screen were retested at 10 μM in 24 well plates for 48 hrs and smears were prepared for microscopic examination after Geimsa staining. Compounds which showed activity by the gold standard of microscopic examination were tested at multiple concentrations for IC_{50} determinations.

Screening of the MMV Malaria Box:

The Medicines for Malaria Venture (MMV) kindly provided the Malaria Box which was comprised of 200 drug like and 200 probe like inhibitors of *P. falciparum* asexual stage. The MMV Box was supplied in 96-well plates at 10 mM stocks in 100% DMSO. We diluted compound library by 50 fold to make master plates at 200 μM and 5 μl of each compound was dispensed into the duplicate assay plates, to achieve final concentration of 10 μM. The first and last columns on each plate were used for the negative (0.1% DMSO) and positive (10 μM pyrvinium pamoate) controls. Plate set up and detection of fluorescence was performed as described above in method section for FDA approved compound library. Compounds showing >50% inhibition in both replicates were considered primary hits. All the primary hits were then retested at multiple doses and IC_{50} values were determined.

Z factor determinations

Z factors were calculated using this equation described previously for validating high throughput assays (σ= standard deviation, μ=mean, s=sample, c=control) (12).

$$Z = 1 - \frac{(3\sigma_s + 3\sigma_c)}{|\mu_s - \mu_c|}$$

Mosquito rearing and membrane feeding assay

Anopheles gambiae Keele strain mosquitoes were maintained on a 10% sugar solution at 27^{o} C and 80% humidity with a 12-h light/dark cycle according to standard rearing methods. Day 15 gametocytes were treated with gametocytocidal compounds or 0.1% DMSO for 48 hr and then were centrifuged and diluted to 0.3% final gametocytemia in a mixture of erythrocytes supplemented with human serum for mosquito membrane feeding assays. Unfed mosquitoes were removed after feeding, and midguts were dissected 7 days later and stained with 0.1% mercurochrome. The number of oocysts per midgut was determined with a phase-contrast microscope, and the median infection intensity was calculated for the control and each experimental group.

RESULTS

SYBR Green I: CyQUANT Suppressor Assay Development and Validation

Using SYBR Green I as a live-cell permeable fluorescent probe, we were able to detect gametocytes based on DNA content, with exflagellation as a means to increase DNA content in viable male gametes. In addition we used a background suppressor from the CyQUANT Direct Cell Proliferation Assay kit which works specifically by entering permeabilized cells or cells with compromised membranes and masking green fluorescence. By using SYBR Green I in conjunction with the background suppressor, we were able to mask the signal from dead or damaged gametocytes and only read SYBR Green I fluorescence from live or intact cells. The assay was optimized to determine sensitivity comparing drug treated and untreated parasites. SYBR Green I fluorescent signal from total and killed (10 µM pyrvinium pamoate treated, Figure 4.1) gametocytes was shown to increase linearly with increasing number of gametocytes (Figure 4.2A) and after subtracting out signal from killed gametocytes, retained fluorescent signal with a coefficient of determination of 0.96, indicating strong predictive value of gametocyte number on fluorescent signal.

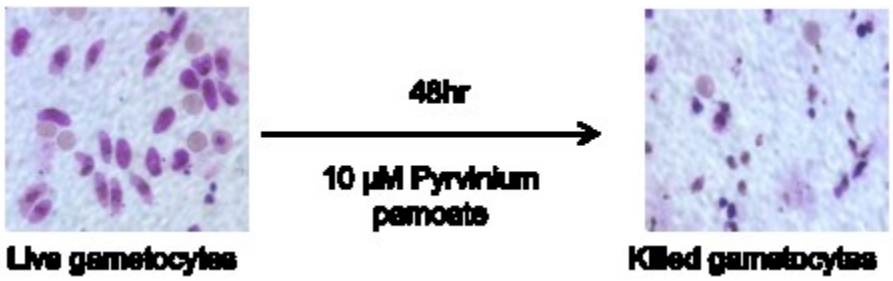

Figure 4.1 Gametocyte culture before and after 48 hr treatment with pyrvinium pamoate.

A

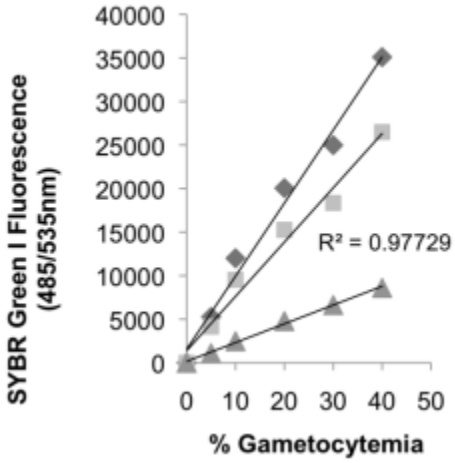

B

Z-factors for SYBR Green I Assay plus background suppressor	
%Gametocytes (2%hct)	Z-factor
40	0.86
30	0.81
20	0.68
10	0.57
5	0.37

$$Z = 1 - \frac{3(\sigma_s + 3\sigma_c)}{|\mu_s - \mu_c|}$$

Figure 4.2 (A) SYBR Green I fluorescence of total (diamond), killed (triangle) and live gametocytes after drug treatment (total minus killed, square) with decreasing number of gametocytes per uninfected cell, diluted with 2% hematocrit erythrocytes in media in presence of CyQUANT background suppressor. (B) Z factors for each dilution were calculated using the equation shown, described previously for validating high throughput assays (σ= standard deviation, μ=mean, s=sample, c=control or in this case zero gametocytes) (12)**.**

To determine the limit of detection and sensitivity of the assay, a Z-factor was calculated for decreasing number of gametocytes, with 5,000-10,000 gametocytes per well providing a Z-factor above 0.5 which is indicative of a good assay (Figure 4.2B). Addition of the CyQUANT background suppressor dye greatly increased the sensitivity of the assay compared to exflagellation, which marginally enhanced the signal of live gametocytes (Figure 4.3). Specifically, beginning with an average ratio of 4:1 female to

male mature gametocytes, exflagellation increased live gametocyte signal from 7000 to 8000 fluorescent units, suggesting a contribution of 10-20% of exflagellation to overall fluorescent signal (Figure 4.3).

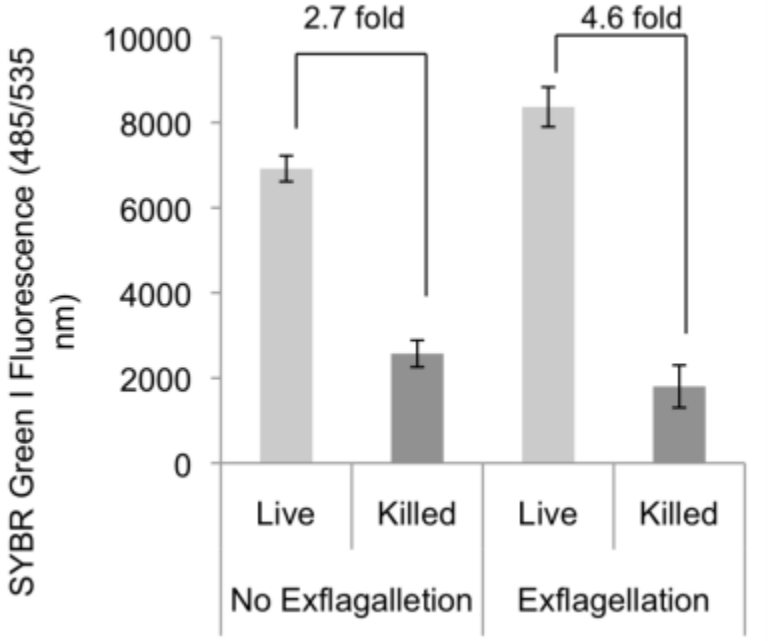

Figure 4.3 SYBR Green I fluorescence of live or pyrvinium pamoate-killed gametocytes in the presence of CyQUANT background suppressor, with and without exflagellation with background well fluorescence (no parasites) subtracted out as a blank.

SYBR Green I Fluorescence Units (484/535 nm)			
sample wells (single drug per well, duplicate plates)		s (no drug)	c (10 µM PP)
12051	6459	13088	6034
10100	11971	13613	6175
11136	11561	13205	6412
12074	12142	12877	6295
	µ	**13196**	**6229**
	σ	**310**	**162**

$$100 - \left(\frac{sample - \mu_c}{\mu_s - \mu_c}\right) \times 100 = \%\, inhibition$$

Figure 4.4 Example of assay plate SYBR green I fluorescence in the presence of background suppressor and calculations for % inhibition. Green indicates a positive hit with high inhibition attributable to gametocyte killing and red indicates an intermediate hit, potentially attributable to inhibition of exflagellation and/or moderate gametocyte killing. Percent inhibition was calculated using the above equation (σ= standard deviation, µ=mean, s=sample, c=control or in this 100% killed gametocytes with 10 µM pyrvinium pamoate). One drug was plated per well using duplicate plates.

Drugs inhibiting exflagellation but not killing the parasites would result in low to intermediate inhibition in this assay (red highlighted value, Figure 4.4), with anything greater than 20% inhibition indicative of some gametocyte killing (green highlighted value, Figure 4.4). Making blood films of positive hits can further differentiate whether parasites are being killed or damaged or whether exflagellation inhibition is occurring.

For our assay, we set a cutoff value of greater than 70% inhibition (equal to or better than clotrimazole) for the FDA drug library screen and greater than 50% inhibition

(using pyrvinium pamoate as a positive control) for the MMV box screen to capture gametocytocidal compounds rather than solely exflagellation inhibitors. The final assay setup for drug screening is briefly illustrated in Figure 4.5.

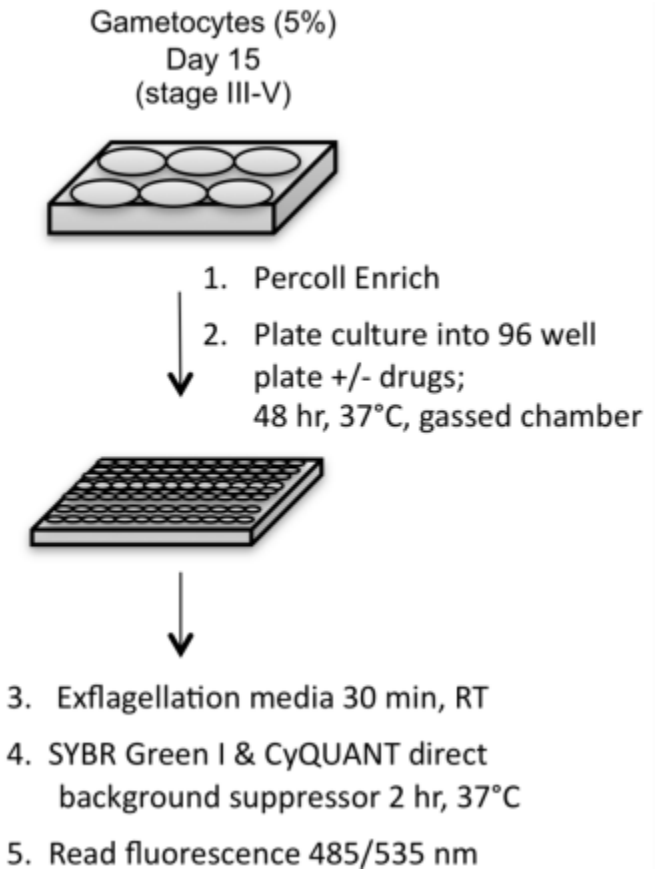

Figure 4.5 Overall assay setup with five steps: 1) Culture and enrich gametocytes. 2) Incubate with drug for 48 hr. 3) Add exflagellation media and incubate 30 min. 4) Add SYBR Green I and background suppressor and incubate 2 hr. 5) Read SYBR Green I fluorescence at excitation 485 nm and emission 535 nm.

Screening of JHU Clinical Compound Library

The Johns Hopkins University Clinical Compound Library version 1.3 of FDA-approved drugs was screened using the assay described above to identify compounds that had gametocytocidal activity, confirmed with Giemsa stained smears of drug treated cultures for the top hits. During the initial screening, clotrimazole was identified as a moderately active gametocytocidal compound, showing 70% inhibition at 20 μM and was then used as a lower cutoff control for identification of screening hits, in order to screen for compounds that were gametocytocidal and did not only inhibit exflagellation. Uninfected erythrocytes were used as baseline for the initial screening.

The FDA approved drug library was screened at 20 μM (Figure 4.6) and we initially selected the top 70 compounds showing more than 50% inhibition for evaluation using microscopic examination and at multiple concentrations IC_{50} determinations (Figure 4.7). As expected most hits showing more than 70% inhibition during initial screening were confirmed to be gametocytocidal by microscopic examination and they showed a clear dose dependent response. Overall we identified 25 compounds with IC_{50} values less than 20 μM, with most less than 10 μM (Table 4.1, Figure 4.7). Most of the compounds with intermediate activity were determined to inhibit exflagellation (data not shown) but were not gametocytocidal as indicated by Giemsa smears of drug-treated gametocytes. The mean Z-factor calculated from the FDA approved drug library screen was 0.61 (SEM=0.05).

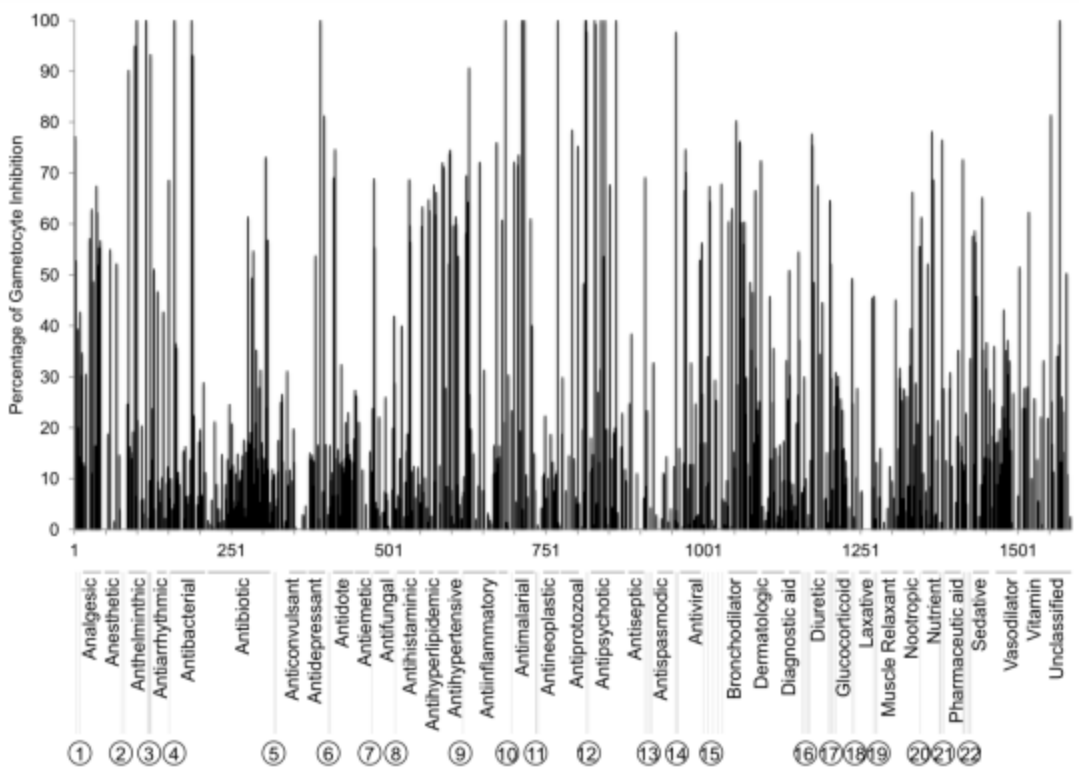

Figure 4.6 SYBR Green I assay results for the Johns Hopkins Clinical Compound Library version 1.3 of FDA approved drugs screened at 20µM. Plot of percentage of gametocytocidal activity of 1,584 compounds compared to clotrimazole control. Numerically referenced drug indications can be found in Supplementary Table 1.

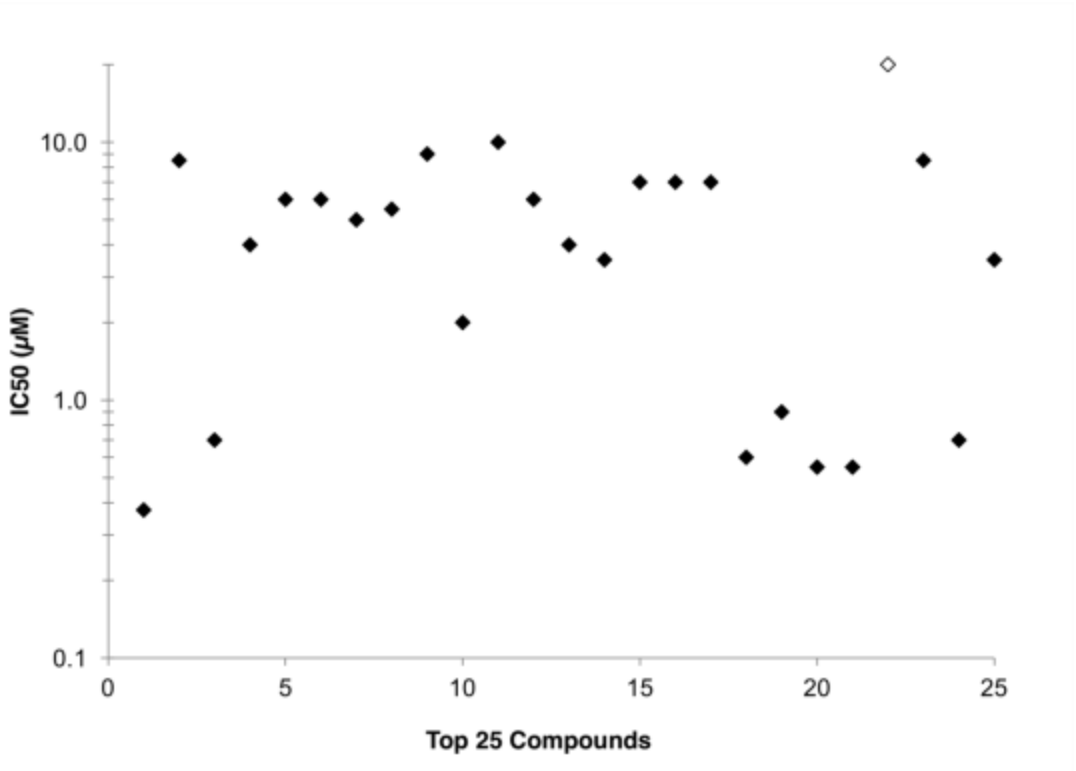

Figure 4.7 IC_{50} values less than or equal to 20 μM of 25 hits from FDA approved drug library screen. Primaquine (open) had an IC_{50} value equal to 20 μM. An IC_{50} for clotrimazole was not determined.

Table 4.1. Gametocytocidal compounds identified in JHU FDA-approved drug library screen with greater than 70% inhibition at 20 μM.

		Gametocyte		Asexual	
Compound	**Indication**	**20 μM % inh (SD)**	**Avg μM**	**10 μM % inh (SD)**	**Avg μM IC_{50}**
Homidium (Ethidium) bromide	Anthelmintic	108.8 (4.7)	0.38	99.3 (0.0)	0.1
Melphalan	Antineoplastic	98.9 (14.9)	4.0	22.9 (2.3)	20.0
Pyrvinium pamoate	Anthelmintic	91.9 (20.0)	4.0	99.6	0.6
Thonzonium bromide	Antiseptic	90.8 (10.6)	6.0	98.1 (0.0)	6.3
Ifosfamide	Antineoplastic	90.6 (15.7)	2.0	0.0 (0.0)	NA
Antimony potassium tartrate	Anthelmintic	88.4 (16.4)	3.5	97.7 (0.0)	NA
Cetalkonium chloride	Antiseptic	88.1 (6.2)	6.0	93.9 (0.1)	12.6
Benzododecinium	Antiseptic	87.5 (6.1)	5.0	98.0[†]	0.1[‡]
Benzethonium chloride	Antiseptic	85.9 (10.3)	6.0	98.6 (0.0)	4.0
Gentian violet	Antiseptic	84.7 (30.5)	8.5	99.2 (0.6)	0.6
Cetylpyridinium chloride	Antiseptic	82.9 (14.2)	7.0	66.4 (8.8)	-
Benzalkonium chloride	Antiseptic	81.4 (7.5)	7.0	98.5 (0.0)	5.0
Tilorone	Antiviral	81.0 (3.0)	5.5	99.2 (0.0)	0.2[‡]
Dithiazanine iodide	Anthelminthic	80.5 (12.0)	7.0	92.9 (0.28)	3.2
Pyrithione zinc	Antiseptic	80.4 (13.7)	0.6	98.6 (0.9)	-
Cetylpyridinium bromide	Antiseptic	78.2 (4.2)	9.0	86.4	6.3
Anastrozole	Antineoplastic	75.7 (22.7)	0.6	-	NA
Methylbenzethonium chloride	Antiseptic	75.2 (5.9)	10.0	98.3 (1.4)	-
Maprotiline	Antidepressant	73.9 (8.1)	0.9	37.4 (0.9)	20
Clotrimazole	Antifungal	70 (-)	-	-	1.3
Acetomenaphthone	Pharmaceutic aid	69.0 (16.4)	8.5	-	12.6
1-Pentanol	Dermatologic	63.8 (18.9)	0.7	5.2 (12.5)	-
Megestrol acetate	Progestogen	62.4 (17.3)	3.5	-0.7 (5.7)	NA
Pentamidine	Antiprotozoal	53.5 (59.5)	0.7	97.7 (0.0)	1.0
Primaquine	Antimalarial	47.8 (15.7)	20	84.2 (10.0)	1.3
Anazolene sodium	Diagnostic aid	34.7 (36.1)	0.6	-6.3 (8.9)	20.0

Asexual stage 10 μM inhibition data was obtained from the Collaborative Drug Discovery Database (CDDD), 10 microM drug 3D7 48hr, ^{3}H hypoxanthine assay for parasite inhibition protocol, and asexual IC_{50} data was obtained from from Eastman et al. or from the CDDD WRAIR IC50 nM D6 protocol as noted [43-44]. Gametocytocidal IC_{50} values were calculated from one experiment with three replicates for top compounds. [†] Data only available for 96 hr assay, [‡] WRAIR D6 data, – Unavailable, NA not active

Major Drug Classes with Gametocytocidal Activity

As a result of the FDA drug library screen, several drug classes were identified that showed activity against gametocytes, including a known antimalarial, primaquine, as well as other classes including antiseptics, antineoplastics, antihelminthics, antivirals, antiprotozoals, antidepressants, and pharmaceutical aids (Figure 4.8). Eight of the twenty-five positive hits were identified as a single class of drugs, quaternary ammonium compounds (QACs) which were classified as antiseptics. Pyrvinium pamoate, an anthelminthic, demonstrated 100% inhibition at 10 μM and was used for further assays as a positive control. By using a positive control of killed parasites in conjunction with the background suppressor rather than uninfected red blood cells, we were able to prevent artificially high inhibition values and screen for live gametocytes, not total gametocytes.

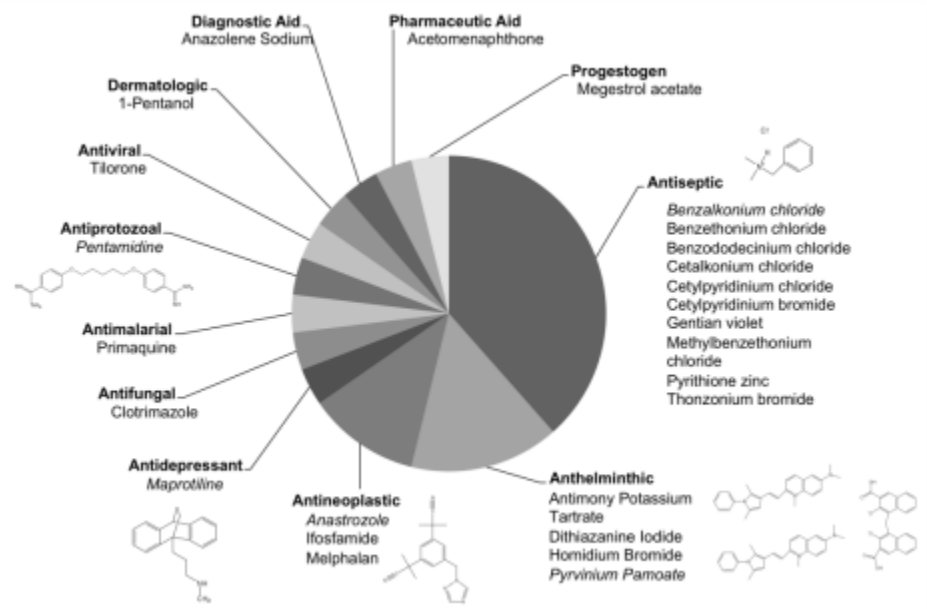

Figure 4.8 Drug class representation of active molecules, IC_{50}< 20 μM. Structures shown correspond to italicized compounds.

Validation of Gametocytocidal Compounds with Membrane Feeding Assay

In order to validate the transmission blocking activity of compounds exhibiting the most potent gametocytocidal activity, mosquito infections through feeding on treated and untreated gametocyte cultures were performed. Gametocyte cultures were treated with methylene blue, a known gametocytocidal compound and clotrimazole, pyrvinium pamoate, and one of the quaternary ammonium compounds cetalkonium chloride for 48 hrs prior to ingestion by mosquitoes through a membrane feeder, and mosquito infections were determined 7 days later as a measure of oocyst stage parasite on the mosquito midgut tissue (Figure 4.9). All compounds demonstrated dose dependent transmission blocking activity, with pyrvinium pamoate showing the highest potency with 100% efficacy at 500 nM.

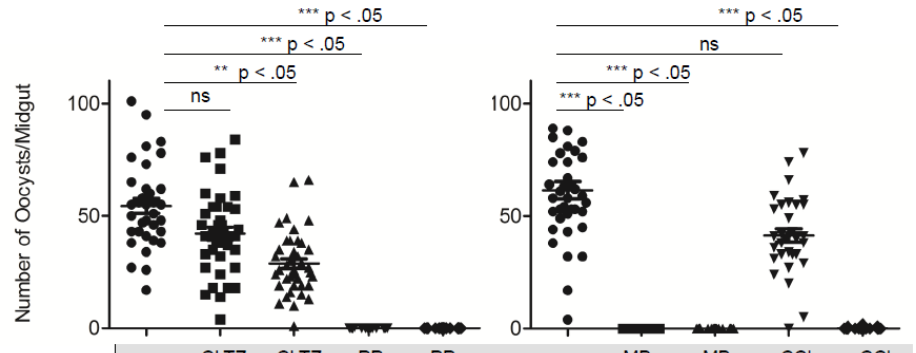

	Ctrl	CLTZ 0.5 µM	CLTZ 5 µM	PP 0.5 µM	PP 5 µM	Ctrl	MB 0.5 mM	MB 5 mM	CCl 0.5 mM	CCl 5 mM
Mean # Oocysts	54	42	29	0	0	61	0	0	41	0
SEM	3.3	2.8	2.1	0.0	0.0	3.8	0.0	0.0	2.9	0.1
Prevalence	1.0	1.0	1.0	0.0	0.0	1.0	0.0	0.0	0.97	0.18

Figure 4.9 Inhibition of oocyst development in mosquito midguts by top compounds from JHU FDA-approved clinical compound library including clotrimazole (CLTZ), pyrvinium pamoate (PP), methylene blue (MB) and cetalkonium chloride (CCl).

MMV Malaria Box Screen

Medicines for Malaria Venture (MMV) has generously put together a 'malaria box' of four hundred compounds with proven antimalarial activity against asexual blood stage parasites and made them freely available for use in the development of effective antimalarial compound screens, particularly those designed to identify liver stage and transmission blocking drugs. We screened these four hundred compounds using our gametocytocidal assay, this time using pyrvinium pamoate as a positive control due to increased efficacy compared to clotrimazole (Figure 4.10). Our initial screen of the MMV box identified eighteen compounds with greater than 80% inhibition at 10 μM which we further screened to determine their IC_{50}s (Table 4.2). Seventeen of the compounds were confirmed as having greater than 50% inhibition at 10 μM and IC_{50}s less than 10 μM, with one compound MMV019918 showing a submicromolar IC_{50}. Of these seventeen compounds with gametocytocidal activity, seven were drug-like, while ten were probe-like, as described by MMV (13). In addition, compounds with the greatest activity against gametocytes also showed nanomolar IC_{50}s against the asexual stage parasite as reported with the compound information by MMV. The mean Z-factor calculated from the MMV malaria box screen was 0.57 (SEM = 0.04).

Furthermore, we compared our MMV box hits with hits from four other assays using different reporters, including luciferase expressing parasites, alamar blue, or confocal fluorescence microscopy (10,14–16). We found that all of our eighteen hits overlapped between different assays (Figure 4.11, see supplementary data available with published manuscript for list of compounds).

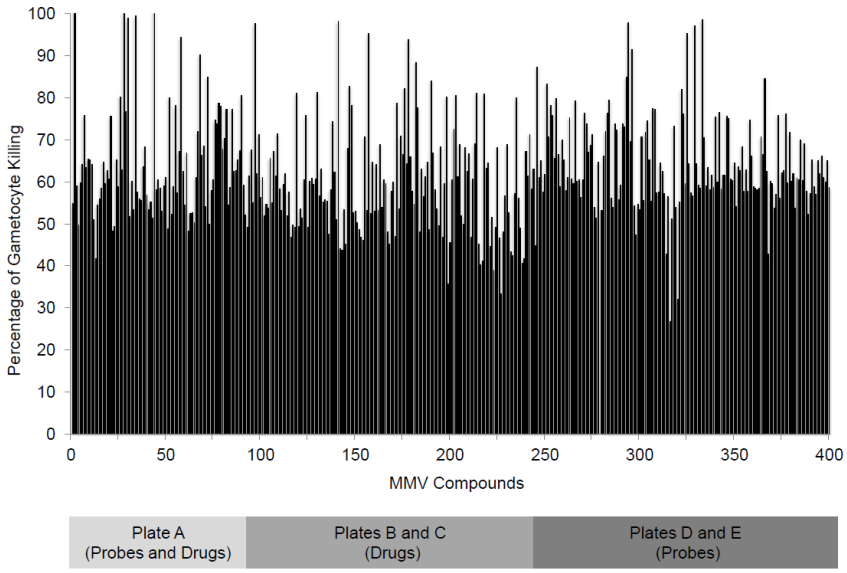

Figure 4.10 SYBR Green I assay results for the MMV box screened at 10 µM. Plot of percentage of gametocytocidal activity of 400 compounds compared to pyrvinium pamoate control.

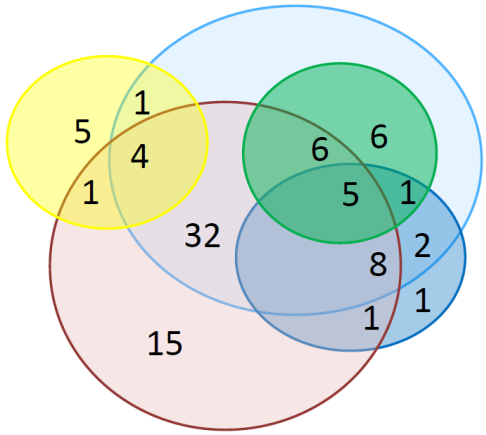

Figure 4.11 Overlap of recent screening assays for MMV Malaria Box. SYBR Green I assay (green) MMV box hits compared with hits from four other assays: Confocal fluorescence microscopy (red), Alamar blue early (dark blue) and late (light blue) and Luciferase (yellow) (10,14–16).

Table 4.2. Gametocidal compounds identified from MMV box with greater than 50% inhibition at 10 μM and available corresponding data on asexual stage inhibition and structure from MMV.

	Gametocyte		Asexual		
MMV #	**% inh 10 μM**	**EC_{50} (SD, μM)**	**% inh 5 μM**	**EC_{50} (nM)**	**CHEMBL EC_{50} (μM)**
MMV665941	122	1.8 (0.2)	96	255	0.62
MMV000448	110	5.4 (1.4)	95	235	0.03, 1.04, 0.53
MMV006172	104	2.6 (0.3)	97	142	0.057, 0.64
MMV396797	100	8.8 (1.2)	-	477	NA
MMV665878	100	1.1 (0.6)	99	139	0.27
MMV667491	99	4.5 (1.5)	-	1230	NA
MMV665830	98	3.3 (0.6)	98	1005	0.25
MMV019780	98	3.8 (0.7)	98	697	0.84
MMV019555	97	3.4 (0.5)	100	376	0.20
MMV019881	96	5.5 (0.9)	98	646	1.04
MMV019918	92	0.9 (0.3)	96	801	1.51
MMV019690	90	>10	97	935	0.78
MMV000445	86	10.00	98	1135	1.97
MMV007591	85	5.4 (1.0)	85	ND	1.12
MMV000848	85	3.6 (3.2)	97	660	1.08
MMV020505	83	6.6 (1.1)	96	876	0.80
MMV006303	82	2.1 (0.6)	-	391	0.03
MMV396794	82	8.2 (0.9)	NA	1160	NA

DISCUSSION AND CONCLUSIONS

To realize the goal of malaria elimination and eradication we need to add new and potent weapons active against multiple life stages of the parasite. Because most of the currently licensed antimalarials target only the asexual intra-erythrocytic stage, which is responsible for the pathology of disease, we urgently need to expand our antimalarial arsenal. Drugs that can effectively eliminate sexual gametocyte stages responsible for transmission to the mosquito vector will be required to move forward towards eventual goal a of malaria free world. In order to find new tools we have established a simple and robust HTS gametocytocidal assay based on DNA content of live gametocytes.

Because gametocytes do not multiply we have utilized male gametocyte exflagellation and a background suppressor to subtract the DNA fluorescence signals from dead cells to achieve robust signal to noise ratio. As emphasized earlier in our description of assay optimization, we carefully took into consideration the contribution of exflagellation to fluorescent signal, and set cutoff values for our assay which allowed us to screen for compounds with gametocytocidal activity and not merely exflagellation inhibition. However, it should be noted that our assay does not allow us to distinguish between male and female gametocyte killing, but instead looks at overall intact gametocytes, and at lower inhibition levels, male gametocyte viability. Linearity of the assay was determined both as function of % gametocytes at 1% HCT (data not shown) as well as actual number of gametocytes per well, which showed a linear relationship with an R^2 value of > 0.95. While many gametocytocidal assays have been developed, many of these assays have features that make them difficult to adapt to high-throughput

screening such as multiple incubations steps or requirement for high gametocytemia, or require transgenic parasites, making it impossible to use field isolates without further genetic manipulation. Our assay is simple enough to be used in any laboratory with access to malaria culture and a fluorescence plate reader, while also maintaining the sensitivity and robustness required for a high-throughput screening assay. We utilized our assay to screen an FDA-approved drug library of 1500 compounds as well as the MMVs Malaria box of 400 compounds to identify new pharmacophores with gametocytocidal activity.

The FDA approved drug library was tested at a concentration of 20 μM in duplicate which led to the identification of several classes of compounds with gametocytocidal activity. Most of the hits from FDA approved library were antiseptic, anthelminthic, and antineoplastic as well as some antimicrobials and an antidepressant drug. Clotrimazole, an antifungal, was identified as having 70% inhibition against gametocytes with an asexual IC_{50} of 1.3 μM, and was recently reported as a hit in another gametocytocidal screen (11).

Pyrithione zinc is an antiseptic which showed activity in our assay with high efficacy against both sexual and asexual stages of the parasite and was also recently reported in the screening of a different library for gametocytocidal drugs (10). As expected our screen identified primaquine as a gametocytocidal compound, albeit at a higher than reported IC_{50} due to lack of metabolism to the highly effective phenolic metabolites of primaquine required for inhibition (17). The antineoplastic compounds, anastrozole, ifosfamide, and melphalan, demonstrated greater than 50% inhibition at

0.55 to 4 μM concentrations against gametocytes (Table 4.1). The data available for melphalan showed 20% inhibition of 3D7 at 10 μM and an IC_{50} of 20 μM. compared to an IC_{50} of 4 μM against *P. falciparum* gametocytes, suggesting that melphalan shows slightly less efficacy against asexual compared to sexual parasites. Of the anthelminthics, homidium bromide and pyrvinium pamoate demonstrated the highest efficacy against gametocytes, with 100% inhibition at 20 μM and IC_{50} values of 0.38 μM and 4 μM respectively, while also effectively inhibiting 70-100% of asexual stages at 10 μM. Homidium bromide (ethidium bromide) is a well-known fluorescent DNA-intercalating agent used in molecular biology and is known to be mutagenic, whereas pyrvinium pamoate is an FDA-approved anthelminthic compound used to treat pinworm, with activity against *Cryptosporidium parvum*, and thought to inhibit mitochondrial NADH-fumarate reductase (18–20). A recent study demonstrates nanomolar inhibition of pyrvinium pamoate against both 3D7 and K1 strains of *P. falciparum* asexual blood stage parasites with further derivatization studies suggesting the quaternary amino group in the quinoline ring is not required for antimalarial activity (21). Removing the positive charge from the molecule may allow better bioavailability of pyrvinium pamoate, and further investigation of gametocytocidal activity of uncharged derivatives is warranted.

The other anthelminthics antimony potassium tartrate and dithiazanine iodide inhibited 80-90% of gametocytes at 20 μM and 90% of asexual stages at 10 μM. Dithiazanine iodide has some structural similarity to pyrvinium pamoate and also possesses a quaternary amine, which raises the question of whether a positive charge is critical for gametocytocidal activity. Interestingly, maprotiline, a tetracyclic

antidepressant similar to the tricyclic antidepressant methylene blue, demonstrated nanomolar inhibition of both gametocyte and asexual stages of *P. falciparum*, but showed greater efficacy against gametocytes. Methylene blue has reported efficacy against gametocytes *in vitro* and also showed *in vivo* efficacy against asexual parasites in multiple murine models of cerebral malaria, protecting 75% of mice at 10 mg/kg for five days post-infection (9,22–25). Our observations suggest further exploration of tetracyclic and tricyclic antidepressants for gametocytocidal activity.

The antiseptic QACs were the most highly represented class of drugs in the hits from the FDA approved library screen, comprising eight out of twenty five hits. Most of the QACs identified in the screen, including cetalkoniumchloride, thonzonium bromide, and benzododecinium chloride, demonstrated almost 100% efficacy against gametocytes at 20 μM with low micromolar IC_{50}s. QACs with antimicrobial activities were identified as early as the 1930s and are among the most useful antiseptics and disinfectants, and have been used for a variety of clinical purposes (26–30). These drugs can function as choline analogs and can inhibit de novo phosphatidylcholine biosynthetic pathway of the malaria parasite. QACs have previously been shown to inhibit asexual blood stages of *P. falciparum* at nanomolar concentrations, with greater activity seen with long alkyl side chains and increased steric hindrance around the nitrogen atom (31).

Phosphatidylcholine, the predominant phospholipid produced by malaria parasites, plays essential structural and regulatory roles in parasite development and differentiation. Previous studies in *P. falciparum* have demonstrated the presence of two pathways for phosphatidylcholine biosynthesis, the cytidine diphosphate (CDP)-choline

pathway, which uses host choline and fatty acids as precursors, and the serine decarboxylase-phosphoethanolamine methyltransferase (SDPM) pathway, which uses host serine and fatty acids as precursors. Recent studies have shown that QACs inhibit multiple steps during phospholipid biosynthesis by targeting the choline carrier as well as enzymes of both the SDPM and the CDP–choline pathways (32,33). A recently published study demonstrates the essentiality of phosphotidylcholine synthesis for gametocyte development and transmission by knocking out or inhibiting the key enzyme in this pathway, phosphoethanolamine methyl transferase, which results in inhibition of gametocyte maturation and also blocks transmission (34). These observations strongly suggest a critical role for phospholipid metabolism during *P. falciparum* gametocyte stages and may present a unique target for multistage drug development. While challenges with poor absorption have been associated with this group of compounds due to a net positive charge, improvements using a prodrug approach have shown promise (31). A choline analog, Albitiazolium is already in clinical trial for complicated malaria using intra-peritoneal or intra-muscular route and efforts are underway to develop this compound for uncomplicated malaria, using an oral route (35). Thus we have not only identified a class of compounds with efficacy against both asexual and sexual stages but also a shared target which can be utilized to identify new pharmacophores active against both asexual and transmission stages of malaria parasites.

In regards to cytotoxicity, route of drug administration and approved drug levels for the aforementioned hits, many of the compounds identified, including the QACs, are topical agents which are not approved for oral drug use. Anthelminthic compounds such

as pyrvinium pamoate and dithiazanine iodide are approved for oral administration, but are not absorbed to appreciable levels by the GI tract and thus are not available in the bloodstream. Antineoplastics such as melphalan can be given orally or intravenously, but perhaps not surprisingly have side effects including bone marrow suppression. Maprotiline, however, is an orally administered antidepressant with an LD_{50} of 90 mg/kg in women, according to DrugBank, and approved prescription of 75-150 mg daily, depending on the severity of depression(36,37). While many of these FDA approved drug hits may not be immediately available or appropriate for oral antimalarial chemotherapy, they do provide novel pharmacophores with gametocytocidal and/or asexual activity, and are suggestive of new drug targets.

The successful screening and hit identification from FDA approved library led us to request the 400 compound malaria box of asexual blood stage active compounds from MMV. We screened the malaria box at 10 μM in duplicate, this time using 10 μM pyrvinium pamoate as a positive control (100% inhibition) and 0.1% DMSO as a vehicle control. As compared to the FDA approved library, we observed a higher number of compounds showing inhibition, which was expected as all these compounds have potent activity against the asexual blood stages. In all we obtained 18 hits, 17 of which showed a dose dependent response against mature gametocytes. The majority of the active compounds were very similar in structure, with seven containing acridine-like structures, three fused benzene rings with a central nitrogen, with varied side chains, one similar to that of chloroquine (MMV665830). Quinacrine and pyronaridine are both acridine-based compounds which have been proven clinically effective against malaria (38). Multiple

mechanisms of action have been proposed and proven for the various acridine-like compounds, including inhibition of hemozoin crystallization (39–41), mitochondrial bc_1 complex (42,43), DNA Topoisomerase II (44,45), and also DNA intercalation, though the latter has not been correlated with increased antimalarial activity (38). Of note, pyronaridine and other Topo II inhibitors have been shown to inhibit both asexual and sexual stages of *P. falciparum* in a previous study, suggesting that Topoisomerase II inhibitors may be utilized to target multiple parasite stages including gametocytes (44).

Towards the end of our library screening and data analysis, four manuscripts describing results of gametocytocidal screening of the MMV malaria box were published. Comparing our MMV hits with these four recent assays, we found that all of our hits overlapped with either the early or late alamar blue or confocal microscopy assays or both, but no hits were shared with the early gametocyte Luciferase based assay (Figure 4.11, see supplementary tables in published manuscript for list of compounds) (10,14,15,46). MMV019918 was a top hit identified by three assays, including our SYBR Green I, the alamar blue and confocal microscopy assays, with nanomolar inhibition against late and early stages (IC_{50}s ranging from 320-890 nM depending on the assay). Four other compounds including MMV000448, MMV006172, MMV007591 and MMV019555 were also identified by all three assays.

We have successfully produced and validated a gametocytocidal drug screening assay that will be easily adaptable to high-throughput format using SYBR Green I and a background suppressor to read DNA content after exposure to drug. Using this assay we screened an FDA-approved drug library and the MMV Malaria box, totaling

approximately 2000 compounds and identified two highly represented classes of compounds, QACs and acridine-like compounds, which were effective against both sexual and asexual stages of the parasite. Further target validation is required to ascertain the mechanism of action of these compounds in gametocytes.

REFERENCES

1. Murray CJL, Rosenfeld LC, Lim SS, Andrews KG, Foreman KJ, Haring D, et al. *Global malaria mortality between 1980 and 2010: a systematic analysis*. Lancet. Elsevier Ltd; 2012 Feb 4;379(9814):413–31.
2. License A, Malaria G, Program E. *A research agenda for malaria eradication: vector control*. PLoS Med. 2011 Jan;8(1):e1000401.
3. Mendis K, Rietveld A, Warsame M, Bosman A, Greenwood B, Wernsdorfer WH. *From malaria control to eradication: The WHO perspective*. Trop Med Int Health. 2009 Jul;14(7):802–9.
4. Birkholtz L-M, Bornman R, Focke W, Mutero C, de Jager C. *Sustainable malaria control: transdisciplinary approaches for translational applications*. Malar J. 2012 Jan;11:431.
5. Peatey CL, Spicer TP, Hodder PS, Trenholme KR, Gardiner DL. *A high-throughput assay for the identification of drugs against late-stage Plasmodium falciparum gametocytes*. Mol Biochem Parasitol. Elsevier B.V.; 2011 Dec;180(2):127–31.
6. D'Alessandro S, Silvestrini F, Dechering K, Corbett Y, Parapini S, Timmerman M, et al. *A Plasmodium falciparum screening assay for anti-gametocyte drugs based on parasite lactate dehydrogenase detection*. J Antimicrob Chemother. 2013 May 3;1–11.

7. Tanaka TQ, Williamson KC. *A malaria gametocytocidal assay using oxidoreduction indicator, alamarBlue*. Mol Biochem Parasitol. Elsevier B.V.; 2011 Jun;177(2):160–3.

8. Lelièvre J, Almela MJ, Lozano S, Miguel C, Franco V, Leroy D, et al. *Activity of clinically relevant antimalarial drugs on Plasmodium falciparum mature gametocytes in an ATP bioluminescence "transmission blocking" assay*. PLoS One. 2012 Jan;7(4):e35019.

9. Adjalley SH, Johnston GL, Li T, Eastman RT, Ekland EH, Eappen AG, et al. *Quantitative assessment of Plasmodium falciparum sexual development reveals potent transmission-blocking activity by methylene blue*. Proc Natl Acad Sci U S A. 2011 Nov 22;108(47):E1214–23.

10. Sun W, Tanaka TQ, Magle CT, Huang W, Southall N, Huang R, et al. *Chemical signatures and new drug targets for gametocytocidal drug development*. Sci Rep. 2014 Jan;4:3743.

11. Tanaka TQ, Dehdashti SJ, Nguyen D-T, McKew JC, Zheng W, Williamson KC. *A quantitative high throughput assay for identifying gametocytocidal compounds.* Mol Biochem Parasitol. Elsevier B.V.; 2013 Mar;188(1):20–5.

12. Zhang J-H, Chung TDY, Oldenburg KR. *A Simple Statistical Parameter for Use in Evaluation and Validation of High Throughput Screening Assays*. J Biomol Screen. 1999 Apr 1;4(2):67–73.

13. Spangenberg T, Burrows JN, Kowalczyk P, McDonald S, Wells TNC, Willis P. *The open access malaria box: a drug discovery catalyst for neglected diseases.* PLoS One. 2013 Jan;8(6):e62906.

14. Duffy S, Avery VM. *Identification of inhibitors of Plasmodium falciparum gametocyte development*. Malar J. 2013 Nov 11;12(1):408.

15. Bowman JD, Merino EF, Brooks CF, Striepen B, Carlier PR, Cassera MB. *Anti-apicoplast and gametocytocidal screening to identify the mechanisms of action of compounds within the Malaria Box*. Antimicrob Agents Chemother. 2013 Nov 18;58(2):811–9.

16. Lucantoni L, Avery V. *Whole-cell in vitro screening for gametocytocidal compounds.* Future Med Chem. 2012;4(18):2337–60.

17. Pybus BS, Marcsisin SR, Jin X, Deye G, Sousa JC, Li Q, et al. *The metabolism of primaquine to its active metabolite is dependent on CYP 2D6*. Malar J. Malaria Journal; 2013;12(1):1.

18. Downey AS, Chong CR, Graczyk TK, Sullivan DJ. *Efficacy of pyrvinium pamoate against Cryptosporidium parvum infection in vitro and in a neonatal mouse model.* Antimicrob Agents Chemother. 2008 Sep;52(9):3106–12.

19. Chong CR, Chen X, Shi L, Liu JO, Sullivan DJ. *A clinical drug library screen identifies astemizole as an antimalarial agent*. Nat Chem Biol. 2006 Aug;2(8):415–6.

20. Tomitsuka E, Kita K, Esumi H. *An anticancer agent, pyrvinium pamoate inhibits the NADH-fumarate reductase system--a unique mitochondrial energy metabolism in tumour microenvironments*. J Biochem. 2012 Aug;152(2):171–83.

21. Teguh SC, Klonis N, Duffy S, Lucantoni L, Avery VM, Hutton C a, et al. *Novel conjugated quinoline-indoles compromise Plasmodium falciparum mitochondrial function and show promising antimalarial activity*. J Med Chem. 2013 Aug 8;56(15):6200–15.

22. Coulibaly B, Zoungrana A, Mockenhaupt FP, Schirmer RH, Klose C, Mansmann U, et al. *Strong gametocytocidal effect of methylene blue-based combination therapy against falciparum malaria: a randomised controlled trial.* PLoS One. 2009 Jan;4(5):e5318.

23. Pascual A, Henry M, Briolant S, Charras S, Baret E, Amalvict R, et al. *In vitro activity of Proveblue (methylene blue) on Plasmodium falciparum strains resistant to standard antimalarial drugs.* Antimicrob Agents Chemother. 2011 May;55(5):2472–4.

24. Dormoi J, Briolant S, Desgrouas C, Pradines B. *Impact of methylene blue and atorvastatin combination therapy on the apparition of cerebral malaria in a murine model.* Malar J. 2013 Apr 15;12(1):127.

25. Dormoi J, Briolant S, Desgrouas C, Pradines B. *Efficacy of proveblue (methylene blue) in an experimental cerebral malaria murine model*. Antimicrob Agents Chemother. 2013 Jul;57(7):3412–4.

26. D'Arcy PF and, Taylor EP. *Quaternary ammonium compounds in medicinal chemistry* I. J Pharm Pharmacol. 1962;14(1):129–46.

27. D'Arcy PF and, Taylor EP. *Quaternary ammonium compounds in medicinal chemistry II.* J Pharm Pharmacol. 1962;14(1):193–216.

28. Bhattacharya BK, Sen AB. *Chemotherapeutic Properties of Some New Quaternary Ammonium Compounds; Their Cesticidal Action Against Hymenolepis Nana.* Br J Pharmacol Chemother. 1965 Feb;24:240–4.

29. Krawczyk J, Keane N, Swords R, O'Dwyer M, Freeman CL, Giles FJ. *Perifosine--a new option in treatment of acute myeloid leukemia?* Expert Opin Investig Drugs. 2013 Oct;22(10):1315–27.

30. Dorlo TPC, Balasegaram M, Beijnen JH, de Vries PJ. *Miltefosine: a review of its pharmacology and therapeutic efficacy in the treatment of leishmaniasis*. J Antimicrob Chemother. 2012 Dec;67(11):2576–97.

31. Peyrottes S, Caldarelli S, Wein S, Périgaud C, Pellet A, Vial H. *Choline Analogues in Malaria Chemotherapy.* Curr Pharm Des. 2012;18:3454–66.

32. Tischer M, Pradel G, Ohlsen K, Holzgrabe U. *Quaternary ammonium salts and their antimicrobial potential: targets or nonspecific interactions?* Chem Med Chem. 2012 Jan 2;7(1):22–31.

33. Calas M, Cordina G, Bompart J, Ben Bari M, Jei T, Ancelin ML, et al. *Antimalarial activity of molecules interfering with Plasmodium falciparum phospholipid metabolism. Structure-activity relationship analysis*. J Med Chem. 1997 Oct 24;40(22):3557–66.

34. Bobenchik A. *Plasmodium falciparum phosphoethanolamine methyltransferase is essential for malaria transmission.* Proc Natl Acad Sci. 2013;110(45):18262–7.

35. Wein S, Maynadier M, Bordat Y, Perez J, Maheshwari S, Bette-Bobillo P, et al. *Transport and pharmacodynamics of albitiazolium, an antimalarial drug candidate*. Br J Pharmacol. 2012 Aug;166(8):2263–76.

36. Drugs.com Maprotiline Dosage [Internet]. Available from: http://www.drugs.com/dosage/maprotiline.html

37. Drug Bank: Maprotiline [Internet]. Available from: http://www.drugbank.ca/drugs/DB00934

38. Valdés AF. Acridine and Acridinones: *Old and New Structures with Antimalarial Activity*. Open Med Chem J. 2011;11–20.

39. Yu X-M, Ramiandrasoa F, Guetzoyan L, Pradines B, Quintino E, Gadelle D, et al. *Synthesis and biological evaluation of acridine derivatives as antimalarial agents*. ChemMedChem. 2012 Apr;7(4):587–605.

40. Fernández-Calienes A, Pellón R, Docampo M, Fascio M, D'Accorso N, Maes L, et al. *Antimalarial activity of new acridinone derivatives*. Biomed Pharmacother. 2011 Jun;65(3):210–4.

41. Guetzoyan L, Yu X-M, Ramiandrasoa F, Pethe S, Rogier C, Pradines B, et al. *Antimalarial acridines: synthesis, in vitro activity against P. falciparum and interaction with hematin.* Bioorg Med Chem. Elsevier Ltd; 2009 Dec 1;17(23):8032–9.

42. Biagini G, Fisher N, Berry N. *Acridinediones: selective and potent inhibitors of the malaria parasite mitochondrial bc1 complex*. Mol Pharm. 2008;73(5):1347–55.

43. Barton V, Fisher N, Biagini G a, Ward S a, O'Neill PM. *Inhibiting Plasmodium cytochrome bc1: a complex issue*. Curr Opin Chem Biol. Elsevier Ltd; 2010 Aug;14(4):440–6.

44. Chavalitshewinkoon-Petmitr P. *Gametocytocidal activity of pyronaridine and DNA topoisomerase II inhibitors against multidrug-resistant Plasmodium falciparum in vitro*. Parasitol Int. 2000;48(4):275–80.

45. Auparakkitanon S, Wilairat P. *Cleavage of DNA induced by 9-anilinoacridine inhibitors of topoisomerase II in the malaria parasite Plasmodium falciparum*. Biochem Biophys Res Commun. 2000 Mar 16;269(2):406–9.

46. Lucantoni L, Duffy S, Adjalley SH, Fidock D a, Avery VM. *Identification of MMV Malaria Box Inhibitors of Plasmodium falciparum Early-Stage Gametocytes Using a Luciferase-Based High-Throughput Assay*. Antimicrob Agents Chemother. 2013 Dec;57(12):6050–62.

NATALIE G. ROBINETT
(Formerly Sanders)
Doctoral Candidate
Johns Hopkins Bloomberg School of Public Health
615 N. Wolfe Street, Rm. W4612
Baltimore, MD 21205
Email: natalie.robinett@gmail.com Phone: (512) 508-1854

EDUCATION

Aug 2010-Present — PhD Candidate, Molecular Microbiology and Immunology
Specialization: Molecular Parasitology and Drug Discovery
Johns Hopkins Bloomberg School of Public Health
Baltimore, Maryland
Defense Date: September 10, 2015

May 2010 — BS, Chemistry with Honors
Southwestern University
Georgetown, Texas (Magna cum laude)

RESEARCH EXPERIENCE

August 2010-Present — PhD Student, Johns Hopkins Bloomberg School of Public Health
H. Feinstone Department of Molecular Microbiology and Immunology
PI: Dr. David Sullivan
Dissertation Topic: Determining the function of Plasmodium hemolysin III and discovery of novel antimalarial drugs

Aim 1: Determine function and virulence of *Plasmodium* hemolysin III in order to discover a potential role in severe malaria anemia

- Characterized stage specific *P. falciparum* HlyIII protein expression using hemolysin-specific polyclonal antiserum and Western blotting
- Genetically modified the murine malaria parasite, knocking out the *P. berghei* HlyIII homolog and characterized virulence and growth rate in mice, as well as essentiality in all stages of the life cycle, comparing the PbHlyIII KO parasite to the wild type *P. berghei* ANKA strain

Aim 2: Discover novel antimalarial compounds to improve current drug regimens in light of current drug resistance and treatment failures

- Synthesized and tested hydroxyethylapoquinine (HEAQ) and derivatives for ability to inhibit heme crystallization
- Demonstrated comparable antimalarial efficacy *in vitro* and *in vivo* (mouse model) and decreased hERG channel inhibition of HEAQ and derivatives when compared to the parent drugs quinine and quinidine
- Developed a high throughput assay to screen for gametocytocidal drugs using a novel combination of SYBR Green I and CyQUANT

background suppressor for efficient and robust detection of gametocyte killing
- Identified new classes of transmission blocking drugs including quaternary ammonium compounds and acridine-like compounds

June 2008 - May 2010

Honors Chemistry Research Student, Southwestern University
PI: Dr. Lynn Guziec, Chemistry Department and
Dr. Martín Gonzalez, Biology Department

Honors Thesis: Synthesis and Antimicrobial Activity of Seleno-Dapsone

Aim1: Synthesize a selenium analog of the antileprotic drug Dapsone in order to make a less toxic derivative of a sulfonamide drug

- Developed a synthetic approach and successfully synthesized and purified Seleno-Dapsone (confirmed by NMR and elemental analysis)

Aim2: Determine whether Seleno-Dapsone is an active antimicrobial agent with comparable efficacy to Dapsone

- Assessed antimicrobial activity of Seleno-Dapsone against *Bacillus subtilis* and *Staphylococcus aureus*, showing dose dependent inhibition of both strains

PUBLICATIONS

1. Moonah S, **Sanders NG**, Persichetti J, Sullivan DJ Jr. (2014) Erythrocyte lysis and Xenopus laevis oocyte rupture by recombinant Plasmodium falciparum hemolysin III. Eukaryot Cell. pii: EC.00088-14.
2. **Sanders, NG,** Sullivan, DJ, Mlambo, G, Dimopoulos, G, Tripathi, A. (2014) Gametocytocidal screen identifies novel chemical classes with Plasmodium falciparum transmission blocking activity. PlosONE 9(8) e105817. doi: 10.1371/journal.pone.0105817. eCollection 2014.
3. Kumar K, Schniper S, González-Sarrías A, Holder AA, **Sanders N**, Sullivan D, Jarrett WL, Davis K, Bai F, Seeram NP, Kumar V. (2014) Highly potent anti-proliferative effects of a gallium(III) complex with 7-chloroquinoline thiosemicarbazone as a ligand: synthesis, cytotoxic and antimalarial evaluation. Eur J Med Chem. 86:81-6. doi: 10.1016/j.ejmech.2014.08.054. Epub 2014 Aug 16.
4. Hain AU, Bartee D, **Sanders NG**, Miller AS, Sullivan DJ, Levitskaya J, Meyers CF, Bosch J. (2014) Identification of an Atg8-Atg3 protein-protein interaction inhibitor from the medicines for malaria venture malaria box active in blood and liver stage Plasmodium falciparum parasites. J Med Chem. 12;57(11):4521-31
5. **Sanders, NG**, Meyers, D., Sullivan, DJ. (2013) Antimalarial efficacy of hydroxyethylapoquinine (SN-119) and derivatives. published online ahead of print on 18 November 2013 Antimicrob Agents Chemother. 58(2):820-7

ORAL PRESENTATIONS

1. **Robinett, NG,** Moonah, S, Sullivan, DJ. What is a hemolytic protein like you doing in a red blood cell parasite like this? or Determining the functional role of *Plasmodium* hemolysin III in the parasite. Emergent Biosolutions, Gaithersburg, MD. April 24, 2015
2. **Robinett, NG,** Moonah, S, Sullivan, DJ. What is a hemolytic protein like you doing in a red blood cell parasite like this? Gordon Research Conference: Tropical Infectious Diseases, Galveston, TX. March 7, 2015

POSTERS

1. **Robinett, NG,** Moonah, S, Sullivan, DJ. What is a hemolytic protein like you doing in a red blood cell parasite like this? Gordon Research Conference: Tropical Infectious Diseases, Galveston, TX. March 2015
2. **Sanders, NG**, Moonah, S, Sullivan, DJ. Characterization of *P. falciparum* hemolysin III in asexual blood stages and expression in *Xenopus* oocytes. 25th Annual Molecular Parasitology Meeting at Woods Hole, MA. September 2014
3. **Sanders, N.**, Meyers, D., Sullivan, D.J. Antimalarial efficacy of hydroxyethylapoquinine (SN-119) and derivatives. 24th Annual Molecular Parasitology Meeting at Woods Hole, MA. September 2013
4. **Sanders, N.**, Meyers, D., Sullivan, D.J. Antimalarial efficacy of hydroxyethylapoquinine (SN-119) and derivatives. (2012) ASTMH 61st Annual Meeting, Atlanta, GA. November 2012
5. **Sanders, N.G.** Sullivan, D.J., Tripathi, A. A high throughput drug screening assay using SYBR Green I identifies novel classes of gametocytocidal compounds. 23rd Annual Molecular Parasitology Meeting at Woods Hole, MA. September 2012
6. **Sanders, N.**, Guziec, L. Synthesis of Seleno-Dapsone. National ACS Meeting, Washington, D.C. August 2009

TEACHING/MENTORING EXPERIENCE

Lecture, Teaching

August 2015	*Guest Lecturer*, Johns Hopkins School of Public Health Course: Introduction to the Biomedical Sciences Lecture: General Immunology Mentor: Dr. Gundula Bosch, Instructor, Johns Hopkins Skills to gain: experience teaching a graduate level course
July 2015	*Guest Lecturer*, Johns Hopkins University Course: Introduction to Biological Molecules Lecture: Protein Architecture and Biological Function (2 sections) Lecture: Translation of RNA (2 sections) Labs: DNA Isolation and Restriction Mapping of DNA Mentor: Dr. Richard Shingles, Professor of Biology, Johns Hopkins Skills gained: experience teaching an undergraduate course

Oct-Dec 2014 Jan-Mar 2014 Jan-Mar 2013	*Teaching Assistant*, Johns Hopkins School of Public Health Course: Biology of Parasitism Role: Assist with laboratory section, identification of parasites via microscopy, utilizing mouse models for parasite infections and host-pathogen interactions (taught small animal handling)
Mar-May 2012	*Teaching Assistant*, Johns Hopkins School of Public Health Course: Malariology Role: Proctor exams, answer questions, manage online lecture material

Mentoring

June 2011-May 2015	*Math tutor*, Pen Lucy Action Network, Baltimore, MD Weekly tutor an elementary school student in mathematics, problem solving, test taking strategies, and memorization
June – Aug 2014	*Mentor*, Undergraduate Research, Johns Hopkins School of Public Health Student: Kalina Martinova (Johns Hopkins University Class of 2016) Project: "Purification of recombinant *P. falciparum* histidine rich protein 2 (HRP2)" Role: Trained in primary literature review and analysis
June – Aug 2013	*Mentor,* Undergraduate Research, Johns Hopkins School of Public Health Student: Promise Okeke (Augsburg College, Class of 2015) Project: "Irreversible heme crystal inhibition by amodiaquine and pyronaridine: a means to circumvent malaria drug resistance" Role: Trained in *in vitro* heme crystallization assay and drug dilutions, and data analysis, buffer composition
June –Aug 2012	*Mentor*, Undergraduate Research, Johns Hopkins School of Public Health Student: Laura Anzaldi (Johns Hopkins Medical Student Class of 2018) Project: "Malaria heme crystallization inhibition: analysis of FDA drugs, parasite inhibition and drug resistance" Role: Trained in *in vitro* biochemical assay techniques, drug dilutions, and data analysis
June – Aug 2011	*Mentor*, Undergraduate Research, Johns Hopkins School of Public Health Student: Melissa Santos (University of Maryland Class of 2014) Project: "Heme crystallization inhibition by novel quinine derivatives" Role: Trained in molecular biology techniques and data analysis

PROFESSIONAL TEACHING DEVELOPMENT
(Preparing Future Faculty Teaching Academy)

Jan-Mar 2015 — Student, Johns Hopkins School of Public Health
Course: Teaching at the University Level (Instructor: Dr. Anne Riley)
Skills gained:

- Developed a deeper understanding of how students learn
- Designed a course syllabus for an upper level college biology class
- Developed active learning activities for my course
- Gave an introductory lecture for my course and received feedback
- Developed a personal teaching philosophy

Sep- Dec 2012 — Student, Johns Hopkins School of Education
Course: Introduction to Effective Instruction (Instructor: Dr. David Andrews)
Skills gained:

- Studied basic teaching pedagogy including: science of learning, formative and summative assessment techniques, and approaches/challenges to small and large group instruction
- Developed a short teaching philosophy and gave a mini-lecture with feedback on body language, speech and presentation skills

OUTREACH/SERVICE

June 2011-May 2014 — Student Facilitator, Public Health Christian Fellowship Student Group
Johns Hopkins Bloomberg School of Public Health

- Engaged public health students in discussions of living out faith in the context of public health challenges and crises
- Organized and led weekly meetings to promote fellowship and growth during graduate school
- Invited faculty and outside speakers to discuss the role of faith-based organizations in public health and to share their perspectives on faith in a public health context

Aug 2012-Aug 2013 — President, Molecular Microbiology and Immunology Student Group
Johns Hopkins Bloomberg School of Public Health

- Created a space for students to express their ideas or concerns and develop better communication between students and faculty
- Organized social events to promote fellowship and collaboration within the department, including organizing our first annual outdoor picnic.
- Organized a canned food drive to support a local women's shelter

RESEARCH GRANTS AND AWARDS

Aug 2012-May 2015	Emergent Biosolutions Fellowship Proposal: Characterizing the role of a putative *P. falciparum* hemolysin III in malarial anemia and as a potential antimalarial drug target Award: $15,000 (Covered lab supplies and travel to scientific meetings)
Aug 2013-May 2014	Frederick Bang Award Proposal: Role of *P. falciparum* hemolysin III in severe malaria anemia Award: $3000 (Covered lab supplies and travel to scientific meetings)
May 2011-May 2012	Eleanor A. Bliss Honorary Fellowship Departmental Award, H. Feinstone Department of Molecular Microbiology and Immunology Award: unknown amount (Covered stipend)

PROFESSIONAL AFFILIATIONS

May 2010-Present	Phi Beta Kappa, Alpha Chi Scholar
Aug 2010-Present	American Society of Microbiology, Student Affiliate